

AN EXPERIMENTAL ANALYSIS OF DEFLECTION AND ULTI-
MATE MOMENT IN THIN, REINFORCED CONCRETE PANELS
AS A FUNCTION OF REINFORCEMENT SPACING

By

GEORGE WILLIAM ARTHUR MAHONEY

Bachelor of Science
University of Illinois
Urbana, Illinois
1949

Master of Science
Oklahoma State University
Stillwater, Oklahoma
1953

Submitted to the Faculty of the Graduate Collège
Oklahoma State University
in partial fulfillment of the requirements
for the Degree of
DOCTOR OF PHILOSOPHY
May, 1971

Thesis
1971D
M216e
cop. 2


OKLAHOMA
STATE UNIVERSITY
LIBRARY
AUG 12 1971

AN EXPERIMENTAL ANALYSIS OF DEFLECTION AND ULTI-
MATE MOMENT IN THIN, REINFORCED CONCRETE PANELS
AS A FUNCTION OF REINFORCEMENT SPACING

Thesis Approved:



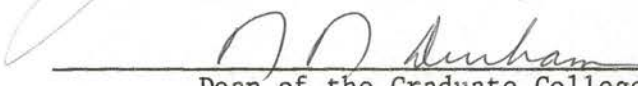
Thesis Adviser











Dean of the Graduate College

788652

ACKNOWLEDGEMENTS

This study was conducted as a part of Oklahoma Agricultural Experiment Station Project 1429.

The author is especially indebted to his previous major advisor, Dr. G. L. Nelson, Agricultural Engineering Department Chairman, Ohio State University. This thesis could not have become a reality without his encouragement, guidance and assistance. The author is also deeply indebted to Dr. James E. Garton who assumed the role of major advisor for the final year of work and the assistance and encouragement received.

My sincere appreciation for their assistance is extended to the other members of the Advisory Committee: Professor E. W. Schroeder, Head of the Agricultural Engineering Department, Dr. R. L. Janes, Associate Professor of Civil Engineering, Dr. John P. Lloyd, Assistant Professor of Civil Engineering, and Dr. Allen F. Butchbaker, Associate Professor of Agricultural Engineering. Their criticisms and suggestions have been invaluable.

For providing facilities and funds during this study, I extend my appreciation to Professor E. W. Schroeder.

For assistance in conducting experiments and in preparation of figures, I extend my appreciation to Jack I. Fryrear, Norman Griffin and Don McCracken.

For the honor of being selected as NSF Faculty Fellow and for the opportunity of attending Iowa State University for one year of my graduate program, I would like to express my appreciation to the National

Science Foundation.

I am grateful to Mrs. Janet Sallee for her efforts in typing the final draft of the manuscript.

Last but not least, I am especially indebted to my wife, Jean, my son, Kevin, and my daughter, Siobhan, for their understanding and many sacrifices. To them I dedicate this thesis.

TABLE OF CONTENTS

Chapter	Page
I. INTRODUCTION.	1
Background	1
The Problem.	4
Objectives	4
II. LITERATURE REVIEW	6
Ferro-Cemento.	7
Crack Arrest	8
Other Materials for Reinforcement.	12
III. REINFORCED CONCRETE THEORY.	14
Straight Line Theory	14
Ultimate Strength Theory	16
IV. THEORETICAL ANALYSIS.	22
V. DESIGN OF THE EXPERIMENT.	31
Similitude and the Buckingham Pi Theorem	31
Definition of the System	32
Dimensionless Parameters, Uncracked Panels	36
Dimensionless Parameters, Cracked Panels	36
Dimensionless Parameters, Ultimate Loads	37
Discussion of Pi Terms, Uncracked Panels	37
Discussion of Pi Terms, Cracked Panels	39
Discussion of Pi Terms, Ultimate Loads	39
VI. DESIGN OF TEST SPECIMENS.	43
Preliminary Tests.	47
VII. EXPERIMENTAL PROCEDURES	50
Casting Procedures	50
Testing Equipment.	54
Instrumentation.	56
Testing Procedures	58
VIII. DISCUSSION OF TESTING	61

TABLE OF CONTENTS (Continued)

Chapter	Page
Modulus of Elasticity for Concrete Cylinders.	61
Modulus of Elasticity for Panels.	67
IX. DATA ANALYSIS.	71
Uncracked Panel Data.	72
Statistical Significance, Uncracked Panels.	74
Cracked Panel Data.	77
Statistical Significance, Cracked Panels.	80
Ultimate Strength Data.	82
Statistical Significance, Ultimate Loads.	83
X. THE PREDICTION EQUATIONS	85
Uncracked Panels.	85
Prediction Equation, Uncracked Panels	89
Cracked Panels.	94
Prediction Equation, Cracked Panels	99
Ultimate Strength of Panels	102
Prediction Equations, Ultimate Strength	107
XI. VALIDATION TESTS	108
XII. SUMMARY AND CONCLUSIONS.	121
The Prediction Equations.	122
Statistical Significance.	122
Suggestions for Further Study	124
A SELECTED BIBLIOGRAPHY.	126
APPENDIX A. PRELIMINARY INVESTIGATIONS.	130
APPENDIX B. CONJUGATE BEAM THEORY	141
APPENDIX C. LOAD-DEFLECTION PLOTS, TEST PANELS.	153

LIST OF TABLES

Table	Page
I. List of Pertinent Quantities	34
II. Pi Term Values Required in Uncracked Concrete Panels for Predicting Deflection Pi Terms	40
III. Pi Term Values Required in Cracked Concrete Panels for Predicting Deflection and Ultimate Moment Pi Terms	42
IV. Physical Properties of Thin Concrete Panels Tested	62
V. Modulus of Elasticity for Panels in Flexure	69
VI. Data for Regression Analysis and Best Fit Curve, Spacing Effect of Reinforcement on Strain	76
VII. Data for Regression Analysis and Best Fit Curve, Load Effect on Panel Deflection at Midspan, Uncracked Panels	88
VIII. Data for Regression Analysis and Best Fit Curve, Spacing Effect of Reinforcement on Panel Deflection at Midspan, Uncracked Panels	91
IX. Data for Regression Analysis and Best Fit Curve, Depth of Panel Effect on Panel Deflection at Midspan, Uncracked Panels	93
X. Data for Regression Analysis and Best Fit Curve, Spacing Effects of Reinforcement on Measured Versus Computed Deflected, Cracked Panels	96
XI. Data for Regression Analysis and Best Fit Curve, Depth of Panel Effect on Measured Versus Computed Deflection, Cracked Panels	98
XII. Data for Regression Analysis and Best Fit Curve, Percent Reinforcement Effect on Measured Versus Computed Deflection, Cracked Panels	101
XIII. Data for Regression Analysis and Best Fit Curve, Spacing Effect of Reinforcement on Ratio of Measured Versus Computed Ultimate Load	104

LIST OF TABLES (Continued)

Table	Page
XIV. Data for Regression Analysis and Best Fit Curve, Depth of Panel Effect on Ratio of Measured Versus Computed Ultimate Load	106
XV. Physical Properties of Wire for Validation Tests.	109
XVI. Wire Surface Area and Dimensionless Terms for Validation Test.	111
XVII. Ultimate Loads for Validation Tests	114
XVIII. Bond Test Results	134
XIX. Physical Properties of Twelve Panels for Preliminary Tests for E_c for Concrete	139

LIST OF FIGURES

Figure	Page
1. Straight Line Theory.	15
2. Ultimate Strength Theory.	17
3. Failure Mode, Under-Reinforced Beams.	20
4. Failure Mode, Over-Reinforced Beams	20
5. Location of Neutral Axis in Cracked Beam.	27
6. Transformed Sections--Uncracked and Cracked Sections.	27
7. Loss of Concrete Tensile Stress at Crack.	28
8. Pertinent Dimensions, Test Panel.	33
9. Stress-Strain Plot, No. 10 Plain Wire	51
10. Test Panels, Five Depths and Lengths.	53
11. Stress-Strain Plot for Test Cylinders	55
12. Test Cylinder at Failure.	57
13. Loading Equipment for Panel Tests	57
14. Load-Deflection Tests, Five Spacings.	65
15. Load-Deflection Tests, Five Depths.	66
16. Data Plot, Strain Versus S/d_s	75
17. Data Plot, Δ/L Versus PL^2/EI	87
18. Data Plot, Δ/L Versus S/d_s	90
19. Data Plot, Δ/L Versus D/d_s	92
20. Data Plot, Δ/Δ_c Versus S/d_s	95
21. Data Plot, Δ/Δ_c Versus D/d_s	97
22. Data Plot, Δ/Δ_c Versus p	100

LIST OF FIGURES (Continued)

Figure	Page
23. Data Plot, P_u/P_c Versus S/d_s	103
24. Data Plot, P_u/P_c Versus D/d_s	105
25. Casting Bed and Wire for Validation Tests	110
26. Stress-Strain Plot, Wire for Validation Tests	112
27. Plot of Validation Test Data.	113
28. Stress-Strain Plot of Validation Test Cylinder.	115
29. Failure Due to Void at Cross Wire	117
30. Failure Due to Compression Surface Spalling	117
31. Failure Sequence, Top View.	118
32. Failure Sequence, Front View.	118
33. Spacing of Cracks, Validation Test.	120
34. Failure at Cross Wires.	120
35. Pull-Out Test Bracket	133
36. Pull-Out Test Specimen.	135
37. Real Beam and Conjugate Beam.	142
38. Cracked Conjugate Beam.	145
39. Cross Section for Computing I of Uncracked Panel.	149
40. Cross Section for Computing I_c of Cracked Panel	151
41. Load-Deflection Plots, Panels 1, 2 and 3.	154
42. Load-Deflection Plots, Panels 4, 5 and 6.	155
43. Load-Deflection Plots, Panels 7, 8 and 9.	156
44. Load-Deflection Plots, Panels 10, 11 and 12	157
45. Load-Deflection Plots, Panels 13, 14 and 15	158
46. Load-Deflection Plots, Panels 16, 17 and 18	159
47. Load-Deflection Plots, Panels 19, 20 and 21	160

LIST OF FIGURES (Continued)

Figure	Page
48. Load-Deflection Plots, Panels 22, 23 and 24.	161
49. Load-Deflection Plots, Panels 25, 26 and 27.	162

CHAPTER I

INTRODUCTION

Background

Reinforced concrete has been used for building construction for over 100 years after receiving recognition as a construction material for boats and flower pots. Louis Lambot of France first used reinforced concrete as we know it in 1848 when he built a small rowboat using thin, iron straps to form a metal grid which he covered with wire netting and plastered with mortar.⁽⁵⁾ The total thickness of his 12 foot rowboat was approximately 1 to 1½ inches, relatively thin when we consider normal reinforced concrete construction.

Lambot's reasons for using concrete for his boats are much the same advantages we think of today in relation to material selection for agricultural applications. They are:

1. Savings in initial cost of construction.
2. Savings in maintenance.
3. Speed of construction.
4. Impermeability.
5. Immediate repairs in case of damage.
6. Incombustibility.
7. Strength and durability.

Lambot's boats were quickly followed by reinforced concrete tubs for orange trees, designed by Monier in 1849, and constructed of a mesh

of iron rods covered with mortar. W. B. Wilmenson patented the first structural reinforced concrete construction system in England the following year, 1850, a floor and roof system reinforced with second hand mining rope.

Reinforced concrete was adapted for construction in Germany and England by 1885. The first completely reinforced concrete building in America was built in 1903. In recent years, reinforced concrete has had even greater acceptance and use with the introduction of prestressed frames, decorative panels, shell structures and new and better handling and erection facilities for precast elements. Still, with all the new methods and applications, concrete has had limited acceptance as a structural material for American agriculture.

The above is not to imply that concrete is not used in American agriculture. American agriculture is one of the largest users of portland cement concrete. The use is primarily for paved feedlots, floors and foundations for large structures, silos and underground tanks. While concrete is used for floors and foundations, the structures are usually prefabricated metal structures or pole frame structures.

Concrete has made some inroads in recent years in structures for agriculture with the introduction of tilt-up wall panels. Although the idea itself is not new, new tilting methods have been developed by agricultural engineers at Texas A. & M. University that have found favor with the farmer-builder. These men developed a tilting frame, made with common iron pipe, that allows the farmer to erect his own wall panels using the farm tractor, and avoiding the expense of heavy equipment. Gin pole trucks, available in most small communities in the Southwest, can also be used at minimal cost and allow a greater freedom in casting

and erecting as compared to the tractor and tilting-frame method that requires the panel to be cast where it is to be erected.

Small concrete plants and rural contractors have made a serious effort, and with much success, of marketing tilt-up buildings in much of the Midwest. The panels are usually cast in their own yard and trucked to the site, rather than being cast on the site on prepared beds or concrete floors. Most contractors have utilized the Texas A. & M. design or their own modifications. This particular tilt-up panel is designed primarily to resist tilting moments, rather than actual building loads. Therefore, most are oversized for the actual building loads, the exception being grain storage structures.

Concrete, as stated by Lambot, has many advantages when we consider the rigors to which a building for agriculture is subjected. Agriculture needs buildings that are fireproof, rodent proof, require little maintenance, and are impervious to the manure and urine encountered in livestock operations. Concrete can provide such structures. However, before concrete structures can receive wide acceptance in agriculture, they must be competitive in price and time of erection. To do so, they must incorporate maximum utilization of materials, minimize cost of fabrication, and reduce erection costs with lighter building elements and improved methods of erection.

One method of better utilization of material is suggested by Nervi (17) in his book, Structures. Nervi implies that concrete in close proximity to steel reinforcement exhibits higher strength properties than plain concrete. If such an effect does exist and can be obtained economically, there is a real possibility that a savings in precasting of structural elements, or a reduced weight and savings in transport of

precast elements and erection, can be obtained. The latter would be especially important in rural construction, where special lifting equipment is often unavailable.

The Problem

Proximity effects of reinforcement in thin concrete sections were investigated to determine if close spacing of reinforcement reduced deformation under load for uncracked and cracked specimens and increased ultimate strength. No specific applications were considered in the design of the experiment. However, if such improved properties could be obtained economically by using minimum spacing of reinforcement, many applications could be made in structures and facilities for agriculture.

A series of tests were conducted using small concrete panels with one way reinforcement. The panels were tested as simple beams and the results were evaluated to determine if close spacing of reinforcement had a significant effect on deformation and ultimate strength of thin concrete sections. Quantities pertinent to the problem were identified and a set of dimensionless parameters developed and tested. Evaluation of the results were made by the application of similitude and statistical analysis.

The Objectives

1. Obtain data suitable for determining if spacing effects have a significant effect on stiffness and ultimate strength of reinforced concrete.
2. Develop prediction equations that describe proximity effects of concrete reinforcement on the deformation and ultimate strength

of concrete panels subjected to flexure.

3. Compare prediction equations obtained with existing design procedures that have been developed for conventional reinforcement.

CHAPTER II

LITERATURE REVIEW

Applied research in reinforced concrete has usually been directed at specific application areas; bridges, building frames, special structures and etc. As most structures of reinforced concrete are rather massive, large diameter reinforcement and relatively low strength concrete are incorporated into the design. The large bars and wire reinforcement are used to minimize labor in alignment and placement of the reinforcing. Low strength concrete is low cost concrete, and adequate for most applications in commercial structures. Therefore, most studies use large bars and lower strength concrete in their investigations. Little information is available on the use of small wire reinforcement and high strength concrete to minimize dead load and erection costs where equipment for handling heavy sections or structural elements is limited.

Precast and prestressed concrete structural elements have to be designed for minimum dead loads, both to minimize the dead load of the structure they must support and to reduce hauling and erection costs. As such, fabricators have utilized higher strength concretes, high tensile strength wire, quality control and skilled personnel to obtain better utilization of materials of construction. One result of this interest in better utilization of materials is new interest in crack spacing and crack arrest and a more careful study of previous works.

One method of eliminating cracking of concrete in the tensile stress

regions of slabs or beams is through prestressing. This practice puts the concrete normally in tension under compressive stress by preloading, or prestressing the member with a reversed moment. This is accomplished by preloading the reinforcement, or prestressing it. Then, when normal design loads are applied, they tend to cancel out the prestressed load and the concrete that was previously under compressive stress now approaches zero stress. In the same manner, the concrete that was subjected to light tensile stresses now assumes compressive stress. However, prestressing requires costly facilities, trained technicians, and little effort has been made by prestress companies to enter the farm market. The latter may seem a bit ironic to many as the first application of prestressed construction in America was for agriculture, prestressed concrete fence posts.

Ferro-Cemento

P. L. Nervi of Italy developed a method of reinforced concrete construction similar to Lambot's, using very thin, highly reinforced sections. Nervi used conventional bar reinforcement to obtain the frame or shape desired for his structural member and then stacked several layers of wire mesh (plaster base) either side of the frame. He then forced high strength mortar between the wires from either side, troweling it in place with little cover over the outside layer of mesh. The mesh used was soft steel, 0.02 to 0.06 inches in diameter, with a mesh spacing of approximately 3/8ths of an inch. Since he had no theoretical explanation for the high strength properties of his ferro-cemento panels, Nervi used model analysis and test specimens extensively in his design.

These ferro-cemento structural sections had steel reinforcement

throughout all stress areas and showed all the mechanical characteristics of a homogeneous material. One concrete plank tested was only five-eighths of an inch thick, yet had twelve layers of mesh, 0.13 pounds per square foot per layer or 1.57 pounds per square foot, equivalent to about 30 pounds of steel reinforcement per cubic foot of concrete. Under test, visible cracks did not appear in the concrete until the steel was stressed to nearly its proportional limit, or yield point. In one experiment, Nervi dropped a 550 pound weight from a height of 10 feet on a five by five foot panel, one and three sixteenths of an inch thick. The panel did not fail but only yielded and cracked in the area of impact.

Nervi liked the freedom of form his ferro-cemento afforded. As such, he used it for structural members in graceful, free-form buildings, as reusable forms for floors, roof decks and beams, and for construction of commercial fishing boats and pleasure craft. The high impact resistance of the ferro-cemento hull, plus the fact that the fine cracks that did occur did not leak and tended to heal with time, made his material ideal for boat construction.

Boat construction using Nervi's method of reinforced concrete construction is currently receiving wide interest. Hurd⁽⁹⁾ refers to Australian and New Zealand interest in ferro-cemento for boats as well as refrigerated storage structures, storage tanks and water troughs for agriculture. This method of construction is economically feasible in craft of the thirty to fifty foot length category

Crack Arrest

Batson⁽²⁾ investigated the mechanics of crack arrest in concrete

with closely spaced wire reinforcement and based his theoretical approach to crack arrest on research in the field of fracture mechanics. He assumed that the extension of cracking can be limited or contained by closely spaced reinforcement. Microcracking, which starts at an internal flaw in the concrete, will propagate out from the initial area with no tendency for the concrete and the reinforcement to move relative to each other. The rods and the concrete are stretched equally. At the crack edges, however, the longitudinal extension due to the stress singularity is resisted by the stiffer rods. The distributed bond stress in the reinforcement acts as a series of finite pinching forces to prevent further propagation of the crack edge. In this manner, the crack will be contained by surrounding rods and will not propagate beyond the rods until the bond stress of the concrete is exceeded. Also, by placing reinforcement throughout the complete tensile area of the beam, cracks starting at the lower surface or near the lower surface of the beam will not propagate up to the neutral axis, as is the normal assumption for beams with reinforcement located in one plane.

Batson used both plain wire and wire mesh, 16, 20 and 34 standard wire gage, as well as standard reinforcement in his experiments. Vertical and horizontal wire spacings were 0.500, 0.333 and 0.167 in. respectively, for the above wire sizes. Wires were placed throughout the tensile section of the beams and a sand mortar, 2.5 parts sand to cement and a water-cement ratio of 0.45, was used to facilitate placing of the concrete with the closely spaced wire. The specimens tested were model beams, six and one half feet long. The beams were haunched with an eighteen inch long test section of constant cross section at midspan. The test section was three inches wide and five inches deep.

Results of Batson's investigations indicate a clear relationship between ultimate strength of beams and average spacing of reinforcing wire. However, this relationship was noted only for wire spacings of less than one half inch with a significant rise in ultimate strength occurring at wire spacings of about 0.3 in. to 0.4 in. An average increase in ultimate strength of fifty per cent over beams with wire spacings of 0.6 in. was noted for beams with 0.2 in. wire spacing.

In 1933, Westergaard⁽²³⁾ extended the Hertz theory of contact stresses to estimate the effects of cracks on concrete in the compression area of reinforced concrete beams in bending. He found that at crack locations, the compressive strains in the concrete above the crack, in the direction of the beam, are not proportional to the distance from the neutral axis. He also developed an equation for approximating the distance to the centroid of bond stresses on either side of a crack, based on measured crack width, for reinforcement stressed below its proportional limit. This distance, u , was used by Westergaard to determine the magnitude of elastic weights to compute deflection of beams due to cracks. This distance, u , is approximated as:

$$u = \frac{E_s A_s Z}{2T} \quad (1)$$

where;

u = distance from the crack to the center of gravity of the diagram of bond stresses

E_s = modulus of elasticity of steel, psi

A_s = area of steel, square inches

Z = crack width, inches

T = total tension in the steel at the crack

This revised picture of crack effects suggested to him the relative advantages of smaller sizes of reinforcement.

Rumaldi and Mandel⁽²⁰⁾ conducted studies on the performance of short wire reinforcement uniformly distributed and closely spaced in concrete in tension. This study was an extension of work by Rumaldi and Batson⁽¹⁹⁾. Mandel used varying amounts of short wires, two inches in length, distributed in the concrete in the mixer in the final states of mixing, for constructing his test beams. Sand mortar was used for the concrete. The beams tested were small in cross section, one and three fourths inches wide by three inches deep. Mandel determined the amount of reinforcement performing in actual tension by determining the orientation of random rods in infinite space and arrived at the conclusion that 41% of his reinforcement was effective. His ratio of steel reinforcement to concrete was varied from 2.1% to 4.3%, or an actual effective ratio, p , of 1% to 2.52%. For very close spacings, he obtained a theoretical increase in strength ratio to conventional reinforcement from 2.5 for the 0.2 inch spacing to 1.2 for the one inch spacing, with a rapid increase when the spacing was reduced to 0.5 inches or less.

One factor that was apparently missed by Mandel was the fact that his beam widths were less than the length of his wire specimens. This would result in a higher percentage of the wires having an effective orientation. Also, with such narrow, shallow beams, he had a pronounced edge effect in that all wires coming into contact with the bottom of the form would be re-oriented in a favorable position to give much more reinforcement in the direction of stress than the 1% to 2.52% computed. These wires reoriented by the forms would be located in the area of highest tensile stress. Therefore, he would have more reinforcement

where it was most needed.

Other Materials for Reinforcement

Hanes and Simons⁽⁸⁾ have developed a reinforced stucco using short fiberglass fibers mixed in the concrete. This is used as a stressed skin for concrete block in lieu of mortar joints for masonry construction. The mixing techniques are similar to those used by Mandel, introducing the reinforcement in the final stages of mixing. No durability tests have been conducted on the effective life of the fiberglass reinforcement.

Many problems have been encountered in attempts to use fiberglass as reinforcement in concrete. One limitation is the fact that the alkali in the concrete causes deterioration of the bonding agents used in the manufacture of fiberglass. Russian studies⁽²⁵⁾ showed deterioration of all strands tested unless coated with synthetic resins. With the use of synthetic resins, however, they found improved bond and no deterioration after 30 months.

Materials such as jute and polypropylene fibers have also been used for closely spaced reinforcement. Billig⁽⁴⁾ used jute sacking as a form and reinforcement for reinforced parabolic structures for low cost dwellings in India. He also used similar construction for his Patrick Huts, prefabricated barracks constructed in the early '40's in England. The prefabricated roof and wall haunched panels consisted of a steel reinforced edge beam with a thin, sacking reinforced curved section plastered between the edge beams.

Shell Chemical⁽²⁶⁾ conducted studies of the use of polypropylene fibers, or packaging twine, for non-load bearing panels. The purpose of

the reinforcement was to improve handling characteristics and reduce damage in handling precast units. Fibers were mixed in the concrete in the final stages of mixing, 0.2 to 0.1% by weight, and the panels tested in bending. Increases in tensile strength of 30% to 50% were recorded. The durability of this material is questionable but for short term handling applications, it is apparently effective.

CHAPTER III

REINFORCED CONCRETE THEORY

Two methods of reinforced concrete design are currently used; the Working Stress Design and the Ultimate Strength Design. The working stress design is applicable for determining stress and strain in reinforced concrete when the stresses are elastic. This limits its use to situations where steel stresses are less than the yield strength of the reinforcement and where concrete stresses are in the relatively linear portion of a stress-strain plot for a particular concrete, usually less than one half ultimate strength of the concrete. The working stress design method can be used for either uncracked or cracked section design. Until a reinforced concrete beam cracks, it will perform as a homogeneous member and the concrete will carry tensile stresses. The ultimate strength design method is used in determining the ultimate load carrying capacity of a reinforced concrete member and only considers a fully cracked section with stresses in the reinforcement and the concrete approaching failure conditions.

Straight Line Theory

Deflection of a cracked beam performing in the elastic range can best be estimated by using the transformed section analysis method. Stress and strain relationships are given in Figure 1.

The straight line theory for a cracked section assumes all concrete

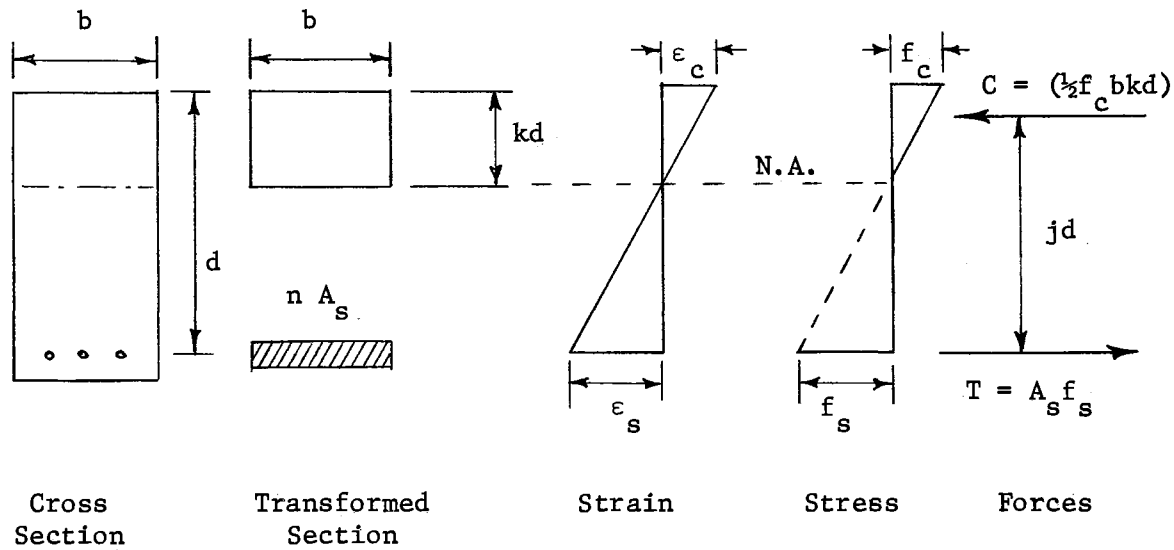


Figure 1. . Straight Line Theory

Stress and strain relationships in the above diagram are based on the following assumptions.

1. Strains have a linear variation.
2. Both steel and concrete have a constant E .
3. Concrete carries no tensile stresses.

taking tensile stress is cracked and therefore, effectively absent. The reinforced section then consists of the concrete in compression above the neutral axis and the steel in tension below the neutral axis. The area of steel reinforcement, A_s , is transformed to an equivalent area of concrete by multiplying A_s by n , the ratio of E_s to E_c . The neutral axis is then located and the moment of inertia and other properties of the transformed section computed. The transformed section analysis method is limited to materials performing in the elastic range.

The straight line theory assumes all concrete cracks due to tensile stresses in a beam will progress to the neutral axis. This is not true in that concrete can take tensile stress, as much as fifteen percent ultimate compressive strength for some concrete. However, the error in determining moment of inertia due to this assumption is small and, for cracked beams stressed within the working range, can be ignored for simplicity and convenience.

When stresses in the concrete or steel exceed the limits of elastic behavior, they are no longer linear as shown in Figure 1 and the neutral axis will move down or up, depending upon whether the concrete or the steel reinforcement is overstressed. If this occurs, the moment of inertia of the section will change and the straight line theory will no longer be applicable in determining the properties of the section.

Ultimate Strength Theory

The ultimate strength theory, suggested by Whitney⁽²⁴⁾, assumes that strain distribution remains linear in concrete stressed to the crushing strength but the stress distribution is not linear. This is based on the assumption that at loads near failure, the concrete at the compres-

sive face of the member has passed the proportional limit of the concrete. The stress-strain relationship for ultimate strength theory is given in Figure 2.

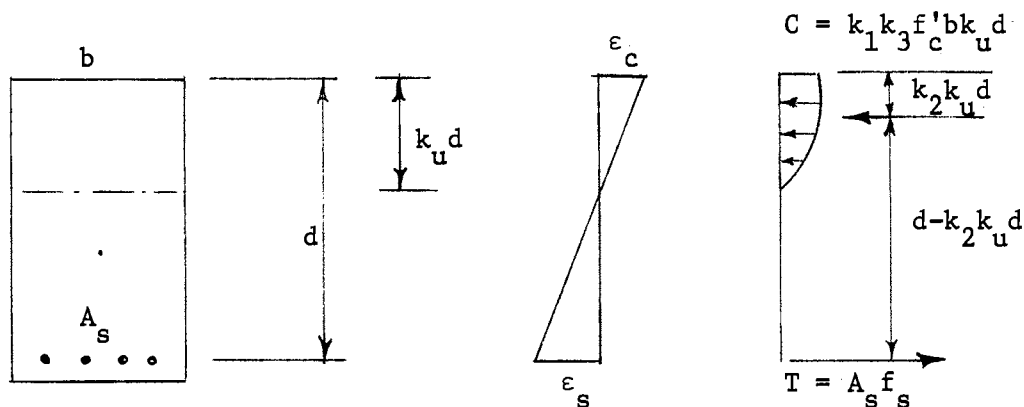


Figure 2. Ultimate Strength Theory

Stress and strain relationships in the above diagram are based on the following assumptions:

1. Strains are distributed linearly.
2. When concrete reaches limiting strain (0.003 to 0.004), it crushes.
3. No tension in the concrete.

where;

$k_1 k_3$ = ratio of average compressive concrete stress in beam at failure to f'_c .

k_3 = ratio of maximum concrete compressive stress in beam to compressive stress of standard cylinder.

k_1 = ratio of average compressive stress to maximum compressive stress.

$$= \frac{\text{area of stress block}}{\text{area of enclosing rectangle}} \leq 1$$

k_2 = 0.42 (general assumption)

The stress distribution in the concrete in compression would take a parabolic shape, as in Figure 2. The shape of the stress block would be similar to the stress-strain diagram for a test cylinder loaded in compression to failure. The stress-strain relationship would be linear for the initial loads, or for low stress, but stress would increase faster than strain once a strain of approximately 0.002 was exceeded. When the crushing strain was reached in the concrete, the stress would decrease as strain increased, resulting in maximum stress occurring at some depth below the compressive surface of the member. The centroid of the compressive force, C , would not be at a point two thirds above the neutral axis, as assumed in straight line theory, but would move down, the location being the centroid of the stress block.

One factor that will control the depth of the neutral axis and the location of the centroid of the compressive force for a reinforced concrete member that is not behaving elastically is the amount of reinforcement used. Balanced beam design assumes the concrete and steel are stressed proportionately, or the tensile reinforcement is stressed to the yield point when the concrete reaches the crushing strain in compression. If the beam is underreinforced, that is, there is less steel used in the fabrication than called for in balanced beam design, the steel will yield first and the beam will fail slowly with extensive cracking in the region of tensile stress. In overreinforced beams, the concrete will crush be-

fore the steel reinforcement yields. In such design, there may be little visible cracking in the concrete in the compressive region due to lack of ductility and the failure may be abrupt.

The location of the neutral axis in both underreinforced and overreinforced beams is not fixed. This is shown in Figures 3 and 4. In an underreinforced beam, the steel starts to yield first and cracks in the tensile region of the concrete which have formed prior to yielding start to progress up as the steel continues to yield and a greater moment arm is required to resist added moments resulting in the neutral axis moving up ahead of the crack. This increases the compressive stress in the concrete above the crack due to the reduced section in compression, or C equals $A_c f_c$. Since tensile force, T equal $A_s f_y$, equal compressive force, C , it could be assumed that steel stresses will be reduced because of the longer moment arm when the neutral axis moves up. However, tensile stress previously carried by the concrete must now be assumed by the reinforcement. As the load on the member continues to increase, cracking will continue to progress upward and the area of concrete in compression will continue to decrease until failure occurs. Failure can be a concrete failure, the crushing strain being reached in the compression area of concrete, or it can be a tensile failure of the reinforcement.

In an overreinforced beam, the concrete at the compressive surface of the beam crushes before the steel yields. Once the point is passed in which the concrete stress cannot be considered proportional to the concrete strain, the neutral axis must move downward and the area of concrete under compression increase to maintain equilibrium of compressive and tensile forces. If additional loads are imposed on the member,

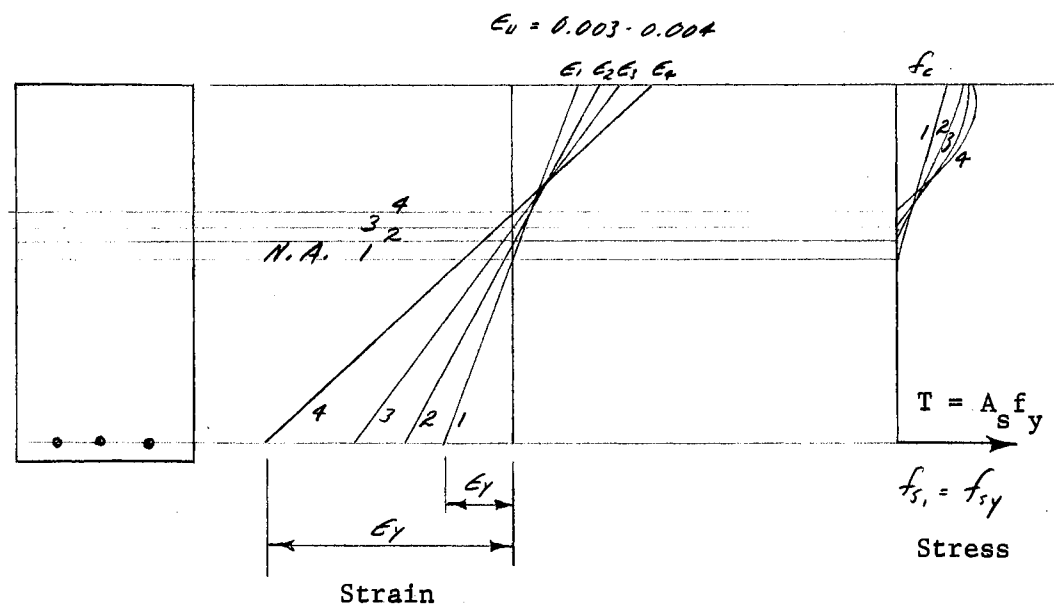


Figure 3. Failure Mode of Under-Reinforced Beam

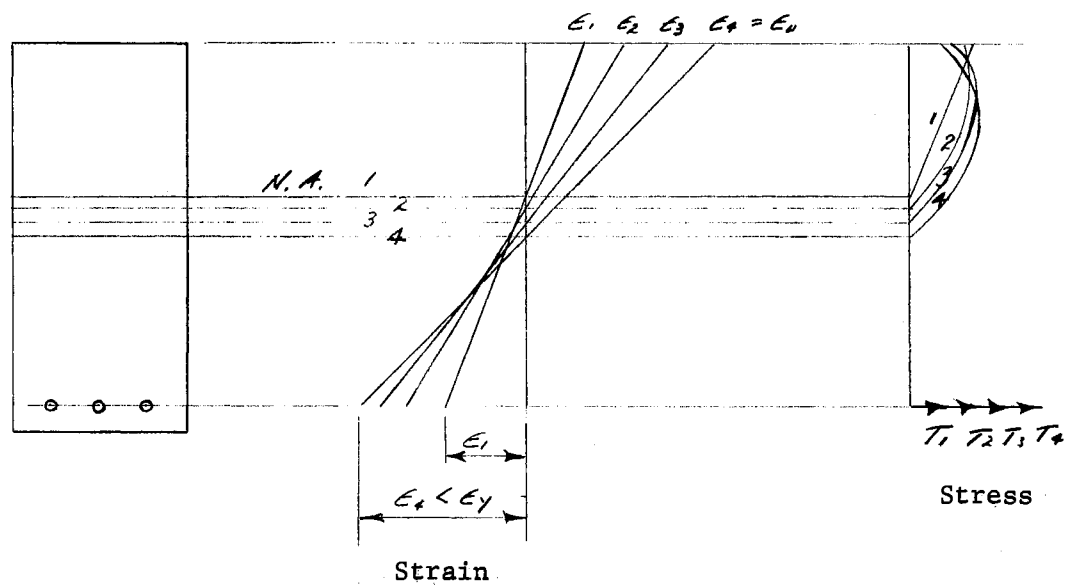


Figure 4. Failure Mode of Over-Reinforced Beam

crushing strain of 0.003 of the concrete in the compressive section of the member may occur and abrupt failure will result.

The reinforcement ratio, p , will vary for balanced design and is not a constant. The physical properties used to compute balanced reinforcement ratio, p_b , are the ultimate strength of the concrete and the yield stress and shape of the stress-strain curve, or E_s , of the reinforcement. Therefore, for a high strength concrete, the value of p_b may be more than double that of a balanced design using concrete with a lower ultimate strength.

This review of reinforced concrete design was included to explain why limitations must be considered when computing deflection using the transformed section moment of inertia. Once maximum strain in tension in the concrete has been exceeded and the member has cracked, transformed section analysis can only be used if both stress and strain retain a linear relationship. After cracking, either elastic or inelastic behavior may occur. The limits in which this linear relationship will occur for a particular beam can only be computed after the stress-strain relationship of both the concrete and the reinforcement used have been determined. If too little reinforcement is used, abrupt failure may occur at initial cracking.

CHAPTER IV

THEORETICAL ANALYSIS

The purpose of this study was to determine if spacing of reinforcement, or proximity effects of reinforcement, has a measurable influence on the performance of reinforced concrete panels with one-way reinforcement. The two performance characteristics by which spacing effects in reinforced concrete panels were evaluated were deflection and ultimate load carrying capacity. The effects of reinforcement spacing on deflection were investigated for both uncracked panels subjected to stresses below the modulus of rupture for concrete in flexure and cracked panels subjected to stresses below the crushing stresses for reinforced concrete subjected to flexure.

If the spacing of reinforcement varied in several beams, the area of reinforcement and all other physical properties of the beam being held constant, the beam should deflect the same amount for the same load and loading conditions. If they did not and deflections were reduced, or increased, it could be assumed that the spacing of the reinforcement had some effect on the physical properties of the beam or the concrete in the beam. Such deviation could then be attributed to spacing effects.

Elastic deflection of uncracked reinforced concrete members can be readily computed using standard deflection equations, the equations used being selected for the type load and load locations. Deflection for a homogeneous member subjected to a given bending stress is inversely

proportional to the stiffness of the member, or the moment of inertia of the member times the modulus of elasticity of the material.

Reinforced concrete is not a homogeneous material. However, it can be treated as such for determining the moment of inertia and deflections by the use of transformed section theory. In determining the moment of inertia by the use of the transformed section, the modulus of elasticity of all materials are reduced to one value and the area of the materials are increased or decreased proportionately. In reinforced concrete, the modulus of elasticity of the reinforcement is usually reduced to the modulus of elasticity of the concrete and the area of the steel is increased n times, where n is the ratio of the modulus of elasticity of steel to the concrete used. The moment of inertia of the section can then be computed and the member treated as a homogeneous beam for computing deflections for any loading conditions within the elastic range.

For this study only a single value of deflection was required to determine stiffness in the member. Therefore, midspan deflection, or deflection at the center of the span, was selected as a measurement of stiffness for convenience and precision of measurement.

If the concrete stress in the tensile region of a reinforced concrete member subjected to flexure exceeds the modulus of rupture, a crack will form which will reduce the moment of inertia of the member in the region of the crack. Variations in the moment of inertia throughout the span will make the calculation of deflection at the center of the span section more difficult and less exact. The deflection at a given point will not only be a function of the moment of inertia at the crack, but will also be a function of crack location. The deflection

will be a function of the angle change at the crack times the length of the member influenced by the crack, plus the deflection due to normal bending in the uncracked section.

The moment of inertia of the member at the crack can still be determined by the transformed section method. The moment of inertia now only includes the concrete above the neutral axis and the transformed area of the steel. Tensile stresses previously carried by the concrete have now been transferred to the reinforcement. The neutral axis has also moved up, toward the compression surface of the member in the region of the crack. This change of location of the neutral axis is not abrupt but a transition from the uncracked section to the fully cracked section, as shown in Figure 5.

The reduced section at the crack results in a much smaller value of EI in the region of the crack and greater deflection of the member since deflection is inversely proportional to the stiffness, or EI . Westergaard⁽²³⁾, using the theory of elastic weights, determined that increases in deflection due to a single crack in a deep reinforced beam could result in deflections one hundred per cent or more greater than deflections in an uncracked beam for the same loading conditions. In thin section concrete, because the reinforcement is restricted to a location at or near the center of the section, to provide cover for the reinforcement, the change in moment of inertia from an uncracked to a cracked section would be proportionately larger. Deflections resulting from these cracks would increase proportionately.

Transformed sections for the uncracked and cracked sections of a reinforced concrete member are shown in Figure 6. This change in moment of inertia from an uncracked to a cracked section is not an abrupt

change at some point along a beam but changes gradually in the region of the crack. This is shown by the change in location of the neutral axis, assumed as shown in Figure 5. This region is shown in Figure 7 as a loss of tensile stress in the concrete region. Concrete in the uncracked section of the beam is taking tensile stress. It is assumed that no concrete below the neutral axis at the crack is subjected to tensile stress other than tensile stress due to bend and tensile stress in concrete above the crack is negligible and can be ignored. Therefore, the shaded area includes all the concrete that is contributing in bond stress only. The shaded area shown is an assumed shape that would be dictated by the change in location of the neutral axis and the stress in the reinforcement.

One wire size was used for all test specimens to eliminate variations in reinforcement and to minimize bond stress effects in the evaluation of panel performance. Ultimate strength theory assumes bond is a function of load, depth of reinforcement, wire surface area and concrete strengths. By using a single size wire, variations in bond stress for a given tensile stress per unit area of wire would be eliminated as wire surface area would be constant. In using a single size wire, the percentage of steel varied directly with the number of wires per panel and inversely with the depth of panel. Since the area of the reinforcement to the effective area of concrete was not a constant for all panels, measured panel deflections were compared directly with calculated deflections of panels which were based on the physical properties of the panel.

Measured deflections were made at the center of the span to give maximum deflection and precision of measurement as well as convenience

in measurement. Computed deflections were determined by the conjugate beam method. The derivation of the equation used to determine the computed deflection, Δ_c , is given in Appendix B under "Conjugate Beam Theory." The equation used to determine deflection at midspan for a total load, P, applied at the third points of a simply supported member and live load only is:

$$\Delta_c = \frac{23 PL^3}{1296 EI} + \frac{PL \ell}{6E} \left(\frac{1}{I_c} - \frac{1}{I} \right) \frac{\Sigma x}{2} \quad (2)$$

where;

- I_c = moment of inertia for the cracked section
- I = moment of inertia for the uncracked section
- ℓ = median length of tensile stress loss
- x = distance from crack to nearest end support
- L = length of the beam
- E = modulus of elasticity of the concrete

Equation 2 gives the deflection at the center of the span for any number of cracks assuming they are all spaced at least a minimum distance, ℓ , apart. The total distance, Σx , is the sum of the distances of all cracks from the end supports of the beam, or the nearest support to the crack. A crack at the center of the member would be considered as a single crack and the distance x would be equal to $L/2$. The length ℓ in the equation is critical as the magnitude of the conjugate weight is the product of this length times the height of the M/EI diagram at the crack.

Westergaard⁽²³⁾ used the length u , the distance from a crack to the centroid of bond stresses on either side of a crack, to determine the

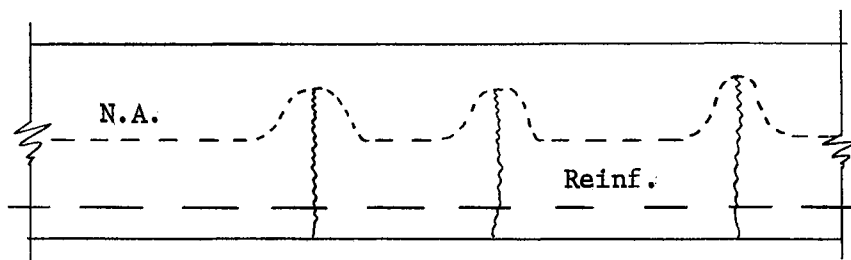
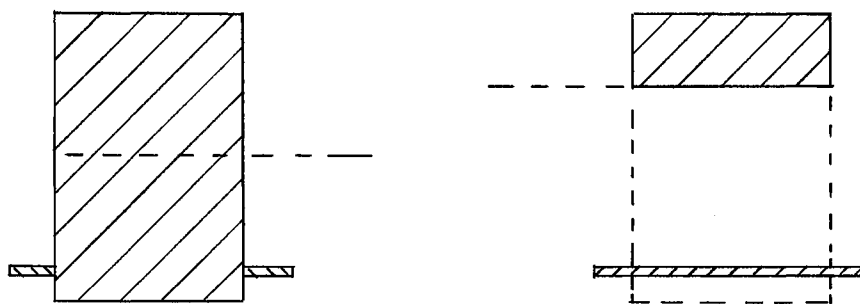


Figure 5. Location of Neutral Axis in a Cracked, Reinforced Concrete Beam



Transformed Section,
uncracked beam.

Transformed Section
at crack.

Figure 6. Transformed Sections of Concrete Beam

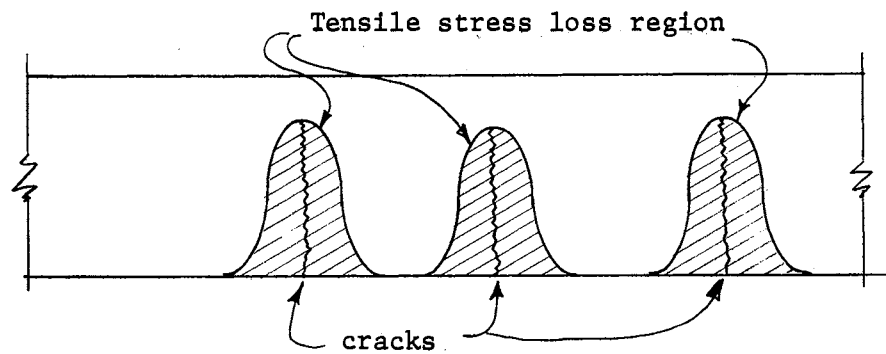


Figure 7. Loss of Tensile Stress in Concrete Either Side of Crack in Beam Subjected to Flexural Stress

magnitude of elastic weights in computing beam deflection due to a crack (Eq. 1). He assumed this distance to be a function of crack width, the modulus of elasticity of the steel, and the steel stress in the region of the crack. Equipment to determine crack width was not available for this experiment. Therefore, the magnitude of the length, ℓ , for computing deflections of the test panels, was determined experimentally from load-deflection measurements taken for the standard test panels. Measured deflections for four load intensities were compared with computed deflections using Equation 2 and trial values of ℓ of two and one half to four inches. Results of these tests showed that a length of three inches for ℓ gave an average ratio of approximately 1.0 for computed versus measured deflections. This length was therefore

used for all computations of panel deflections. Deflection data used was limited to data obtained for loads that produced computed reinforcement stresses of 55,000 to 70,000 psi.

The shape of the conjugate weights was assumed to be rectangular for convenience of computations. Since the conjugate moment resulting from the conjugate weight is determined by the distance from the free end of the member to the centroid of the weight, any shape could be assumed as long as the area of the conjugate weight remained constant and the centroid was located at the crack.

Ultimate loads for the reinforced panels were also compared directly with computed ultimate loads to determine if spacing effects or reinforcement had a significant effect on the ultimate loads of the panels. If measured ultimate loads for panels with various spacing of reinforcement deviated consistently from computed ultimate loads, it could be assumed that proximity effects had some effect on ultimate strength of reinforced concrete panels and a prediction equation could be developed to compute ultimate moment as a function of reinforcement spacing.

The computed ultimate load at failure, P_c , was determined from Equation 16-1 of the ACI Standard Building Code, 318-63, which gives the ultimate design resisting moment for rectangular beams with tension reinforcement only as:

$$M_u = \phi (bd^2 f'_c q (1.0 - 0.58q))$$

where;

$$q = p f_y / f'_c$$

$$\phi = \text{a capacity reduction factor } (\phi = 1.0 \text{ for determining } p_c)$$

$$bd^2 = \text{effective area of concrete}$$

f'_c = compressive strength of the concrete

p = area of reinforcement/ bd^2

f_y = yield strength of the reinforcement

The above ultimate moment is based on failure when the yield point of the reinforcement is reached or exceeded. It is applicable only to reinforced concrete members that are underreinforced. Measured ultimate loads for this study, P_u , were maximum loads prior to complete failure of the reinforced panels. Therefore, the computed ultimate load, P_c , should be less than measured ultimate load, P_u , for these tests. Since all reinforced panels in this test were designed as underreinforced members, use of P_c , obtained from Equation 16-1, for comparative purposes was acceptable.

CHAPTER V

DESIGN OF THE EXPERIMENT

The principles of engineering similitude and dimensional analysis were utilized in the design of the test procedures to reduce the number of variables to be investigated.

An ideal study of proximity effects of reinforcement would include many specific variables. If all were included as variables to be investigated in the experiment, with two or more values of each variable and a minimum of three replications of each test specimen, the number of individual specimens, and the number of individual tests, would be prohibitive. Therefore, the number of variables had to be reduced in scope yet still retain meaning and meet the objectives of the experiment.

Similitude and the Buckingham Pi Theorem

Similitude, which Murphy⁽¹⁶⁾ states includes both similarity and dimensional analysis, allows mathematical analysis to be simplified by the use of the Buckingham Pi Theorem. The Buckingham Pi Theorem significantly reduces the number of required experiments by reducing the parameters to dimensionless terms. As such, it provides a method of formation of general equations from component equations and the development of a prediction equation for the performance of one dimensionless parameter as a function of the other parameters of the system. The general equation form of the theorem is written:

$$f(\pi_1, \pi_2, \dots, \pi_n) = 0$$

where

f = an arbitrary function

π_n = any dimensionless group

The only restriction imposed on dimensionless groups is that they be independent. The number of dimensionless groups required to define a physical phenomenon is, according to Murphy, equal to the number of pertinent quantities required to adequately define the physical system minus the number of dimensions or basic quantities such as force, time, length, etc. A second method of describing the number of dimensionless groups required, as defined by Skoglund⁽²¹⁾, is equal to the number of physical quantities required to adequately define the system minus the rank of the dimensional matrix. This definition is the same as the simplified version given by Murphy but has one added advantage. If the length dimension can be considered as three dimensions, or length, width and height, additional reduction in the number of dimensional groups may be possible due to an increased rank of the dimensional matrix. This "addition" to Buckingham's theorem is known as Huntley's Addition.

Definition of the System

The physical system shown in Figure 8 represents a thin plate section loaded at the third points. The pertinent quantities for evaluation of the load-deflection behavior of this physical system are listed in Table I. The principles of similitude were utilized in the selection of the system dimensions and in the design of the series of tests. Dependent variables in the system are strain, deflection and

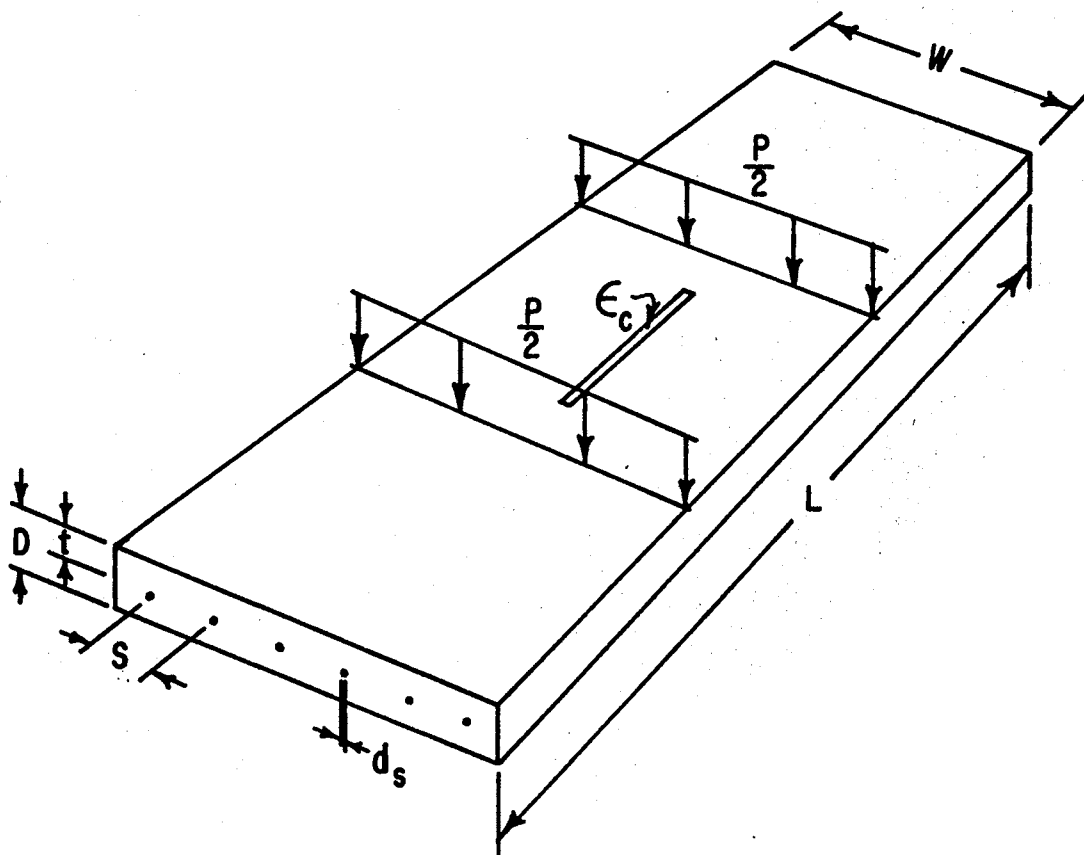


Figure 8. Pertinent Dimensions, Test Panel.

TABLE I
LIST OF PERTINENT QUANTITIES

No.	Symbol	Description	Dimensional Symbol
1	e	Strain	-----
2	Δ	Deflection at midspan of panel, inches	L_y
3	L	Length of panel, inches	L_x
4	D	Depth of panel, inches	L_y
5	d_s	Diameter of wire reinforcement, inches	L_z
6	t	Depth of reinforcement, inches	L_y
7	P	Load on panel, pounds	F
8	E_c	Modulus of Elasticity, concrete, psi	$F/L_y L_z$
9	E_s	Modulus of Elasticity, steel, psi	$F/L_y L_z$
10	S	Wire spacing, reinforcement, inches	L_z
11	K	Stiffness factor, EI	FL_y
12	d_a	Diameter of max. size aggregate, inches	L_z
13	w	Width of panel, inches	L_z
14	Δ_c	Computed deflection at midspan for cracked panel, inches	L_y
15	P_c	Computed ultimate load	F
16	P_u	Ultimate load	F

ultimate load.

Selection of pi terms is accomplished by forming the dependent pi terms using the pertinent dimensions to be investigated. The remaining dimensional terms are used for forming the independent pi term for analysis of the dependent pi terms.

Table I lists a total of sixteen pertinent quantities needed to describe the system for the three series of tests conducted. The three series are; tests of uncracked panels performing in the elastic limits of the concrete, tests of cracked panels performing in the elastic limits of the concrete and reinforcement, and ultimate strength tests conducted in the inelastic range of the reinforcement and the concrete. The first thirteen pertinent quantities listed were needed to describe the system for the uncracked panel tests. Number fourteen, the computed deflection for cracked panels, was needed for the tests of cracked section concrete. The last two quantities, ultimate load and computed ultimate load, were needed only in the test for ultimate load as a function of the independent pi terms.

A maximum of thirteen pertinent quantities were needed to describe the physical system for both uncracked and cracked panel tests. Using Huntley's addition in considering length, width and depth as separate dimensions, the rank of the dimensional matrix was found to be four. Therefore, a total of thirteen minus four, or nine pi terms, was the absolute minimum needed to be formed to describe the system. Ten dimensionless parameters were used for the uncracked panel tests.

Dimensionless Parameters, Uncracked Panels

$$\begin{array}{ll}
 \pi_1 = e & \pi_8 = D/t \\
 \pi_2 = \Delta/L & \pi_9 = S/d_s \\
 \pi_3 = PL^2/EI = PL^2/K & \pi_{10} = D/d_s \\
 \pi_6 = E_s/E_c = n & \pi_{11} = d_a/d_s \\
 \pi_7 = L/D & \pi_{12} = w/d_s
 \end{array}$$

The dimensionless parameters needed to investigate cracked panels included the combined deflection and load-stiffness pi terms to give a direct comparison of measured versus computed deflection. They were:

Dimensionless Parameters, Cracked Panels

$$\begin{array}{ll}
 \pi_1 = e & \pi_9 = S/d_s \\
 \pi_4 = \Delta/\Delta_c & \pi_{10} = D/d_s \\
 \pi_6 = E_s/E_c = n & \pi_{11} = d_a/d_s \\
 \pi_7 = L/D & \pi_{12} = w/d_s \\
 \pi_8 = D/t &
 \end{array}$$

Dimensionless parameters needed to investigate the ultimate moment as a function of the independent pi terms do not include the deflection and strain but do include a direct comparison of measured and computed ultimate load. Therefore, only eight pi terms were needed. They were

Dimensionless Parameters, Ultimate Loads

$$\begin{array}{ll} \pi_5 = P_u/P_c & \pi_9 = S/d_s \\ \pi_6 = E_s/E_c = n & \pi_{10} = D/d_s \\ \pi_7 = L/D & \pi_{11} = d_a/d_s \\ \pi_8 = D/t & \pi_{12} = w/d_s \end{array}$$

Discussion of Pi Terms, Uncracked Panels

$\pi_1 = \epsilon$ describes the strain at the surface of the panel at mid-point of the span, the region of constant moment for a member loaded at the third points. For the conditions selected, strain was considered over the center third of the panel. Strain is a dimensionless term and is a dependent pi term as used.

$\pi_2 = \Delta/L$ is the dependent parameter that describes deflection, or deflection versus the length of the panel. All deflection measurements were made at the midspan of the panel. This pi term was used in determining the stiffness performance of uncracked panels.

$\pi_3 = PL^2/K$ is the pi term that describes the stiffness of various sizes of panel for variations of load and length of panel. This independent pi term was used in determining the performance of uncracked panels. Four values were used.

$\pi_6 = E_s/E_c = n$ is the relationship of the modulus of elasticity of steel and the modulus of elasticity of concrete. This relationship was considered a constant for this experiment since the values of E_c varied only slightly and all computations compensated for these variations.

$\pi_7 = L/D$ is the ratio of the length of test panel to the depth of the panel. This was a constant value for all panels.

$\pi_8 = D/t$ is the ratio of depth, or thickness of the panel, and the depth of the reinforcement. This was a constant, with all wire located at one half the depth of the panel.

$\pi_9 = S/d_s$ is the independent parameter that describes the spacing effects of reinforcement as a function of reinforcement diameter. All reinforcement was in one plane and one size wire was used. Five spacings of reinforcement were investigated.

$\pi_{10} = D/d_s$ is the independent parameter describing the effects of depth of panel as a function of reinforcement diameter. Five depths, and five values of the pi term, were investigated.

$\pi_{11} = d_a/d_s$ is the independent parameter describing the maximum size aggregate as a function of wire diameter. This was a constant for this study.

$\pi_{12} = w/d_s$ is the independent pi term describing the width of panel as a function of wire diameter. One width of panel was used so this was a constant for this study.

Table II gives the three pi terms varied for the uncracked panel tests. Four values of π_3 were used and five values of π_9 and π_{10} were used. The specific values of each pi term are given in the table. Only one pi term was varied for each test. All other pi terms were held constant. The values of π_6 through π_{12} were held constant for all tests. These values are not included in the formation of pi terms. However, any pi terms developed from the tests would be restricted to the conditions of these tests, or to the conditions described by all pi terms. Prediction equations for uncracked panels were;

$$\pi_1 = e = f(\pi_3, \pi_9, \pi_{10}) = f(PL^2/K, S/d_s, D/d_s)$$

$$\pi_2 = \Delta/L = f(\pi_3, \pi_9, \pi_{10}) = f(PL^2/K, S/d_s, D/d_s)$$

Discussion of Pi Terms, Cracked Panels

$\pi_4 = \Delta/\Delta_c$ is the dependent pi term that describes the measured deflection versus the computed deflection for cracked panels. Due to the restrictions imposed on the experimental design by the use of a single size wire for reinforcement, the deflection pi term, Δ/L , and the load-stiffness pi term, PL^2/K , were combined to give a direct comparison of measured and computed deflection as a function of the spacing and depth pi terms. Determination of the computed deflection was based on crack location, panel length, and the EI_c for individual panels at specific loads.

Table III gives the two pi terms varied for the cracked panel tests. Five values of each were used. The tests were conducted on panels with constant thickness and five spacings of wire and panels with constant wire spacing and five thicknesses. The values of π_6 through π_{12} were held constant for all tests. The prediction equations for cracked panels were:

$$\pi_4 = f(\pi_9, \pi_{10}) = f(S/d_s, D/d_s)$$

Discussion of Pi Terms, Ultimate Loads

$\pi_5 = P_u/P_c$ is the dependent pi term that describes the measured failure load versus the computed ultimate load for the individual panels used in the test. The single size wire used for all spacings and depths restricted the development of pi terms to direct comparisons. All fail-

TABLE II
 PI TERM VALUES REQUIRED IN UNCRACKED CONCRETE PANELS
 FOR PREDICTING DEFLECTION PI TERMS

Test	$\pi_3 = \frac{PL^2}{K}$	$\pi_9 = \frac{S}{d_s}$	$\pi_{10} = \frac{D}{d_s}$
	$(\pi_3)_1 = 0.014$		
	$(\pi_3)_2 = 0.021$		
A	$(\pi_3)_3 = 0.028$	$\bar{\pi}_9 = 10$	$\bar{\pi}_{10} = 10$
	$(\pi_3)_4 = 0.035$		
		$(\pi_9)_1 = 5$	
		$(\pi_9)_2 = 7.5$	
B	$\bar{\pi}_3 = 0.021$	$(\pi_9)_3 = 10$	$\bar{\pi}_{10} = 10$
		$(\pi_9)_4 = 15$	
		$(\pi_9)_5 = 20$	
			$(\pi_{10})_1 = 5$
			$(\pi_{10})_2 = 7.5$
C	$\bar{\pi}_3 = 0.021$	$\bar{\pi}_9 = 10$	$(\pi_{10})_3 = 10$
			$(\pi_{10})_4 = 15$
			$(\pi_{10})_5 = 20$

ure loads were measured at complete collapse of the panel, or destruction loads.

Table III gives the two pi terms varied for the ultimate load tests. Five values of each were used. Values of π_6 through π_{12} were held constant for all tests. The prediction equation for ultimate loads was:

$$\pi_5 = f(\pi_9, \pi_{10}) = f(S/d_s, D/d_s)$$

TABLE III
 PI TERM VALUES REQUIRED IN CRACKED CONCRETE PANELS FOR
 PREDICTING DEFLECTION AND ULTIMATE MOMENT PI TERMS

Test	$\pi_9 = S/d_s$	$\pi_{10} = D/d_s$
A	$(\pi_9)_1 = 5$	
	$(\pi_9)_2 = 7.5$	
	$(\pi_9)_3 = 10$	$\bar{\pi}_{10} = 10$
	$(\pi_9)_4 = 15$	
	$(\pi_9)_5 = 20$	
B	$\bar{\pi}_9 = 10$	$(\pi_{10})_1 = 5$
		$(\pi_{10})_2 = 7.5$
		$(\pi_{10})_3 = 10$
		$(\pi_{10})_4 = 15$
		$(\pi_{10})_5 = 20$

CHAPTER VI

DESIGN OF TEST SPECIMENS

The specimens tested were considered to represent small segments of full scale structural elements and not models. Therefore, coarse aggregate concrete was used to fabricate the specimens. In a model tests, mortar made with sand and cement is often substituted as a model concrete. However, Kaplan⁽¹⁰⁾ found that mortar and coarse aggregate concrete vary greatly in many ways. His flexure tests showed that initial cracking in concrete with fifty percent coarse aggregate occurred at about half the tensile strain of concrete with no coarse aggregate in the mix, and that the relation of strain at cracking versus coarse aggregate content was linear. The strain-percent coarse aggregate relationship at ninety five percent ultimate load was not linear but strain increased more rapidly as the percent of coarse aggregate by volume was decreased. He also compared load-strain ratios for plain concrete in flexure using gravel as aggregate, crushed limestone as aggregate, and sand only with no coarse aggregate, all at a water cement ratio of 0.6. While the mortar specimens carried the highest ultimate stress, 9,720 lb as compared to 8,520 lb for the limestone concrete and 6,850 lb for the gravel aggregate concrete, the strain per unit load below the proportional limit was 25 percent lower for the limestone and 12 percent lower for the gravel aggregate as compared to the mortar mix.

Geometric size effects in modeling scale models of reinforced con-

crete beams were investigated by Little and Paparoni⁽¹²⁾, using scale models of models, with scales of 1:1.5 to 1:4. They tested one hundred thirty two model beams using five geometric scale ratios and two reinforcement ratios. They found significant increases in relative strength for the smallest specimens. They also found significant increases in ultimate strength for small wire reinforcement, #18 and #24 wires, as compared to conventional bar reinforcement of 3/8 and 1 in. diameter.

A standard size reinforcing wire and a coarse aggregate concrete mix were used to fabricate the reinforced concrete panels to avoid discrepancies that might occur in model tests. Also, the physical properties of the panel sections tested were designed to meet proposed minimum standards for thin section precast concrete construction as proposed by ACI Committee 324⁽¹⁾. The proposed recommendations are:

- 1) Minimum ultimate strength of 5,000 psi for unprotected concrete.
- 2) Limits on air entrainment.
- 3) Accurate reinforcement placement with minimum spacing of one and one half times maximum aggregate size.
- 4) Minimum concrete cover of 3/8 in. for reinforcement on slabs.

One objective of any thin section concrete would be to minimize weight in precast sections, reducing transport and erection costs and building dead loads. High strength concrete is recommended as it not only provides higher flexural strength but can reduce creep, provide high bond strength, superior durability, and increased resistance to water penetration and corrosion of the reinforcement. High strength concrete also allows for earlier handling of precast elements and an earlier reuse of the casting beds or forms.

Entrained air gives increased durability and workability to the

mix. However, ultimate strength of the concrete decreases linearly with increased amounts of entrained or entrapped air. This strength loss can be offset by the use of a reduced water-cement ratio since the entrained air gives a more workable mix. The amount of air entrained and the water-cement ratio used would be dependent upon the use of the prefabricated elements and the equipment and casting procedures of the fabricator.

Minimum spacing of reinforcement is dependent upon aggregate size and the method of concrete application. Minimum spacing should provide sufficient space between wires to assure easy passage of the aggregate and assure a good coverage and surround of the reinforcement.

The size of the reinforcement used was selected as a basic dimension of this experiment. The size wire used, No. 10, is a common size readily available from local suppliers. Wire diameter is 0.135 in., the cross section area is 0.0143 square in., and as welded wire mesh, it is available in many mesh spacings. Cold drawn steel has a minimum ultimate strength of 80,000 psi, a yield strength of 70,000 psi (ASTM Designation A82-66) and exhibits a relatively straight stress-strain relationship to yield point.

Commercially available wire spacings for welded wire mesh could not be utilized as they would limit the spacings available for the experiment. Therefore, straight wire was selected for the experimental panel reinforcement and a basic spacing of ten wire diameters, 1.35 in., was established. Four more spacings were selected to provide the five values of the spacing p_i term, S/d_g . These were; 0.675 in., 1.012 in., 2.025 in., and 2.70 in., or 1/2, 3/4, 1.5 and 2 times the basic spacing of 1.35 in. Total reinforcement, or the ratio of reinforcement to con-

crete, varied directly as the number of wires for a given depth.

The use of a single size wire eliminated the need for matching wire reinforcement physical properties. When more than one size wire is used, modulus of elasticity can vary slightly and yield point and ultimate strength can vary as much as twenty percent. The use of several sizes of wire can also cause wide variations in bond stress at the interface of the wire and the concrete for equal tensile stress in the wire, due to the greater surface area per square inch cross section of wire for smaller sizes. All wire used for reinforcement came from the same roll, minimizing variations in size as well as other physical properties.

Depth of the standard panel was also selected as 10 wire diameters, or 1.35 in. Four other depths, to give a total of five values to the depth ρ term, D/d_s , were selected. Depths were; 0.675 in., 1.012 in., 2.025 in. and 2.70 in. Values of the reinforcement ratio varied inversely with the depth of reinforcement, the amount of reinforcement being constant.

Location of the reinforcement was at mid depth of the panel. This location was dictated by the depth of the minimum panel thickness, 0.675 in., and the minimum recommended cover.

The width of panels was restricted in obtaining an equal distribution of wires based on some multiple of spacing, and to assure adequate space between minimum spaced wires for the concrete aggregate used. The panel width selected was 8.1 in., or 60 wire diameters. This provided for a maximum of 12 wires at a minimum spacing of 0.675 in., 8 wires at 1.0125 in. spacing, 6 wires at 1.35 in. spacing, 4 wires at 2.025 in. spacing, and 3 wires at 2.70 in. spacing. Side cover for all panels was

one half the spacing between wires.

The length of the panels was arbitrarily selected for desired moments and to assure adequate length for test equipment and strain measurement. The length of the panels with $D = 1.35$ in. was selected as 24 in., or approximately 180 wire diameters. Lengths of the other four depths of panels were proportionally reduced or increased to maintain the same L/D ratio, resulting in panel lengths of 12, 18, 24, 36 and 48 in. This was the length of the test span of the panel and not actual length. Actual lengths of the panels were approximately two in. longer than the test length, to provide a bearing at the ends and subsequent shortening of the panel at excessive deflection and failure.

A crushed limestone aggregate mix was selected to give higher values of E_c , a linear stress-strain relationship over much of the testing range, and a higher ultimate flexural strength than other coarse aggregates. A water-cement ratio of 0.45 by weight was selected for the concrete mix. Cement to aggregate mixture selected was 1:2.5:2.2 by weight. Cement used was Type I portland cement. All materials were purchased locally.

Preliminary Tests

Two preliminary tests were conducted to determine if the proposed panels would meet the requirements of the experiment and to determine testing procedures. A complete discussion of these tests is included in Appendix A.

Bond tests were conducted to determine if the No. 10 wire developed sufficient bond in the shear region of the panels to prevent pullout of the wire reinforcement at tensile stresses below the proportional limit

of the wire. The embedment length used was the bond length on the smallest specimens, the length from the load application to the end of the panel. The smallest panels were 12 in. in length for the test section with an extra inch of length to assure adequate end support. For loads at the third points of the panel, this provided a total bond length of five in.

Pullout specimens of 3, 4, and 5 in. bond length were tested. All specimens developed tensile stresses in the wire approximately equal to the yield point stress before the wires pulled out or failed. Specimens with 5 in. embedment length all failed at wire stresses in excess of yield point. Two of the four specimens tested failed when the wire fractured. First free end slip in three of the specimens occurred near yield point stresses and one specimen did not exhibit any slip prior to failure.

The findings of the preliminary test showed that a five inch wire embedment length was adequate for the No. 10 wire used for reinforcement. No special anchorage was needed to prevent pullout of the reinforcement. A complete discussion of the test is included in Appendix A.

Another preliminary test was conducted to determine if the modulus of elasticity of the concrete was the same for both the finished surface and form surface of the panel. Previous work by Mensch⁽¹⁵⁾, with pneumatic applied concrete, indicated that the modulus of elasticity varied between the two sides of a panel. If such a condition did exist, it would have to be considered in the design of the experiment, in the analysis of the data, and would determine if the form side or the finished side of the panels would be loaded in compression.

Twelve panels were cast and tested to determine if the deflection

and ultimate load carrying capacity of the panels varied, dependent upon the side of the panel loaded in compression. Six of the panels were reinforced with No. 10 wire, six wires per panel, and six had no reinforcement. The size of the panels was the same as the standard panel for the proposed tests; 1.35 in. thick, 8.1 in. wide, 24 in. long and with six wires spaced at 1.35 in. for the reinforced panels. Two castings were required to fabricate all twelve panels so three panels each, reinforced and nonreinforced, were cast each time. The panels were then randomly selected as to which side would be tested in compression, or three of each the reinforced and unreinforced for form side in compression, three each for the finished or troweled side in compression.

All panels were loaded at third points and deflection and strain was recorded for each load increment. The panels were loaded to failure and the data tested for statistical significance. Both deflection tests and ultimate loads were not found to be significant at the 0.95 confidence level. Therefore, it was assumed that the side loaded would not be a factor in testing procedures. A complete discussion of the test is included in Appendix A.

Visual results obtained from the panel test indicated that cracking would be best observed if the form side of the panel were subjected to tensile stress in bending. Also, the form gave a smooth, true surface to the panel at the end where the panel was mounted against the load blocks, giving a firm, even seating of the panel. Based on these observations, all subsequent panel tests were conducted with the form side of the panel in tension.

CHAPTER VII

EXPERIMENTAL PROCEDURES

Casting Procedures

Forms for casting the test panels were constructed on a plywood frame surfaced with plastic sheeting. Side and end forms for the panels were two inch dimensional lumber cut to the required depth of panel and nailed to the plywood casting bed. Holes were drilled in the end forms at the proper spacings and depths and the wires were run through the holes and anchored at the end of the forms. All forms for a particular depth of panel and wire spacing were located end to end to facilitate wire placement.

All panels were not cast at the same time. The forms were prepared first to cast all panels of 1.35 in. depth and five wire spacings. After this group of panels were removed from the forms, the forms were cleaned, a new plastic sheeting applied, and the side and end forms for the panels with five depths and one wire spacing were installed.

The wire used was No. 10 cold drawn steel wire and all wire used was obtained from the same roll of wire to minimize variations in the reinforcement. The wire was clean when received so no attempt was made to clean it or to age it by weathering prior to use to obtain improved bond. Specimens of the wire were tested from various locations on the roll for modulus of elasticity, yield and ultimate strength. The stress-strain relationship and ultimate strength for the wire is shown

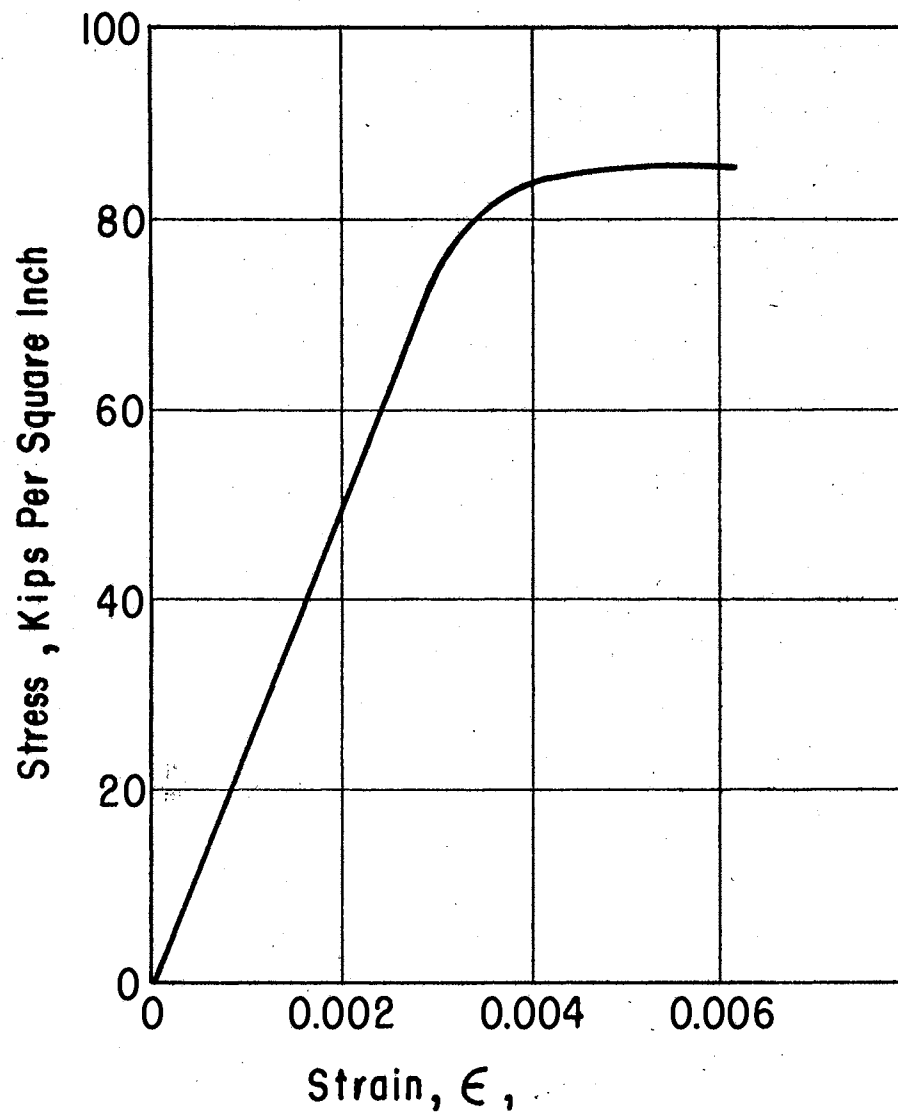


Figure 9. Stress-Strain Plot, No. 10 Plain Wire

in Figure 9.

Because initial casting of the panels was done in very hot weather, small batches of concrete were prepared so the panels could be quickly finished before mixing water was lost to evaporation. The mix used was a relatively stiff mix and slump tests varied from one to two inches. All concrete was hand placed and vibrated into position around the reinforcement. The depth of the wires were maintained during placing of the concrete by the use of strike boards cut to the wire depth. The concrete for the bottom of the panel was worked into position and struck off at wire level. This left a rough surface for bonding the top layer of plastic mix and a visual check would be made to be sure all wires were in place before the final placement of concrete. If any wires were displaced in initial casting, they were carefully worked back into position and the concrete worked under them to prevent further displacement.

After all concrete was placed in the forms, the panels were given a wood float finish and checked for accuracy of depth. They were then allowed to set for approximately thirty minutes for initial set before they were given a steel trowel finish. No water was added at any time after mixing and the panels were allowed to surface dry before plastic sheeting was applied for curing.

The panels were moist cured under plastic and wet burlap for two days prior to removal from the forms. They were then moist cured for twenty six more days and then dried and stored until tested. Spacer blocks were used between each panel in storage to assure air movement and uniform drying. This is shown in Figure 10. Test cylinders were cast from each batch of concrete used for the panels. These cylinders were tested after curing to determine if the concrete met minimum speci-

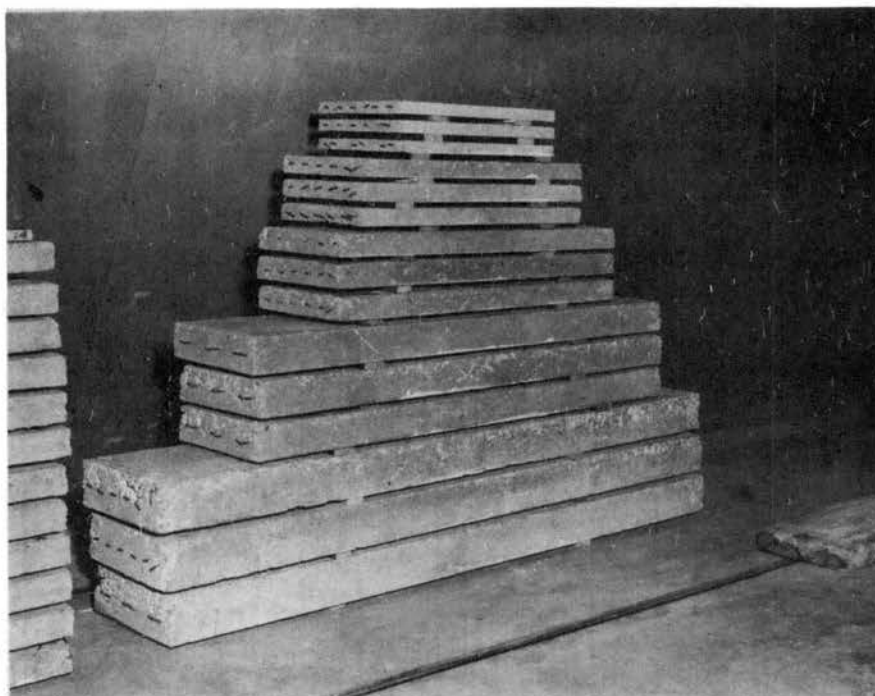


Figure 10. Five Depths of Panels, All With 6 Wires for Reinforcement. Lengths were 48, 36, 24, 18, and 12 inches, bottom to top.

fications of 5,000 psi and whether a uniform value of modulus of elasticity of the concrete for all panels was obtained.

Modulus of Elasticity for Concrete Cylinders

The test cylinders for each group of panels was tested immediately after the panel tests were conducted. The stress-strain relationship for each mix used to cast panels is shown in Figure 11. All concrete cylinders tested showed a relatively straight stress-strain relationship below 5,000 psi and all approached or exceeded 7,000 psi ultimate strength. The secant modulus of elasticity, taken at 70 percent to 80 percent ultimate strength, is given for the concrete used for each panel in Table IV.

The modulus of elasticity for the concrete test cylinders was obtained from compression tests using the universal testing machine. A single strain gage was cemented to each cylinder to determine strain. Strain gages used were four inch gages to minimize strain errors caused by local variations in stiffness caused by tamping or aggregate proximity. All cylinders were capped in the capping machine and checked for vertical positioning in the testing machine prior to loading to avoid eccentric loading and bending stresses. All cylinders were loaded to destruction, Figure 12. Two groups of panels were discarded due to irregularities in mixing and casting procedures. Three castings were required before satisfactory results were obtained.

Testing Equipment

A hydraulic loading device was constructed to load the test panels with load increments of approximately 100 pounds. Loads were applied at

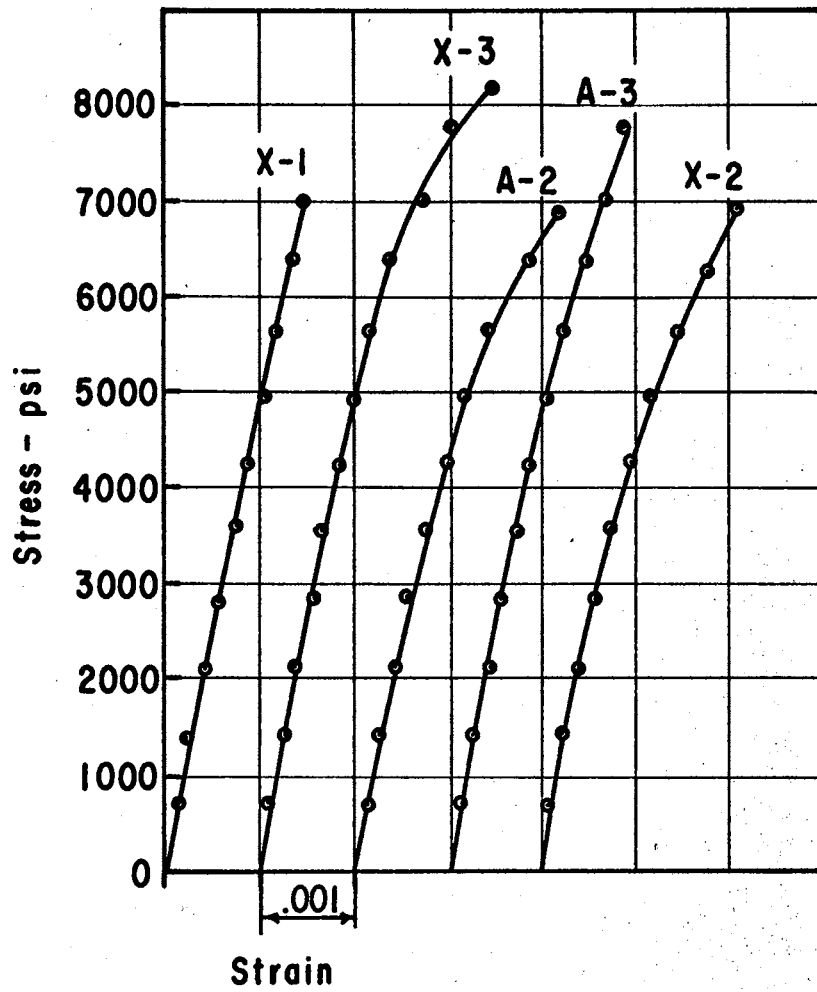


Figure 11. Stress-Strain Plot for Test Cylinders

the third points of the panels to provide a uniform moment and zero shear at the middle third of the span. This loading equipment is shown in Figure 13. The loading device consisted of a hydraulic pump and hydraulic cylinder, a load cell for accurate measurement of load, and a load bracket with two load knives to apply line loads at the third points of the panels. Stationary end supports for the panels were provided by two heavy load blocks bolted to the concrete floor.

The load knives were made of heavy plate, one half inch by three inch stock, and a 3/8 in. rod was welded to the load surface of each knife to give a line loading. The rod was omitted at the center section of each load knife to allow space for lead wires for the strain gages. The pulling bracket for the load knives was designed to be hinged at the center to allow some freedom of movement and to retain a uniform load at the two vertical load lines of the panel if one end of the panel deflected more than the other due to unsymmetric cracking.

Instrumentation

Strain gages were cemented to the compressive side of one group of panels and to both sides of the second group of panels to measure strain at the center of the span. Six in. strain gages were cemented to all panels twenty four in. or longer and three in. gages were applied to the smaller panels. Strain readings and load cell readings were obtained with a slide-wire type strain indicator.

Deflection readings were obtained by measuring deflection at the center of the span with two micrometer dials. One dial was also installed at each end of the panel to measure any relative movement at the support. The difference in readings between the center of the span and

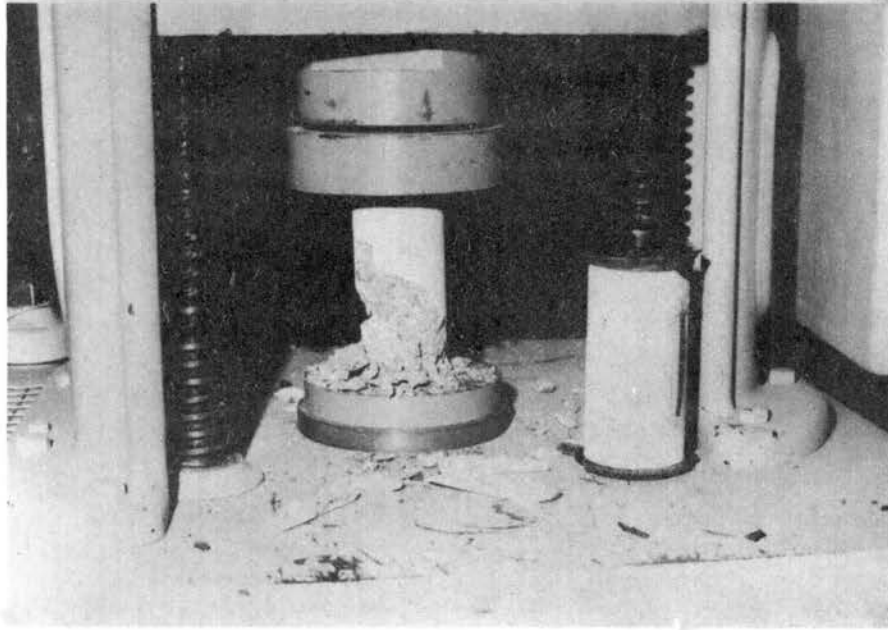


Figure 12. Concrete Test Cylinder for Panel Tests at Failure. Wire resistance strain gages, SR4 type A-9, were used for all tests of

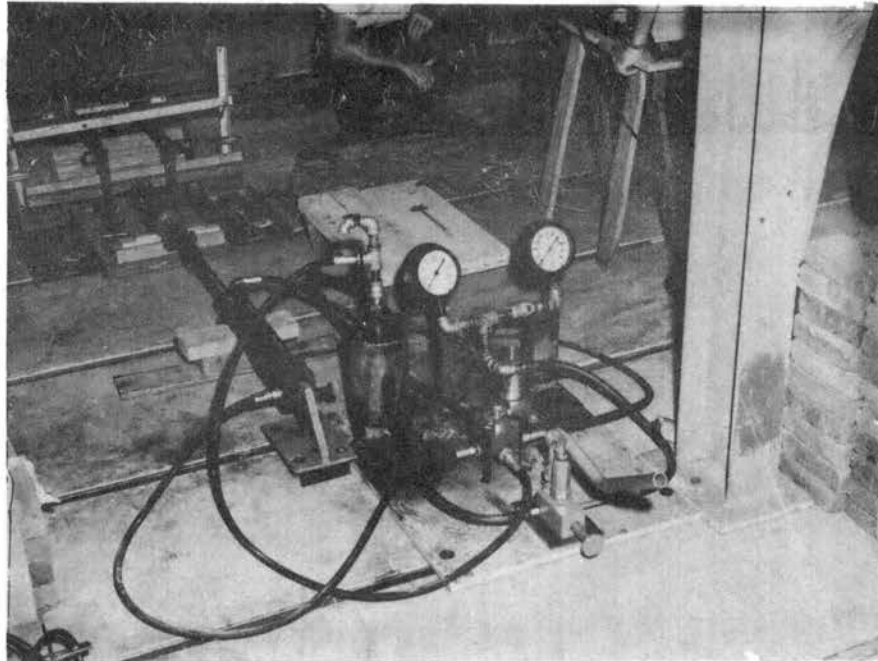


Figure 13. Loading Equipment Used for Test Showing Hydraulic Pump and Gages, Hydraulic Cylinder, Load Cell and Load Knives With Panel in Test Position.

the supports was used as the deflection. The dials were mounted on movable brackets and were positioned at the middle of the panel at either end and one and one half inches in from either edge of the panel at the center of the span.

Load increments used were hydraulic load readings obtained from a dial gage installed at the hydraulic pump. There was some lag in the system and gage readings were not uniform over the entire loading range. The use of these readings was required in that the load was applied and held on the concrete panel by the pump operator while the load cell and strain readings were being made. Using the hydraulic pressure gage gave the operator a specific load to hold, resulting in a non-varying load while data were being recorded. Actual loads at each load increment were measured with the electronic load cell.

Testing Procedures

Prior to testing, the depth dimensions of all panels were measured and recorded to determine the actual depth of panel. Three depth measurements were made at the third points and at midspan, two inches in from either edge at the midline of the panel. Values of D given in Table IV are the average depths. The depth varied between panels in the same group but variations within a panel were very small.

The panels were tested on edge to eliminate dead load effects in determining load-deflection data. The panels were set on edge against one inch rollers positioned against the load blocks and were seated against the rollers with a light loading. The micrometer dials were then installed and, when the positioning load was released, zero readings were obtained for the micrometer dials and the load cell and strain

gages.

Three people were required for each test; a pump operator, an operator for the strain and load cell readings, and a recorder to read the micrometer dials and record all data. Loads were applied monotonically in approximately one hundred pound increments. After each load was applied, the load was held by the pump operator while strain, load cell and micrometer dial readings were obtained. After the data was recorded for a load increment, the next load increment was applied. No attempt was made to maintain a constant loading rate but loading rate was fairly uniform. The panels were tested to failure and panel deflections were recorded for the panel for the uncracked phase and the cracked phase of the test.

When the panels cracked, the cracks were noted and their location and the load recorded. Their location was measured after the panel had failed rather than during loading so a fairly constant loading rate could be maintained. Most cracks were quite obvious, due to the placement of the reinforcement at the center of the panel. Initial cracking in most panels occurred at the load knives, a point of maximum load and shear. Cracks were indicated by large increases in deflection and in strain if the crack occurred below a strain gage.

The type of failure observed varied with panel depth and the amount of reinforcement. Panels with three and four wires for reinforcement failed at relatively low loads with large deflections, final failure being a wire fracture failure following extensive yielding. Panels 1.35 in. thick with 6, 8 or 12 wires failed in combined yielding of the wire and crushing of the concrete. Failures of the 1 and 2 in. thick panels with 6 wires were similar. The thin panels simply folded in failure

while two of the deepest panels, 2.7 in. thick, failed abruptly at initial cracking due to wire fracture.

CHAPTER VIII

DISCUSSION OF TESTING PROCEDURE

The hydraulic loading device used resulted in complete collapse of the panels. The stored energy in the hydraulic system pulled the load knives through the panels or folded the panels and pulled them off the load blocks once the panel started to fail. All failure loads recorded were maximum load prior to or at failure. This destruction of the panels was convenient in that the panels were broken at failure, exposing the reinforcement. Wire depths were easily determined at the point of failure.

The locations of all wires were measured after failure at the line of failure and at one or two other crack locations, depending upon the location and extent of cracking. This information was recorded and the depth of reinforcement, t , listed in Table IV, is the computed mean depth of all wires.

Ultimate load for many panels exceeded the computed moment and some exceeded the maximum moment possible if the centroid of compression was located at the surface of the panel. It was assumed that the one inch steel rollers would roll at the supports and yield with the panel as it deformed due to bending stresses and deflection. This was apparently not the case. A panel in bending will contract in the region of compressive stress and expand in the region of tensile stress, getting longer at the bottom and shorter at the top as bending stresses increase.

TABLE IV

PHYSICAL PROPERTIES OF THIN CONCRETE PANELS TESTED

Panel No.	Wires No.	Depth in.	Length in.	Wire Depth in.	Reinforcement ratio, per cent	E_c psi	f'_c psi	I in. ⁴	I_{c4} in. ⁴
1	3	1.47	24	0.78	0.68	4.39×10^6	8492	2.1442	0.1002
2	3	1.45	24	0.70	0.76	4.39	8492	2.0792	0.0784
3	3	1.46	24	0.57	0.93	4.39	8492	2.1007	0.0505
4	4	1.46	24	0.62	1.14	4.39	8492	2.1007	0.0769
5	4	1.49	24	0.68	1.04	4.39	8492	2.2329	0.0936
6	4	1.47	24	0.62	1.14	4.39	8492	2.1442	0.0763
7	8	1.40	24	0.54	2.60	4.88	7431	1.8522	0.0863
8	8	1.45	24	0.54	2.60	4.88	7431	2.0578	0.0863
9	8	1.44	24	0.64	2.22	4.88	7431	2.0155	0.1274
10	12	1.48	24	0.61	3.47	4.88	7431	2.1882	0.1508
11	12	1.48	24	0.59	3.60	4.88	7431	2.1882	0.1367
12	12	1.41	24	0.62	3.42	4.88	7431	1.8922	0.1537
13	6	0.73	12	0.37	2.78	4.61	7006	0.2615	0.0307
14	6	0.73	12	0.38	2.80	4.11	6950	0.2658	0.0353
15	6	0.75	12	0.37	2.78	4.52	8195	0.2905	0.0311
16	6	1.065	18	0.55	1.93	4.61	7006	0.8154	0.0764
17	6	1.105	18	0.45	2.38	4.11	6950	0.9107	0.0623
18	6	1.020	18	0.50	2.12	4.52	8195	0.7163	0.0523
19	6	1.38	24	0.70	1.52	4.61	7006	1.7855	0.1337
20	6	1.35	24	0.70	1.52	4.11	6950	1.6424	0.1434
21	6	1.40	24	0.71	1.50	4.52	8195	1.8364	0.1401

TABLE IV (Continued)

Panel No.	Wires No.	Depth in.	Length in.	Wire Depth in.	Reinforcement ratio, per cent	E_c psi	f'_c psi	I in. ⁴	I_c in. ⁴
22	6	1.99	36	1.00	1.06	4.11	6950	5.3034	0.3006
23	6	2.04	36	1.02	1.05	4.61	7006	5.7305	0.3040
24	6	2.02	36	1.01	1.05	4.52	8195	5.5802	0.3022
25	6	2.68	48	1.35	0.78	4.11	6950	12.9929	0.6183
26	6	2.70	48	1.41	0.75	4.61	7006	13.2860	0.6151
27	6	2.75	48	1.35	0.78	4.52	8195	14.0378	0.6185

Based on the results noted, the rollers did not provide a free lateral movement of the panel but held it in place by friction forces, resulting in reduced stresses in the lower portion of the panel. This restriction of the panels would explain in part the fact that most of the panels exceeded the ultimate computed moment based on the loads and the physical properties of the panels.

The concrete used for fabricating the panels exhibited high tensile stress prior to rupture and exceeded the expected cracking loads for all panels. Cracking stress for the panels varied from 1,000 to 1,200 psi for the panels, or 12 to 15 percent of the compressive stress of the concrete. This high tensile strength in flexure reduced the data for cracked panel deflection to one or two readings for many panels prior to yielding of the reinforcement. The three wire panels and the 2.7 in. thick panels were completely eliminated as far as useful data for deflection of cracked panels. The 2.7 in. thick panels failed at initial cracking loads and only one panel could be reloaded to the cracking load after initial cracking and deflecting. One failed completely at initial cracking and the second failed before the full cracking load was again applied. The panels with three wires had also exceeded yield stress of the wire following cracking.

The load-deflection plots for all panels are given in Figures 41 through 49 in Appendix C. Plots for selected panels are shown in Figures 14 and 15. Deflection due to cracking is readily noted by the large deflections. Many panels cracked while data was being recorded and this is shown by horizontal lines on the plot. The micrometer dials at the center of the panel span were constantly monitored while loads were being applied and any deflections due to cracking were noted as they occurred.

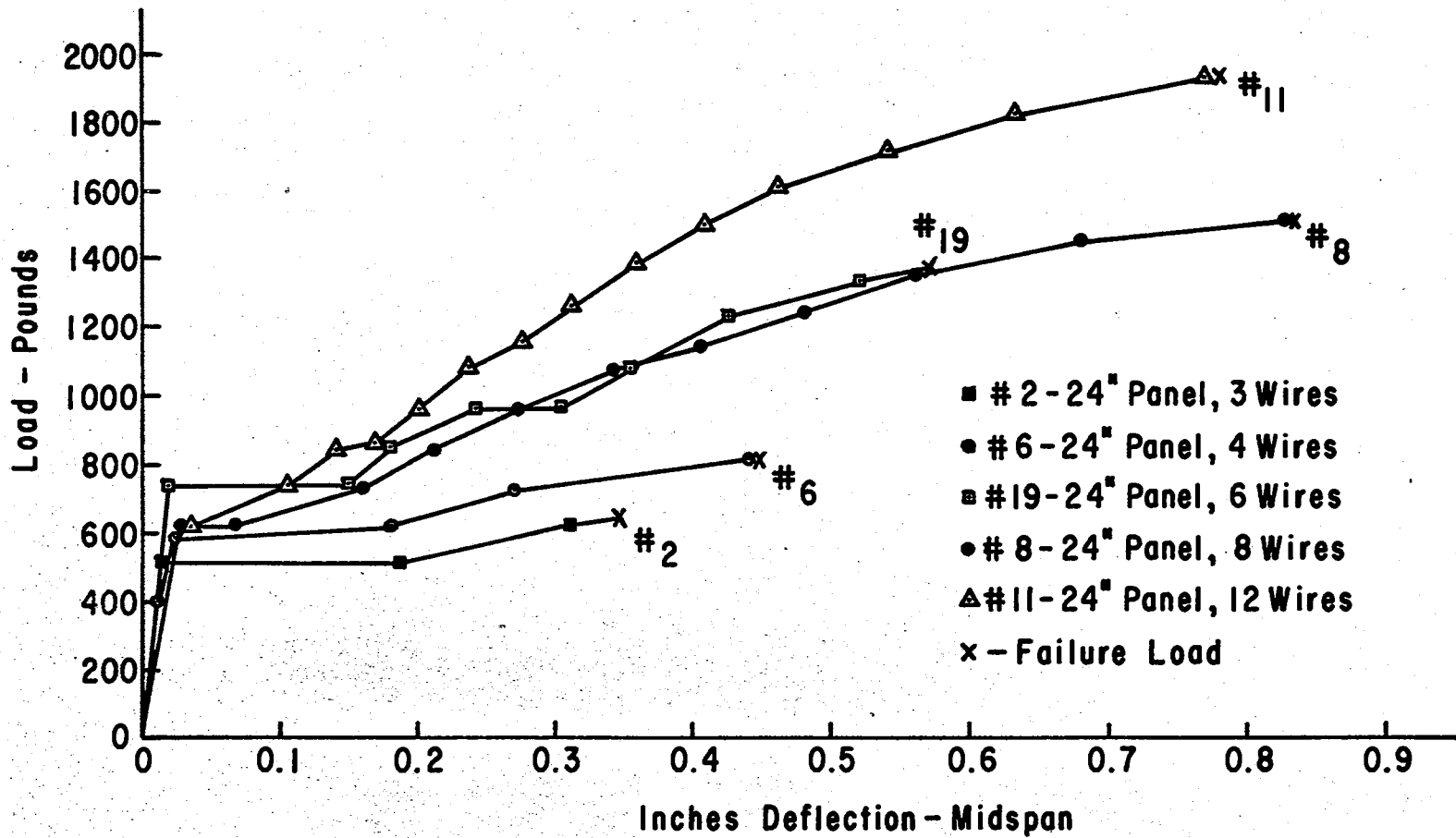


Figure 14. Load-Deflection Tests, Five Spacings

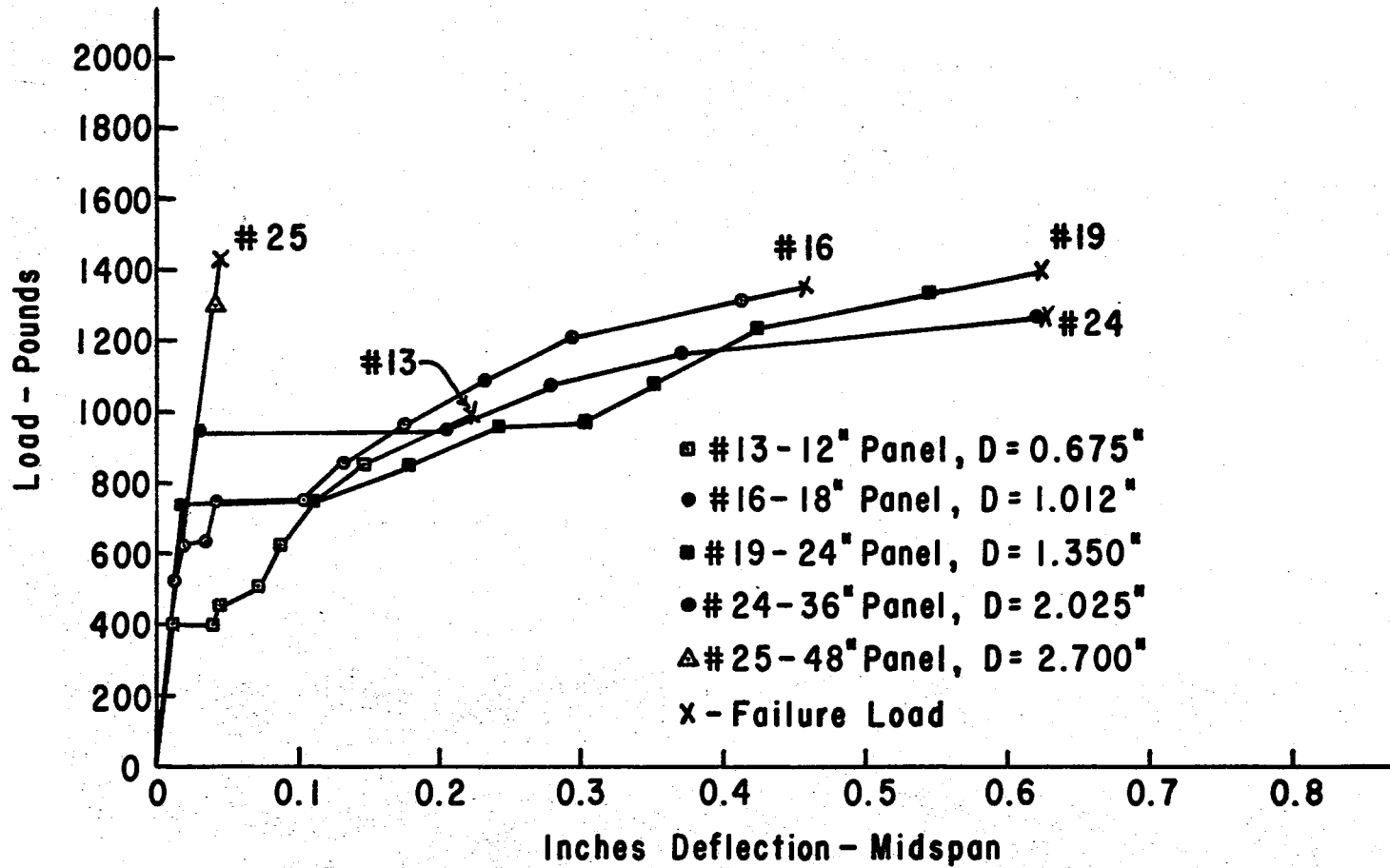


Figure 15. Load-Deflection Tests, Five Spacings

Modulus of Elasticity for Panels

Strain measurements were recorded for all panel tests. However, erratic results were obtained for all panels where depth of panel was varied, panels 13 through 27. This group of panels had been cast three times. The first casting had been rejected due to wide variations in modulus of elasticity of concrete. The second group were cast on plastic sheeting that wrinkled as the concrete was worked into the forms and the panels were not acceptable due to ridges and grooves caused by the plastic. The final casting had been delayed and by the time the panels were finished and the strain gages applied, the shelf life of the strain gage cement had apparently been exceeded. These panels included all in which strain gages had been applied to both the compressive and tensile sides of the panels.

Strain readings from the panels were intended to be used to evaluate reinforcement spacing effects for panels in flexure and to develop a prediction for strain at the surface of the panel as a function of load, spacing of reinforcement and panel depth. Strain readings are useful in that the performance of the concrete in the member and strain data obtained from cylinder tests can be compared to determine if the test cylinder value of modulus of elasticity is representative of the modulus of elasticity of the concrete used in the member. The failure of the strain gages for fifteen panels prevented this check of modulus of elasticity of the panels versus test cylinders.

The modulus of elasticity of the concrete in the panel and how well this value was represented by modulus of elasticity from cylinder tests was critical to evaluation of computed deflections of the panels for analysis of data. The deflection of a concrete member subjected to

flexural stress is inversely proportional to the modulus of elasticity of the concrete. Therefore, it was necessary to determine if the values of E_c obtained from the concrete cylinder tests was comparable to the values of E_c for the concrete for the panels, and could be used to determine the theoretical deflection of the panels.

Strain data was obtained for twelve panels. However, strain gages of only eleven apparently functioned correctly. One gage, panel 5, exhibited erratic characteristics and panel 5 data was excluded from this analysis. Only strain data for eleven panels were included in the test of E_c for the panels versus E_c for the test cylinders.

The modulus of elasticity for each of the concrete panels was computed from strain and deflection data obtained in panel tests for loads in the elastic, uncracked region of the test. Strain and deflection data were selected from test data the third and fourth load increments for each of the eleven panels, the two load increments prior to minimum cracking loads. The modulus of elasticity was computed from both strain and deflection by mechanics. The modulus of elasticity obtained using recorded strain is shown as E_c -Strain in Table V. The modulus of elasticity determined by deflection is given as E_c -Deflection in Table V. Strain for the test cylinders given in Table V is the tangent modulus since the tests in flexure were conducted at low stresses, or about five percent of ultimate strength.

Standard deviation of E_c values obtained from strain and deflection data as compared to values of E_c for cylinder tests were computed. Standard deviation for modulus of elasticity computed from deflection was 0.45×10^6 psi, or 9.3 per cent of E_c of the cylinders. The mean was 3.5 per cent less. Standard deviation for modulus of elasticity

TABLE V
MODULUS OF ELASTICITY FOR PANELS IN FLEXURE

Panel Number	E_c Cylinder psi	E_c Deflection psi	E_c Strain psi
1	4.80×10^6	5.12×10^6	4.48×10^6
2	4.80	4.95	5.67
3	4.80	4.98	5.96
4	4.80	4.78	5.52
6	4.80	4.95	5.58
7	4.88	4.50	4.12
8	4.88	3.82	5.63
9	4.88	4.07	4.46
10	4.88	4.83	4.87
11	4.88	4.55	4.58
12	4.88	4.70	4.69

E_c Cylinder - Obtained from stress-strain relationship for concrete test cylinders.

E_c Deflection - Obtained from computed values of modulus of elasticity based on measured load and deflection for panel loaded at third points, moment of inertia from Table IV.

E_c Strain - Obtained from measured strain and stress computed from load at third points, moment of inertia from Table IV.

computed from strain data was 0.619×10^6 , or 37 per cent higher than the standard deviation of E_c obtained from deflection data. The mean for E_c obtained from strain data was 4.5 per cent more than E_c for the test cylinders. It will be noted in Table V that many values agreed quite well with the test cylinders, especially those obtained from deflection data.

Based on the results obtained, the values of E_c obtained from test cylinders were deemed sufficiently accurate for use in computing the theoretical values of deflection for the experimental panels. It will be noted that only two values of E_c for cylinders were included in the above test. Panels fabricated with other concrete mixes were those that encountered strain gage failures and no comparison of the modulus of elasticity based on strain could be made.

CHAPTER IX

DATA ANALYSIS

Data obtained in the tests of thin concrete panels were reduced and transferred to data cards for computations and analysis. Test data for uncracked panels included, deflection and strain at each load increment. Cracked panel data included load, deflection, strain, number and location of cracks for each load increment, ultimate load at failure and mode of failure.

A least squares multiple regression program was used to determine the regression of the dependent π terms on the independent π terms and to determine if spacing of the reinforcement, depth of panel, and load had a significant effect on strain, deflection and ultimate strength. The multivariable program calculated the response surface, developed a polynomial equation up to third degree, ran a regression on observed versus calculated values, and gave the correlation coefficient and standard deviation of observed and calculated values. The equations developed were used to determine the best fit curves for the prediction equations for the dependent variables as functions of the independent variables.

The equations selected for best fit curves were selected for minimum standard deviation and correlation coefficient. The first, second and third order equations were investigated separately and the higher equations were selected for prediction equations only if they were sig-

nificant improvements over the lower order equations. The purpose of this was to obtain the best equation for the data while retaining simplicity of calculations for users of the prediction equations.

Uncracked Panel Data

The moment of inertia of uncracked panels will usually be little affected by a nominal amount of reinforcement due to the small transformed area of the area of steel. Since the reinforcement in the test panels investigated was located at the neutral axis, the area of reinforcement would not contribute to the moment of inertia of the uncracked panels. Therefore, the reinforcement was ignored in computing the moment of inertia used in the load pl term, PL^2/EI .

The values of I and E_c were assumed constant within individual panels. They were not constant for all panels of the same depth, D , or reinforcement spacing, S , due to slight variations in depth of panels and slight variations in E_c . The moment of inertia of uncracked panels is proportional to the depth cubed, all panels being the same width. Small variations in depth caused large variations in I between panels supposedly of the same depth. This is shown in Table IV for panels 17 and 18. The intended depth of these panels was 1.012 in. Actual depths were 1.02 and 1.105 in. respectively, resulting in a moment of inertia twenty seven per cent higher for panel 18 as compared to panel 17. Therefore, moment of inertia for each individual panel was computed. Values of E_c for the individual panels was obtained from standard compression tests of concrete cylinders cast from the individual batches of concrete from which the panels were cast. The values of EI were then determined for each individual panel.

One of the major objectives of this study was to determine if wire spacings, or S/d_s , would have any influence on strain and deflection for a given value of load, or a given value of PL^2/EI . It would be assumed that if the value of PL^2/EI and all other variables were held constant, any variation in the deflection and strain for a specific value of PL^2/EI would be a function of reinforcement spacing. The same would also hold true if the depth pi term, D/d_s , were varied and all other variables were held constant.

It would also be assumed that the relationship between the deflection and strain pi terms and the load pi term, PL^2/EI , may be evaluated by considering L^2/EI as a constant and varying load, P . As P is increased, the value of the pi terms will increase. If the panel material demonstrates a linear stress-strain relationship, the variation of deflection and strain should be directly proportional to variations in the load, P .

The relationship between the deflection pi term, Δ/L and the load pi term, PL^2/EI , was determined for the panels in which the spacing and depth pi terms were held constant, the standard panels of 1.35 in. depth and with a reinforcement spacing of 1.35 in. Values of P to be investigated were to be four load levels from 200 to 500 lb, or four specific values of PL^2/EI . Since load levels were measured on the pressure gages of the hydraulic system and the fact that the values of L^2/EI varied for the three panels tested, the loads used were not the previously determined increments but were the measured loads obtained from the load cell for gage readings of 200, 300, 400 and 500 lb., plus the 100 and 600 lb. readings. The latter were added to include all applicable data for improved sensitivity of test.

No relationship between the strain π term and the load π term, PL^2/EI , was determined due to strain gage failures on the standard panels, panels 19, 20 and 21. As stated previously, the strain gage cement apparently failed and erratic results were obtained for this group of panels. Insufficient data was obtained to make valid comparisons.

Statistical Significance, Uncracked Panels

The effect of reinforcement spacing on strain for uncracked panels for a constant value of PL^2/EI of 0.0021 was tested by linear regression. The correlation coefficient of linear regression was 0.199 and Fisher's F for this test was 0.332. Therefore, the effect of spacing on strain was not found to be significant at the 0.95 confidence level. This too was the anticipated result for uncracked panels with the reinforcement located at the neutral axis. Data for this test are given in Table VI.

The value of the load π term, PL^2/EI , selected for testing both the spacing and depth effects π terms was 0.0021, or an equivalent load of 300 lb. for the standard panel. This resulted in a wide variation in flexure stress in the panels because of the variations in L^2/I for five panel lengths and five panel depths. However, all panels were tested in the linear stress-strain region of the concrete at loads well below cracking stresses. Deflection values used were obtained by interpolation from the load-deflection data for the individual panels owing to the previously mentioned restrictions on the loading equipment.

A linear regression analysis of the deflection π term, Δ/L , on the load π term, PL^2/EI were conducted to determine if load effects on deflection were significant. The correlation coefficient of linear regression was found to be 0.989. Fisher's F was 10.515. The relationship

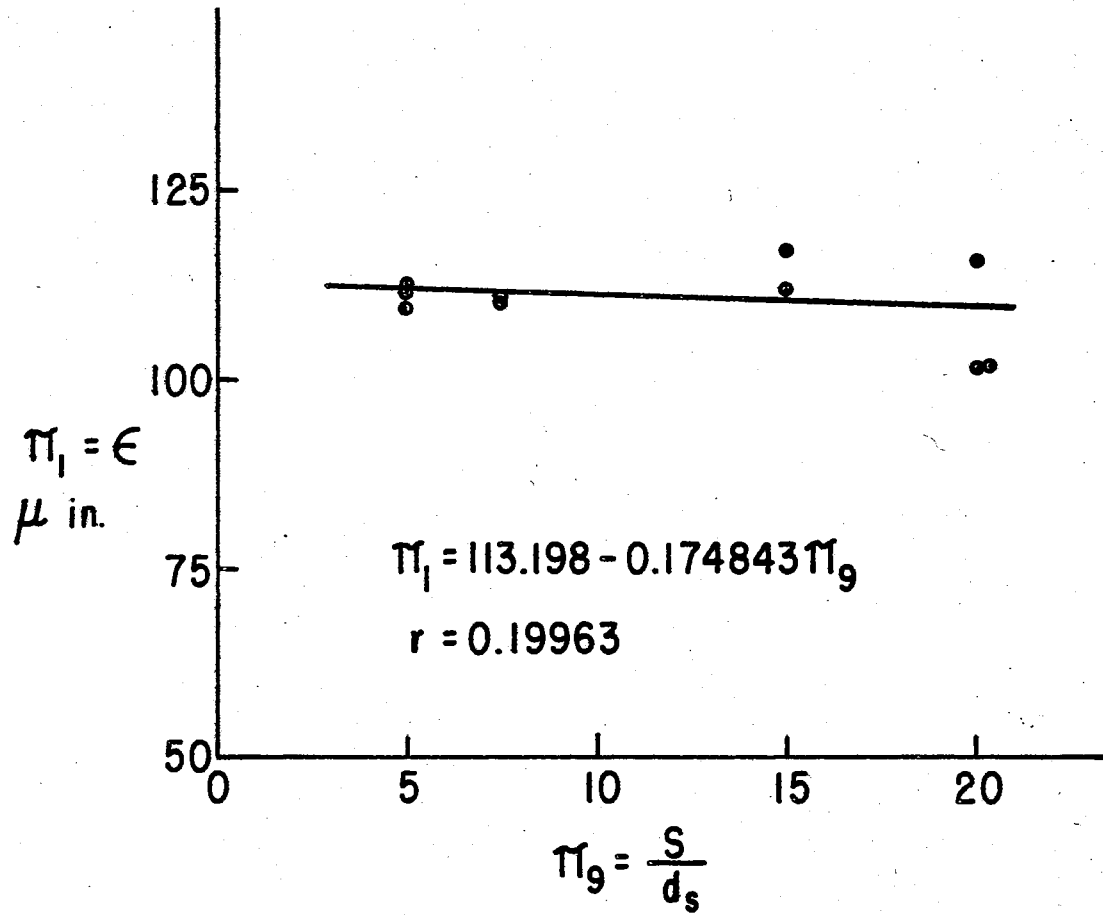


Figure 16. Data Plot, Strain Versus S/d_s

TABLE VI
 DATA FOR REGRESSION ANALYSIS AND BEST FIT CURVE,
 SPACING EFFECT OF REINFORCEMENT ON STRAIN

S/d_s	Strain, Microinches
20.0	102
20.0	115
20.0	102
15.0	117
15.0	120
7.5	111
7.5	110
5.0	109
5.0	113
5.0	112

Polynomial Equation, $\epsilon = 113,198 - 0.17484 S/d_s$

Correlation coefficient = 0.199635

Standard deviation = 6.04926

of deflection versus load was therefore significant at the 0.995 confidence level, using Fisher's F test for significance. A data plot and a plot of the linear regression of deflection pi term on load pi term is shown in Figure 17. Data for this test is given in Table VII.

The effects of both spacing and depth on deflection per unit length of uncracked concrete panels for a constant value of PL^2/EI of 0.0021 were investigated for statistical significance. The spacing pi term, S/d_s , had a linear regression correlation coefficient of 0.069 and a Fisher's F test value of 0.062. The depth pi term, D/d_s , had a linear regression correlation coefficient of 0.225 and a Fisher's F test value of 0.867. The effects of both wire spacing and panel depth on the deflection pi term were found to be not significant at the 0.95 confidence level. This was the anticipated results of this phase of the test as the reinforcement was located at the neutral axis of all panels and all panels were tested in the elastic range of the concrete. All twenty seven panels were included in the test. Data for these tests are given in Tables VIII and IX.

Cracked Panel Data

Selection of a single value of the load pi term, PL^2/EI , as used in the analysis of performance for uncracked panels was not possible for determining the performance of cracked panels. First, no single value of PL^2/EI would apply for all panels for loads greater than cracking loads but less than failure loads. Values that would represent ultimate loads for some panel treatments would represent loads less than cracking loads for other panel treatments. Second, deflection of panels after initial cracking is primarily a function of the number and location of

cracks. Since cracking was not uniform, either in number or location for the various wire spacing and depth treatments, any deflection π term that did not consider crack number and location as a function of load would not be applicable. Deflection is also a function of the amount of reinforcement, or I_c . Panels with larger amounts of reinforcement deflected less under the same load. This is shown in Figure 14. Therefore, the deflection π term used is a direct comparison of measured and computed deflections.

Development of the equation for computing the deflection of cracked panels, and examples as applied to the size panel and type loading used, are given in Appendix B. The conjugate beam method was used to compute deflections of cracked panels. The effective distance, ℓ , for determining the magnitude of the elastic weights at a cracked section, or the length at a crack in which tensile stress is lost in the concrete and the cracked section moment of inertia is effective, was determined by testing, as stated in Chapter IV, Theoretical Testing. This distance was found to be three inches in length, or one and one half inches either side of a crack. Method of obtaining effective length, ℓ , is given below.

Minimum crack spacing in panels tested was noted to be approximately three inches. Therefore, deflections based on load and crack locations for the three standard panels, Panel 19, 20 and 21, were computed by the conjugate beam method using trial values of ℓ of two in., two and one half in., three in., three and one half in., and four in. Deflections were computed for each of the three panels for four load increments and computed deflections for the four loads, using the five values of ℓ . Deflections computed were compared with measured values

of deflection for the four load increments, to determine an effective length of ℓ , or length of tensile stress loss in the concrete. The four loads used were cracking loads and the three subsequent load increments.

A trial length of three inches for ℓ gave an average value of 1.159 for the ratio of measured deflections versus computed deflections for the four load increments investigated. The wire reinforcement stresses were then computed for the four loads for each of the three panels to determine if the yield stress of the wire reinforcement had been exceeded by the loads. The two higher load increments were found to produce wire stresses in excess of seventy thousand pounds per square inch. Since these stresses were in excess of minimum yield strength of the wire, these load values were excluded and the average deflection ratio for the two remaining loads for the three panels was again computed. The average deflection ratio for the six remaining data points, for ℓ equal to three inches, was found to be 1.0025, measured deflection versus computed deflection. Therefore, three inches was accepted for the length of ℓ for computing panel deflection due to cracked panel moment of inertia for all panels.

The minimum stress in the reinforcement after initial cracking for the three standard panels were determined to be 55,000 psi. Therefore, measured deflections used for computing the deflection π term, Δ/Δ_c , were selected for loads that produced a stress in the reinforcement of 55,000 to 70,000 psi. This was to ensure uniformity of bond stresses in the panels for comparative values of computed and measured deflections. All other data points were excluded from analysis of cracked panel performance.

Strain data were recorded for the cracked panel tests but no attempt was made to determine spacing effects or depth effects on strain. Due to the thin section of the panels, two and three fold increases in strain were frequently noted when cracks occurred in the concrete below a strain gage and progressed to near the compressive face of the panels. If the crack occurred outside the portion of the panel monitored by the strain gage, no increase in strain was noted. Therefore, it appeared that recorded strain was a measure of strain at the gage location, not necessarily panel performance.

All panels had been designed to perform as under-reinforced beams to assure ductility and to allow the panels to fail due to yielding of the reinforcement. Balanced design for the concrete and wire reinforcement used was approximately three and one half per cent. It was assumed that a valid moment of inertia of all cracked panels could be computed, using transformed section methods, for computing I_c for determining computed deflections. A check on the validity of this assumption, the effect of the percentage of the reinforcement of the panels as a function of the deflection Δ term for all data points used in the analysis, was investigated for statistical significance.

Statistical Significance, Cracked Panels

The effects of both reinforcement spacing, S , and depth of panel, D , on the deflection of cracked panels were investigated for significance. A linear regression analysis of the effects of spacing versus the ratio of measured and computed deflections, or S/d_s versus Δ/Δ_c , gave a correlation coefficient of 0.329 and a Fisher's F value of 3.03. The effect of depth treatment versus the ratio of measured and computed

deflection, or D/d_s versus Δ/Δ_c , gave a linear regression correlation coefficient of 0.292 and a Fisher's F value of 2.23. Both spacing and depth effects were found to be not significant at the 0.95 confidence level. Data used for these tests is given in Tables X and XI.

Data points used for the above analysis were limited to loads that produced reinforcement stresses from fifty five to seventy thousand pounds per square inch. Three data points were used for each panel with S/d_s and D/d_s values of 5.0 and 7.5. Only two data points for each of the standard panels, or S/d_s and D/d_s value of 10, were used, as explained previously in determination of ℓ . Only one data point was acceptable for each of the three panels with S/d_s values of 15. Only two panels, with one data point each, of the three with D/d_s values of 15 were acceptable. All other panels exceeded the reinforcement stress limit of 70,000 psi after initial cracking. Therefore, none of the panels with S/d_s or D/d_s values of 20 are included in the cracked panel data.

The effect of the ratio of the reinforcement ratio, p , as a function of computed versus measured deflection was also investigated to determine if using transformed section analysis would be valid for values of p tested. A linear regression of the deflection ratio as a function of per cent reinforcement gave a correlation coefficient of 0.133 and a Fisher's F value of 0.795. Therefore, the effect of reinforcement ratio on the ratio of measured versus computed deflections was not found to be significant at the 0.95 confidence level. Data is given in Table XII.

Ultimate Strength Data

The ultimate strength value used for analysis of reinforced concrete panel performance was the total destruction load, or P_u . This load is the maximum load recorded prior to complete failure of the panels. The computed maximum load was determined by dividing the computed ultimate moment for the individual panels by the length from the load knife to the support, or $L/3$. Computed ultimate moments was determined by the ACI Standard Building Code Equation 16-1, page 68. The equation is;

$$M_u = \phi (wt^2 f'_c q (1.0 - 0.59q))$$

where

- ϕ = capacity reduction factor
- w = width of panel, in.
- t = effective depth, in.
- q = $p f_y / f'_c$
- p = A_s / wt
- f'_c = ultimate compressive strength of concrete, psi.

The effective depth of the reinforcement was t , the depth to the centroid of the reinforcement for the individual panels, as given in Table IV. The value for p , or per cent reinforcement, for each individual panel is also given in Table IV.

The computed values of P_c are based on the yield strength of the reinforcement and not on the collapse load. Therefore, the ratio of actual failure load to ultimate computed load should be unity or greater. Ultimate measured load for most panels was twenty five to thirty five

per cent above the computed ultimate load based on yield point of the reinforcement. Some panels exceeded computed ultimate moments by as much as fifty per cent, and also exceeded the ultimate moment possible if the centroid of compressive stresses was at the surface of the concrete. As stated previously, this would be possible only if the supporting rollers offered restraint, reducing the tensile stress in the lower portion of the panel.

The thinnest panels, D/d_s equal 5.0, did not exceed the design load by a large margin. One panel failed at design load and the other two exceeded the design load by about ten per cent. This reduction in the ultimate moment pi term value for this group of panels is probably due to the fact that they had the highest percentage of reinforcement of all panels tested and exceeded the limits of the ultimate moment equation. The reinforcement for these thinnest panels was at or very near balanced design, reducing the ductility of the panels.

Statistical Significance, Ultimate Loads

The effect of the spacing pi term, S/d_s , on ultimate load versus computed ultimate load, or P_u/P_c , was investigated for all fifteen panels with spacing treatment. The correlation coefficient for the linear regression analysis was 0.269 and the value of F was 1.01, or, using Fisher's F test, S/d_s effects on ultimate strength was found to be not significant at the 0.95 confidence level.

The effect of depth, or D/d_s , versus the ultimate moment pi term was investigated for thirteen panels, the two panels that failed at initial cracking being excluded. The correlation coefficient of linear regression was found to be 0.513 and the F value was 3.93. This F value

was found to be not significant at the 0.95 confidence level, using Fisher's F test.

Based on the above findings, it can be assumed that neither spacing of the reinforcement or the depth of the panels have significant effect on the actual ultimate moment other than as provided for in computed value of ultimate moment. No increase in ultimate moment other than the expected increase due to a higher percentage of reinforcement was noted for the closer spacing of reinforcement. Data for the above tests are given in Tables XIII and XIV.

CHAPTER X

THE PREDICTION EQUATIONS

The final form of the prediction equation for a series of equations for pi terms plotted in arithmetic space is obtained by combining the various independent equations by addition and subtracting the number of pi terms minus two, or $s - 2$, times the value of any pi term where all values are constant. The general equation for a system involves only those pi terms that are varied in the study, or s number of pi terms. The equation is of the form:

$$\begin{aligned} \pi_1 = & F(\pi_2, \bar{\pi}_3, \dots, \bar{\pi}_s) + F(\bar{\pi}_2, \pi_3, \dots, \bar{\pi}_s) \\ & + \dots + F(\bar{\pi}_2, \bar{\pi}_3, \dots, \pi_s) - (s-2) \\ & F(\bar{\pi}_2, \bar{\pi}_3, \dots, \bar{\pi}_s) \end{aligned}$$

All computations of prediction equations were obtained for this study by the use of the multiple regression program. Use of the multiple regression program to determine the prediction equation allowed a more useful evaluation of the data as the correlation coefficient and the standard deviation of observed versus computed values of the pi term were obtained directly.

Stiffness of Uncracked Panels

Data for the three test series for deflection pi terms for uncracked panels are tabulated in Table VII, Table VIII and Table IX.

Table VII lists deflection pi term values for tests of uncracked panels in which the independent pi term PL^2/EI was varied while the other independent pi terms were held constant. Table VIII lists data recorded for the tests in which the independent pi term S/d_s was varied while the other independent pi terms were held constant. Table IX lists data recorded for the tests in which the independent pi term D/d_s was varied while the other independent pi terms were held constant.

Three curves were plotted for uncracked panels using data listed in Tables VII, VIII and IX. The data plotted represent the effects of the three independent pi terms, PL^2/k , S/d_s and D/d_s respectively, on the dependent pi term, Δ/L , the deflection at the center of the panel divided by the length of panel. The function used to describe the relationship between the dependent pi term, plotted as ordinate, and the independent pi term, plotted as abscissa, was obtained using least squares multiple regression analysis. The intercept of Y, the equation of the line and the correlation coefficient are given on each plot in addition to actual data plots.

Experimental data showing the relationship between Δ/L at the center of the panel and PL^2/EI for the six selected values of load, or four load increments, are shown in Figure 17. The plot indicates that the data fit a linear equation of the type, $Y = A + BX$, or:

$$\Delta/L = -0.0000054 + 0.01361 (PL^2/EI)$$

The values of the intercept, A, and the slope of the line, B, were obtained by linear regression, using a least squares multiple regression analysis program. Correlation coefficient of 0.989 indicates a high statistical significance, or Fisher's F is significant at the 0.995 con-

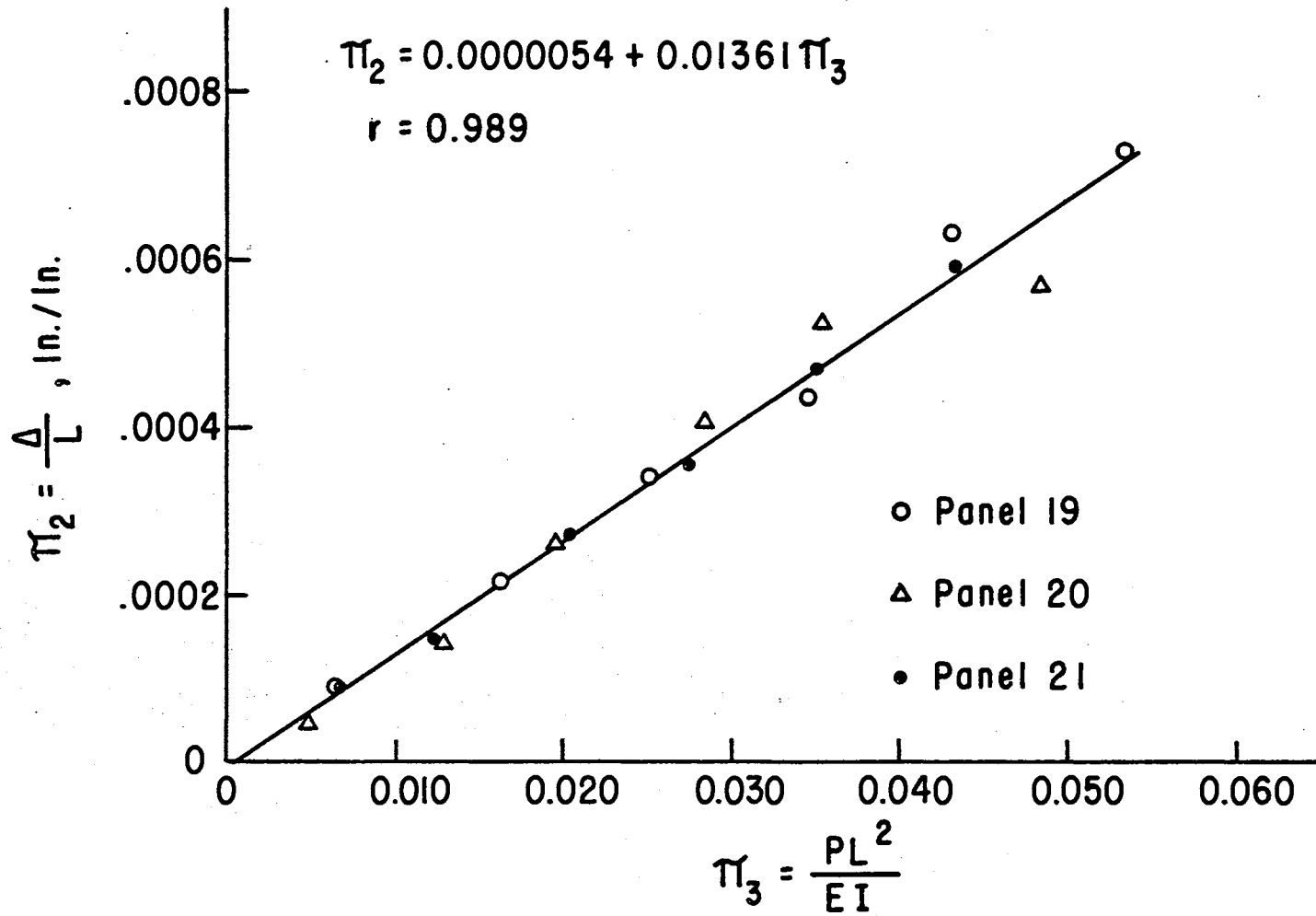


Figure 17. Data Plot, Δ/L Versus PL^2/EI

TABLE VII
 DATA FOR REGRESSION ANALYSIS AND BEST FIT CURVE, LOAD EFFECT
 ON PANEL DEFLECTION AT MIDSPAN, UNCRACKED PANELS

Panel Number	PL^2/EI	Δ/L
19	0.00646	0.000092
	0.01615	0.000216
	0.02495	0.000342
	0.03450	0.000438
	0.04300	0.000634
	0.05330	0.000725
20	0.00474	0.000046
	0.01275	0.000142
	0.01942	0.000262
	0.02830	0.000404
	0.03520	0.000522
	0.04830	0.000567
21	0.00646	0.000092
	0.01230	0.000146
	0.02020	0.000274
	0.02750	0.000358
	0.03500	0.000471
	0.04320	0.000593

Polynomial Equation, $\Delta/L = - 0.000005401 + 0.01361 PL^2/EI$

Correlation Coefficient = 0.989

Standard Deviation = 0.00003

fidence level.

The equation for deflection of a simple beam is given as a function of PL^3/EI , or $\Delta/L = f(PL^2/EI)$, assuming all other variables were held constant. It would be assumed that if the value of PL^2/EI were held constant, any variation in the deflection for the given value of P would be a function of reinforcement spacing.

Experimental data showing the relationship between Δ/L and S/d_s are shown in Figure 18. The equation of the plot, in the form $Y = A + BX$, is:

$$\Delta/L = 0.00036614 - 0.000000704138 (S/d_s)$$

This is an almost horizontal line with the intercept at A , as shown in Figure 19. Spacing effects of reinforcement on deflection was found to be not significant at the 0.95 confidence level.

The relationship between deflection and depth of panel, or Δ/L and D/d_s , is illustrated in Figure 19. The equation of the slope of the line and the intercept were obtained by least squares linear regression analysis. The equation, of the form, $Y = A + BX$, was found to be:

$$\Delta/L = 0.00027181 + 0.00000159618 (D/d_s)$$

The slope of the line is practically zero. The depth of panel has no significant effect on deflection per unit length for values of PL^2/EI in the elastic range of the panel, 0.95 confidence level.

Prediction Equation, Uncracked Panels

The final form of the prediction equation for the effects of load, wire spacing and depth of panel on deflection was found to be:

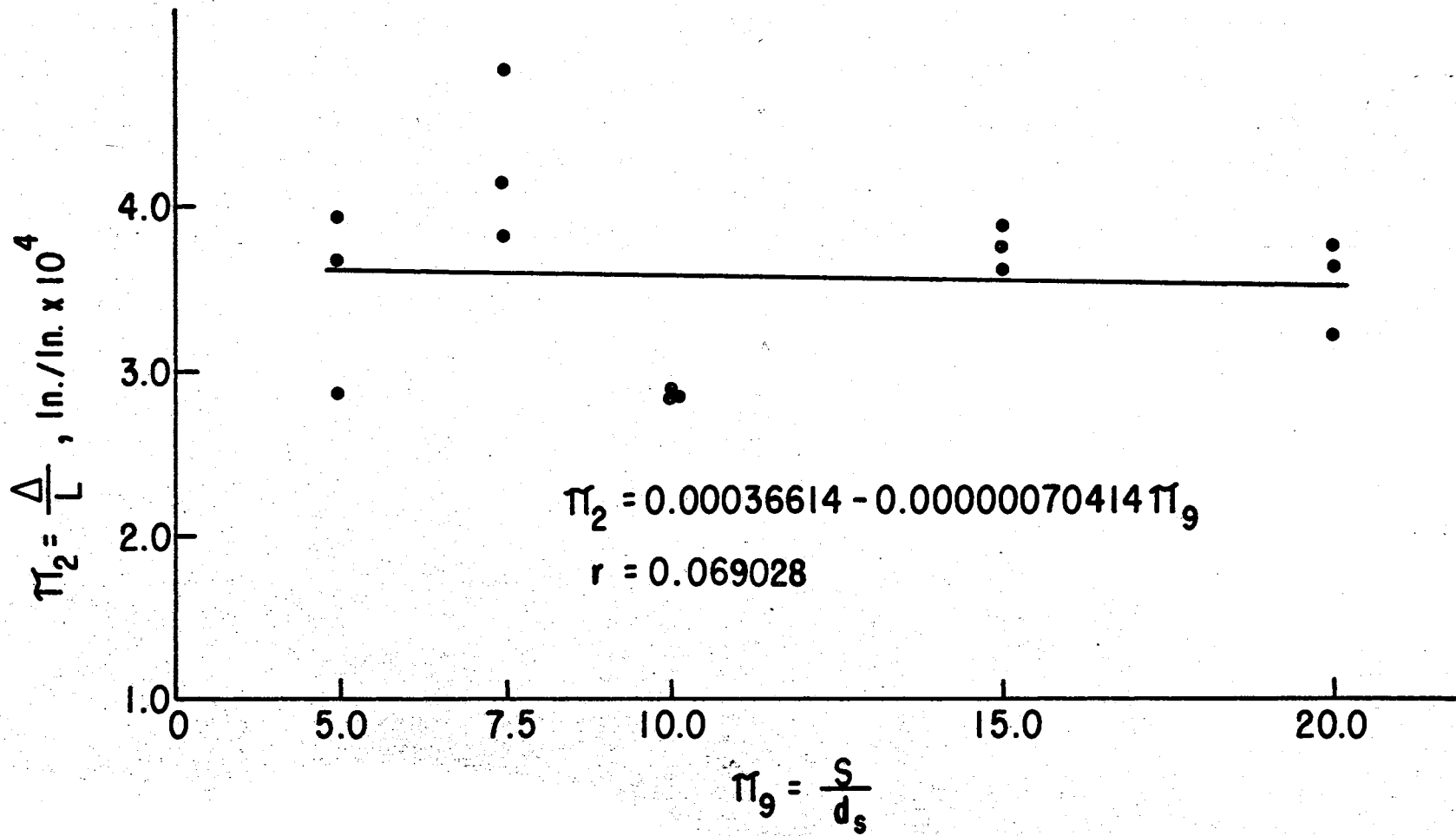


Figure 18. Data Plot, Δ/L Versus S/d_s

TABLE VIII
 DATA FOR REGRESSIONAL ANALYSIS AND BEST FIT CURVE,
 SPACING EFFECT OF REINFORCEMENT ON PANEL
 DEFLECTION AT MIDSPAN, UNCRACKED PANELS

s/d_s	Δ/L
20.0	0.0003625
20.0	0.0003750
20.0	0.0003208
15.0	0.0003625
15.0	0.0003875
15.0	0.0003750
10.0	0.0002833
10.0	0.0002833
10.0	0.0002875
7.5	0.0003833
7.5	0.0004833
7.5	0.0004167
5.0	0.0002875
5.0	0.0003958
5.0	0.0003667

Polynomial Equation, $\Delta/L = 0.0003661 - 0.00000070413 \frac{s}{d_s}$

Correlation Coefficient = 0.069028

Standard Deviation = 0.000058866

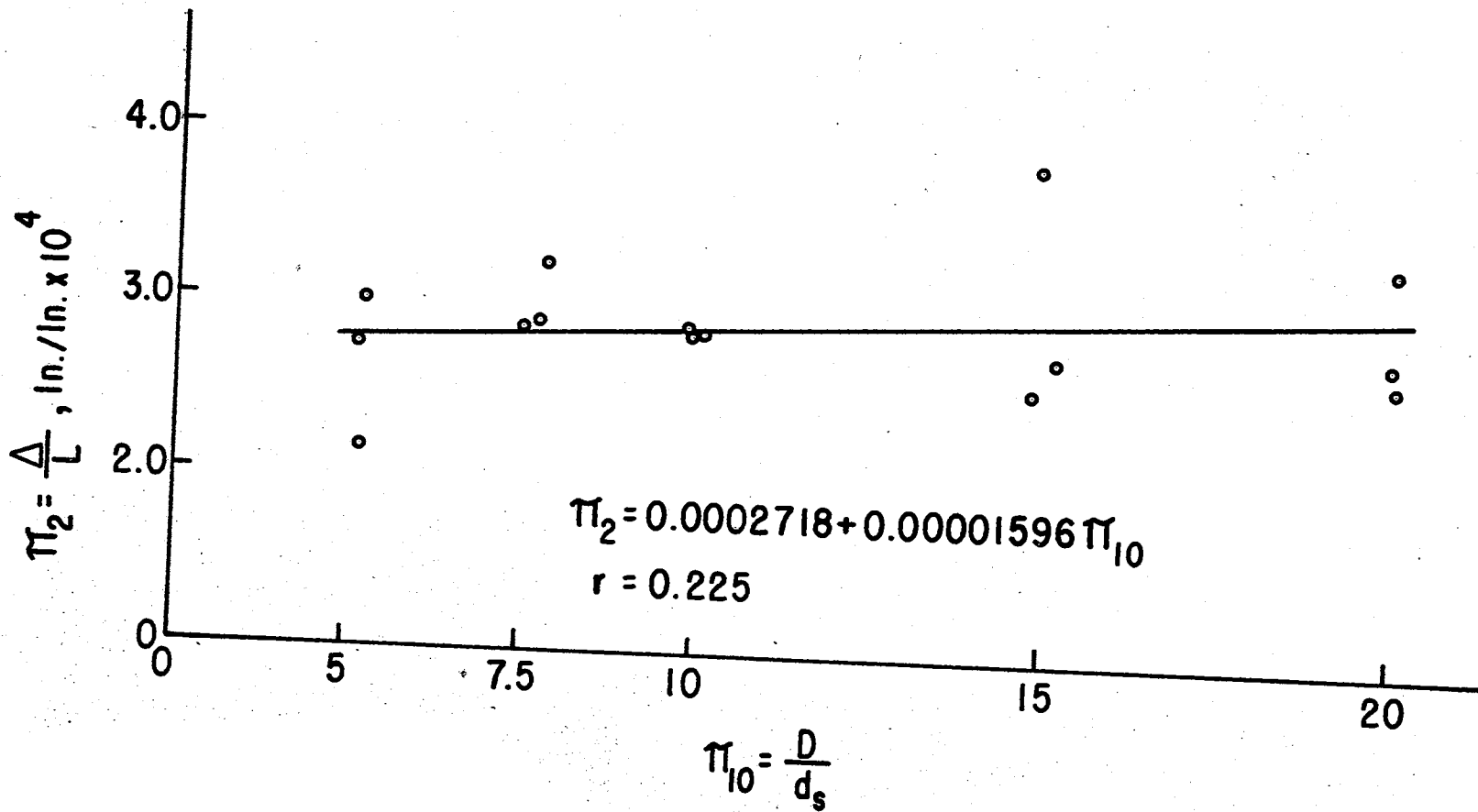


Figure 19. Data Plot, Δ/L Versus D/d_s

TABLE IX
 DATA FOR REGRESSION ANALYSIS AND BEST FIT CURVE,
 DEPTH OF PANEL EFFECT ON PANEL DEFLECTION
 AT MIDSPAN, UNCRACKED PANELS

D/d_s	Δ/L
20.33	0.0003333
20.04	0.0002687
19.87	0.0002792
14.98	0.0002583
15.11	0.0002778
14.72	0.0003889
10.34	0.0002833
9.96	0.0002875
10.24	0.0002833
7.56	0.0002889
8.18	0.0003278
7.89	0.0002889
5.59	0.0003000
5.43	0.0002167
5.40	0.0002750

Polynomial Equation, $\Delta/L = 0.0002718 + 0.000001596 \frac{D}{d_s}$

Correlation Coefficient = 0.225

Standard Deviation = 0.00004

$$\Delta/L = 0.000009983 + 0.000001562 (S/d_s) + 0.000001299 (D/d_s) + 0.01295 (PL^2/EI)$$

The equation of observed versus calculated values of the above prediction equation was $Y = -0.00000001 + 1.000X$ where Y is the observed values of Δ/L and X is the values of Δ/L from the prediction equation. Correlation coefficient was 0.917 and the standard deviation was 0.00006.

Stiffness of Cracked Panels

Data for the deflection tests of cracked panels are tabulated in Tables X, XI and XII. Table X lists deflection pi term values, Δ/Δ_c , for tests in which the independent pi term S/d_s was varied while π_{10} , D/d_s , was held constant. Table XI, lists data recorded for the tests in which the independent pi term D/d_s was varied while π_9 , S/d_s , was held constant. Experimental data showing values of π_4 , Δ/Δ_c , for four values of π_9 , S/d_s , are shown with the equation of the plot in Figure 20. Data are given in Table X. The equation was obtained by least squares multiple regression analysis and is of the quadratic form, $Y = A + B_1X + B_2X^2$. The best fit equation of the curve is:

$$\Delta/\Delta_c = 1.38822 - 0.115318 (S/d_s) + 0.00730266 (S/d_s)^2$$

The correlation coefficient is 0.46548 and the standard deviation 0.2148. Spacing effects of reinforcement on deflection of cracked panels was not significant at the 0.95 confidence level.

The relationship between the deflection pi term and the depth in term for cracked panels is shown in Figure 21. Data is given in Table

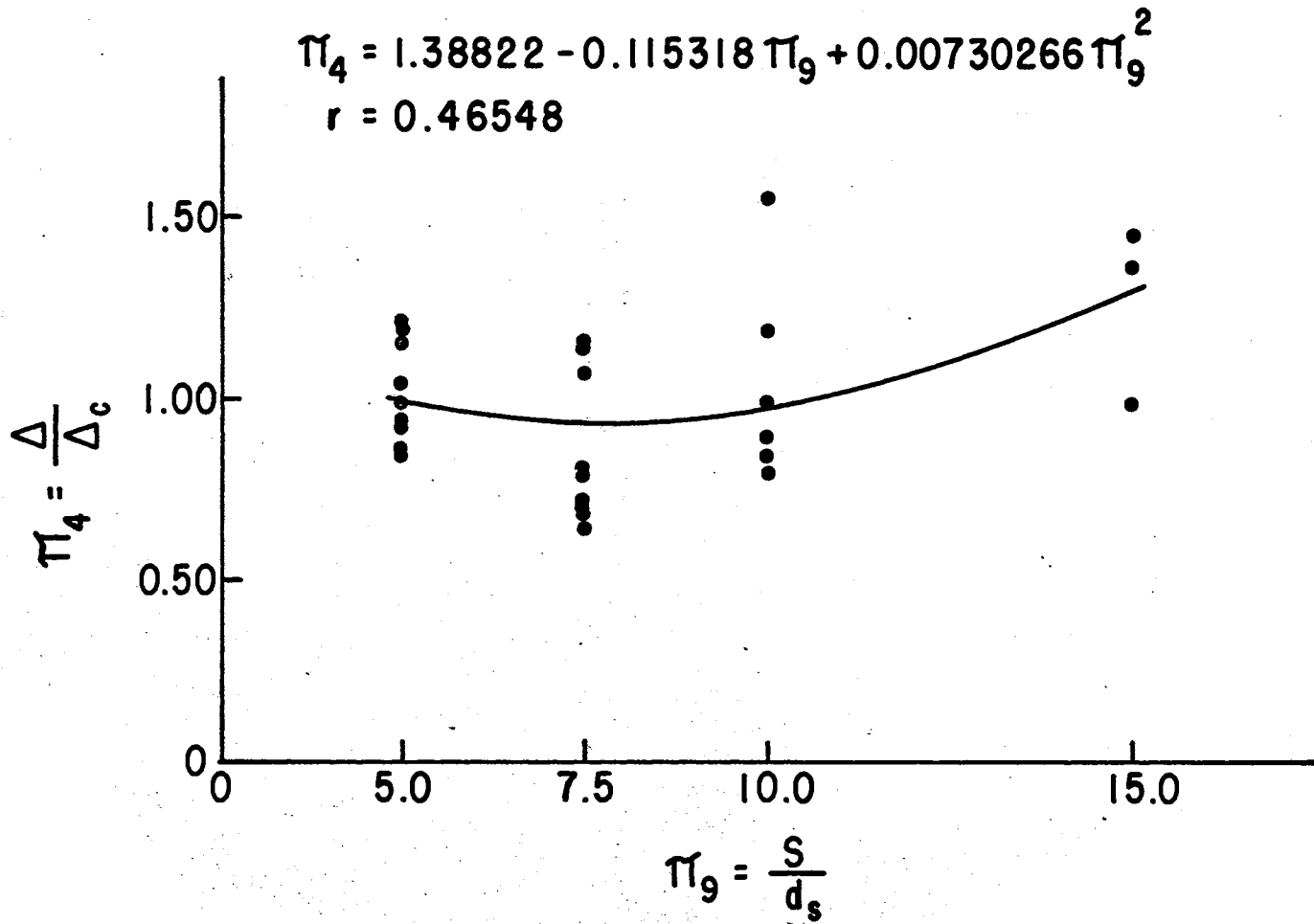


Figure 20. Data Plot, Δ/Δ_c Versus S/d_s

TABLE X
 DATA FOR REGRESSION ANALYSIS AND BEST FIT CURVE,
 SPACING EFFECTS OF REINFORCEMENT ON MEASURED
 VERSUS COMPUTED DEFLECTION, CRACKED PANELS

S/d_s	Δ/Δ_c
15.0	1.4457
15.0	1.3777
15.0	0.9964
10.0	1.5670
10.0	1.1970
10.0	0.9002
10.0	0.9973
10.0	0.7994
10.0	0.8400
7.5	0.6435
7.5	0.6985
7.5	0.8093
7.5	0.6978
7.5	0.7049
7.5	0.7895
7.5	1.0762
7.5	1.1649
7.5	1.1436
5.0	1.2144
5.0	1.1671
5.0	1.1984
5.0	0.9193
5.0	0.9949
5.0	1.0496
5.0	0.8608
5.0	0.8570
5.0	0.9408

Polynomial Equation, $\Delta/\Delta_c = 1.38822 - 0.1153 S/d_s + 0.0073027 (S/d_s)^2$

Correlation Coefficient = 0.4655

Standard Deviation = 0.21488

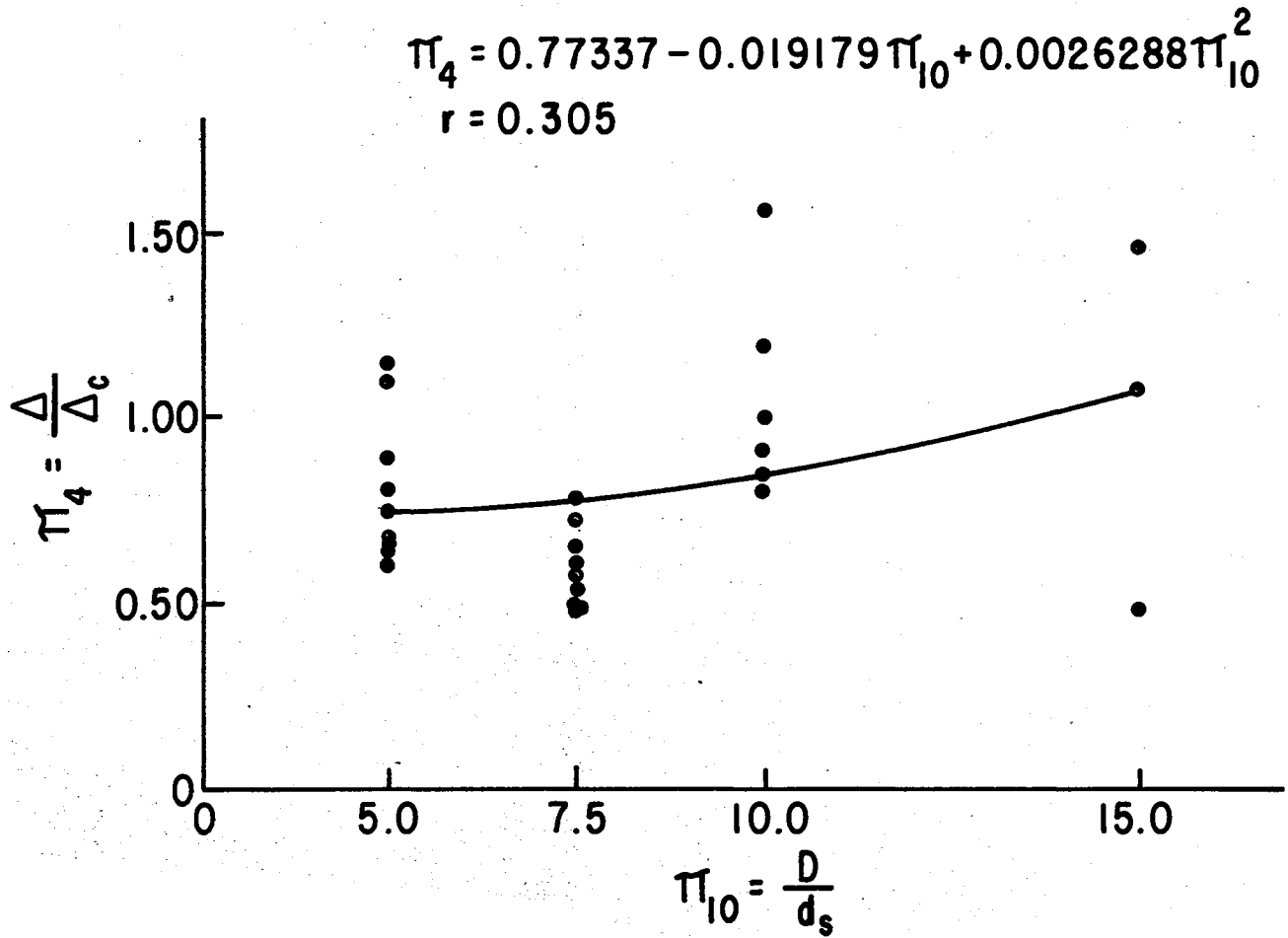


Figure 21. Data Plot, Δ/Δ_c Versus D/d_s

TABLE XI
 DATA FOR REGRESSION ANALYSIS AND BEST FIT CURVE,
 DEPTH OF PANEL EFFECT ON MEASURED VERSUS
 COMPUTED DEFLECTION, CRACKED PANELS

D/d_s	Δ/Δ_c
15.0	0.4891
15.0	1.4595
10.0	1.1970
10.0	1.5670
10.0	0.9002
10.0	0.9973
10.0	0.7994
10.0	0.8400
7.5	0.7220
7.5	0.6015
7.5	0.4936
7.5	0.5331
7.5	0.4943
7.5	0.4913
7.5	0.7825
7.5	0.6573
7.5	0.6753
5.0	0.6876
5.0	0.6423
5.0	0.8063
5.0	0.7574
5.0	0.6008
5.0	0.6624
5.0	1.1586
5.0	1.1025
5.0	0.8879

Polynomial Equation, $\Delta/\Delta_c = 0.77337 - 0.01918 D/d_s + 0.0026288 (D/d_s)^2$

Correlation Coefficient = 0.30586

Standard Deviation = 0.28323

XI. The equation for the deflection Δ term versus the depth d_s term, obtained by least squares multiple regression analysis, is of the quadratic form, $Y = A + B_1X + B_2X^2$. The equation is:

$$\Delta/\Delta_c = 0.77337 - 0.019179 (D/d_s) + 0.0026288 (D/d_s)^2$$

The correlation coefficient is 0.305 and the standard deviation is 0.2832. The effect of depth of panel on deflection of cracked panels was found to be not significant at the 0.95 confidence level.

The reinforcement ratio, p , could not be held constant while varying spacing of reinforcement and depth of panel for a single wire diameter. Therefore, a regression analysis was conducted to determine if the reinforcement ratio had a significant effect on the computed versus measured deflection. Data used are given in Table XII. Results of the least squares multiple regression analysis of the deflection Δ term for cracked panels and the reinforcement ratio, p , are shown in Figure 22. The equation of the best fit plot is of the quadratic form $Y = A + B_1X + B_2X^2$. The equation is:

$$\Delta/\Delta_c = 2.1875 - 1.1803 (p) + 0.2419 (p)^2$$

The correlation coefficient is 0.132887 and the standard deviation is 0.2785. Effects of per cent of reinforcement on cracked panel deflection was found to be not significant at the 0.95 confidence level.

Prediction Equation, Cracked Panels

The final form of the prediction equation for deflection of cracked panels was also determined by least squares multiple regression analysis. The prediction equation, combining the three dimensionless parameters,

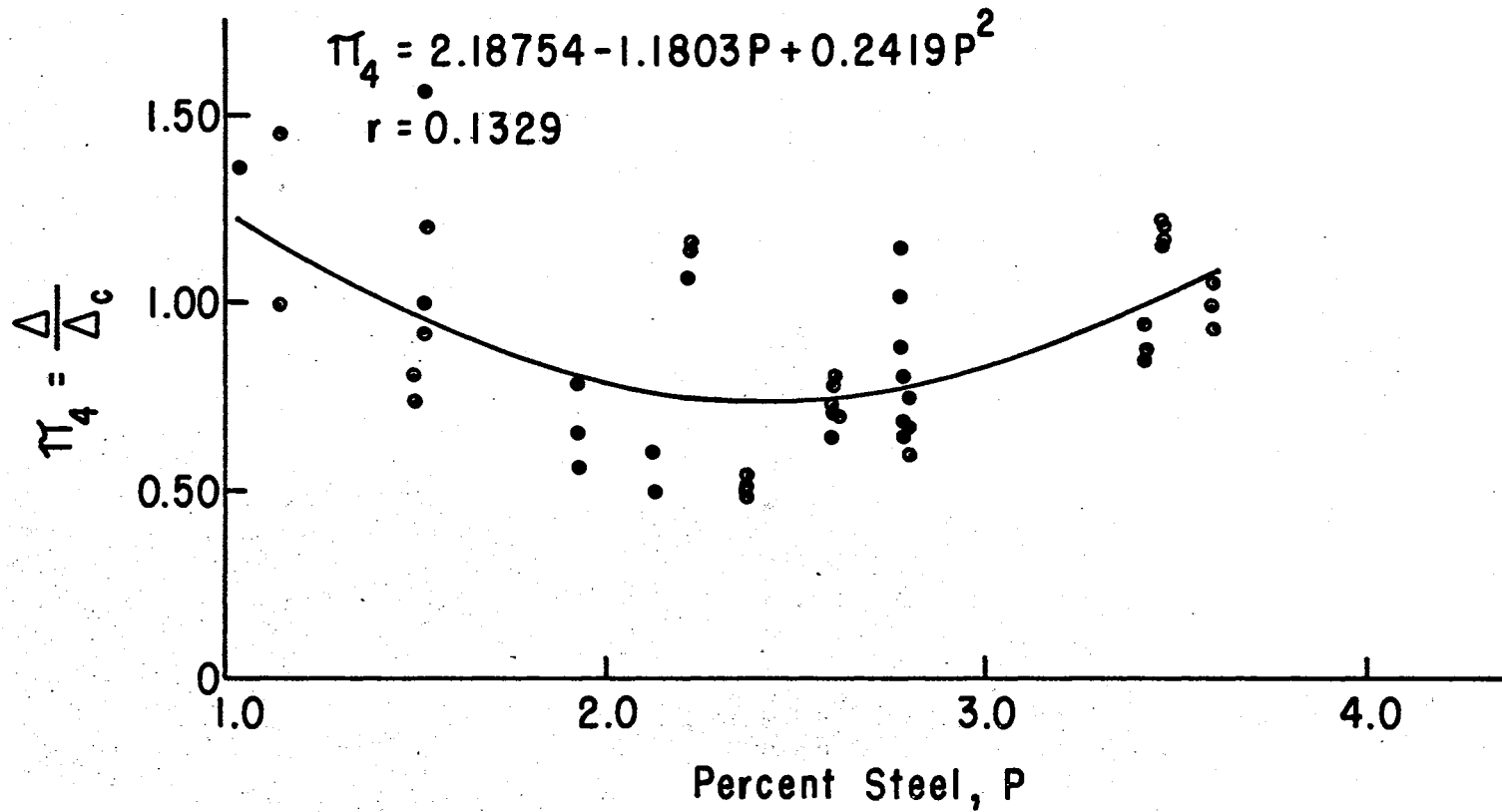


Figure 22. Data Plot, Δ/Δ_c Versus p

TABLE XII

DATA FOR REGRESSION ANALYSIS AND BEST FIT CURVE,
PER CENT REINFORCEMENT EFFECT ON MEASURED VERSUS
COMPUTED DEFLECTION, CRACKED PANELS

P	Δ/Δ_c	P	Δ/Δ_c
1.04	1.3777	2.60	0.6978
1.05	1.4595	2.60	0.7049
1.06	0.4891	2.60	0.7895
1.14	1.4457	2.78	0.8063
1.14	0.9964	2.78	0.6423
1.50	0.8400	2.78	0.6876
1.50	0.7994	2.78	1.1025
1.52	0.9973	2.78	1.1586
1.52	0.9002	2.80	0.6624
1.52	1.1970	2.80	0.6008
1.52	1.5670	2.80	0.7574
1.93	0.5753	3.42	0.8608
1.93	0.6573	3.42	0.8570
1.93	0.7825	3.42	0.9408
2.12	0.4936	3.47	1.2144
2.12	0.6015	3.47	1.1671
2.12	0.7220	3.47	1.1984
2.22	1.0762	3.60	0.9193
2.22	1.1649	3.60	0.9949
2.22	1.1436	3.60	1.0496
2.38	0.4913		
2.38	0.4943		
2.38	0.5331		
2.60	0.6435		
2.60	0.6985		
2.60	0.8093		

Polynomial Equation, $\Delta/\Delta_c = 2.18754 - 1.1803p + 0.2419 p^2$

Correlation Coefficient = 0.132887

Standard Deviation = 0.2785

resulted in a higher correlation coefficient than that obtained for any of the individual pi term plots. The prediction equation is of the quadratic form $Y = A + B_1X_1 + B_2X_1^2 + B_3X_2 + B_4X_2^2 + B_5X_3 + B_6X_3^2$, or:

$$\begin{aligned} \Delta/\Delta_c = & 8.698 - 0.7389 (S/d_s) + 0.02934 (S/d_s)^2 - 0.2975 (D/d_s) \\ & + 0.009945 (D/d_s)^2 - 0.9515 (p) + 0.05074 (p)^2 \end{aligned}$$

Correlation for the above equation is 0.637 and the standard deviation is 0.21662. The equation for observed versus calculated values of deflection is $Y = 0.000269 + 0.9997 X$ where Y is the observed values of Δ/Δ_c and X is the predicted values of Δ/Δ_c from the prediction equation.

Ultimate Strength of Panels

Ultimate strength properties for the two test series of panels is tabulated in Table XIII and Table XIV. Table XIII lists ultimate load versus computed ultimate load for fifteen panels with five values of S/d_s , with three replications of each, and the depth term D/d_s held constant. Table XIV lists ultimate load versus computed load for fifteen panels with five values of D/d_s , with the reinforcement spacing pi term S/d_s being held constant.

The ratio of ultimate load, P_u , to computed ultimate load, P_c , for the panels with five values of S/d_s is shown in Figure 24. The intercept and the slope of the line, of the form $Y = A + BX$, was obtained by linear regression for the data plotted in Figure 23. Y is the dependent variable P_u/P_c and X is the independent variable S/d_s . The intercept of the line is A and the slope of the line is given as B. The best fit equation of the line, determined from the data plotted, is:

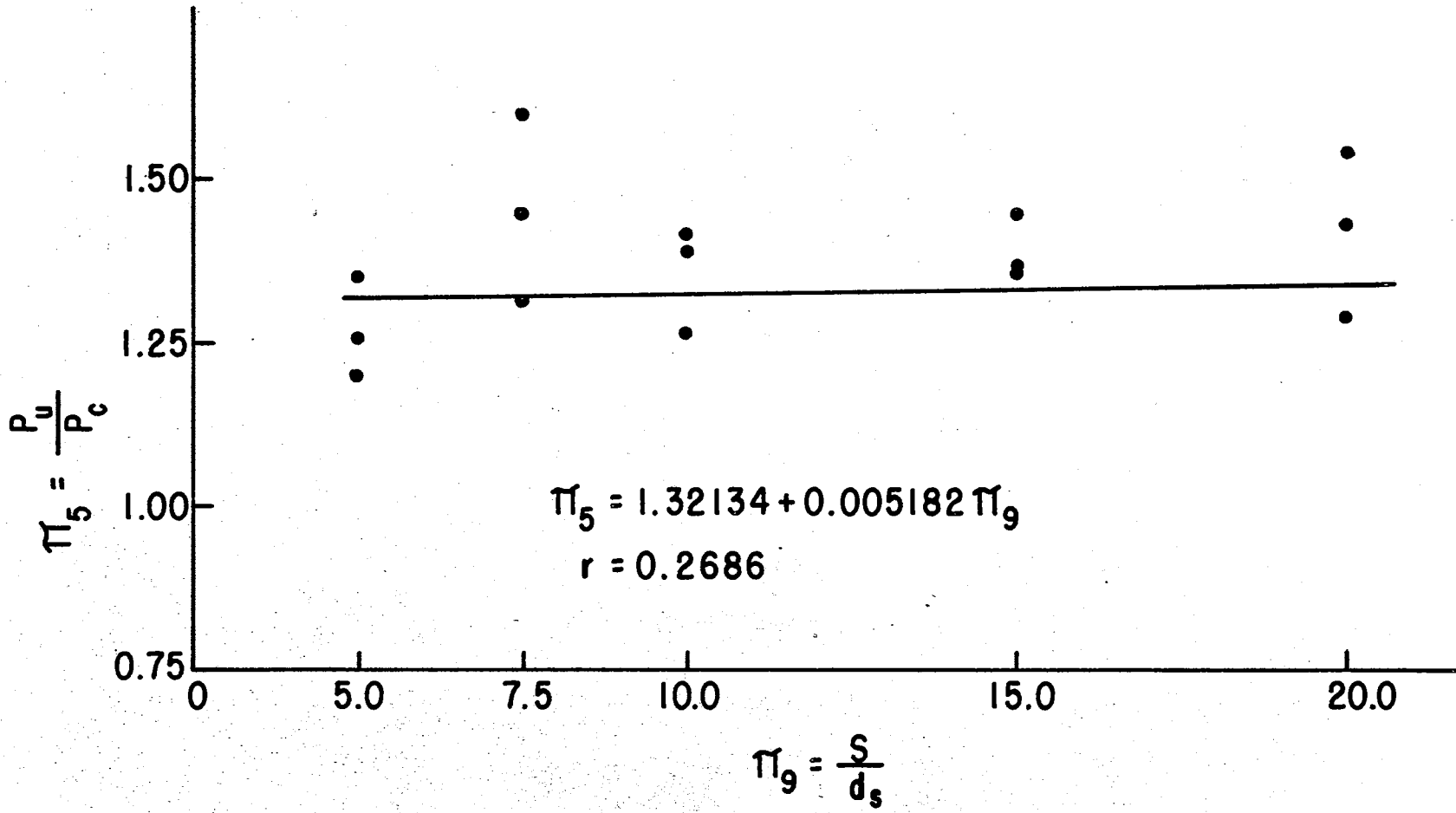


Figure 23. Data Plot, P_u/P_c Versus S/d_s

TABLE XIII

DATA FOR REGRESSION ANALYSIS AND BEST FIT CURVE,
SPACING EFFECT OF REINFORCEMENT ON RATIO OF
MEASURED VERSUS COMPUTED ULTIMATE LOAD

s/d_s	P_u/P_c
20.0	1.4228
20.0	1.2876
20.0	1.5476
15.0	1.3552
15.0	1.4488
15.0	1.3599
10.0	1.4192
10.0	1.3852
10.0	1.2785
7.5	1.4543
7.5	1.6097
7.5	1.3247
5.0	1.2092
5.0	1.3516
5.0	1.2597

Polynomial Equation, $P_u/P_c = 1.32134 + 0.00051822$

s/d_s

Correlation Coefficient = 0.26865

Standard Deviation = 0.10748

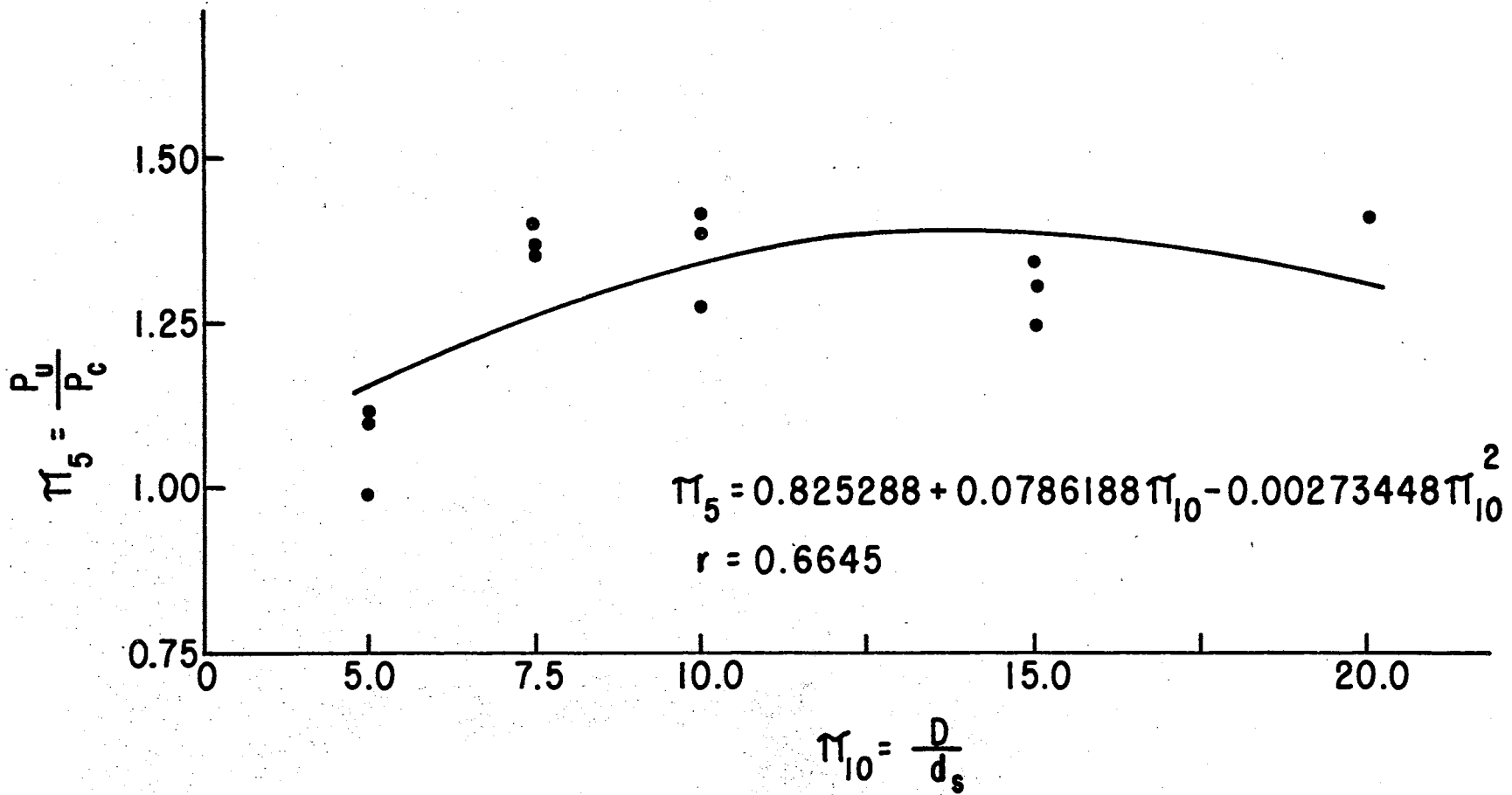


Figure 24. Data Plot, P_u/P_c Versus D/d_s

TABLE XIV
 DATA FOR REGRESSION ANALYSIS AND BEST FIT CURVE,
 DEPTH OF PANEL EFFECT ON RATIO OF MEASURED
 VERSUS COMPUTED ULTIMATE LOAD

D/d_s	P_u/P_c
20.0	1.4123
15.0	1.3023
15.0	1.3415
15.0	1.2416
10.0	1.2785
10.0	1.3952
10.0	1.4192
7.5	1.3580
7.5	1.3988
7.5	1.3685
5.0	0.9925
5.0	1.1048
5.0	1.1161

Polynomial Equation, $P_u/P_c = 0.82588 + 0.07862$

$D/d_s - 0.0027345$

$(D/d_s)^2$

Correlation Coefficient = 0.6645

Standard Deviation = 0.10603

$$P_u/P_c = 1.32133 + 0.0051822 (S/d_s)$$

The correlation coefficient for the above equation is 0.26865 and the standard deviation is 0.1074798. Effects of reinforcement spacing on ultimate load were not significant at the 0.95 confidence level.

Values of P_u/P_c for five values of D/d_s and the equation of the regression line are shown in Figure 24. The equation of the curve plotted for ultimate strength of panels as a function of depth is shown in Figure 25. The curve was obtained for best fit using the least squares multiple regression analysis program and is of the form, $Y = A + BX + BX^2$. The equation is:

$$P_u/P_c = 0.825288 + 0.0786188 (D/d_s) - 0.0027345 (D/d_s)^2$$

The correlation coefficient is 0.305859 and the standard deviation is 0.28323. Depth effects on ultimate load were not significant at the 0.95 confidence level.

Prediction Equation, Ultimate Strength

The final form of the prediction equation for $P_u/P_c = f[(S/d_s), (D/d_s)]$ is given below. The equation obtained, of the partial quadratic form, is:

$$P_u/P_c = 0.6679 + 0.005711 (S/d_s) + 0.09955 (D/d_s) - 0.003584 (D/d_s)^2$$

The correlation coefficient is 0.637 and the standard deviation is 0.10973. The equation of observed vs. calculated values of $Y = 0.00089172 + 1.0007X$, where Y is the observed values of P_u/P_c and X is the computed values of P_u/P_c from the prediction equation.

CHAPTER XI

VALIDATION TESTS

Because of the limitations imposed on the original test series of placement of all reinforcement at the center of the panel, the neutral axis of uncracked panels, and the use of the same wire size of all spacings, a validation of all prediction equations was not attempted. Instead, a test was conducted to determine if spacing effects would have an influence on panel stiffness and ultimate strength if wire sizes were varied and the amount of steel, or p , were held constant.

Three wire sizes were selected for the test and two panels were cast with each of the three wire sizes. The test was limited to six panels so all could be cast from the same batch of concrete. The panels were approximately the same size as the original test panels, 1.5 in. in depth and 9.0 in. in width. The span was the same as the original test panels for 1.35 in. depth, or 24 in. test span. The same mix was used as had been used in previous tests, as given on page 45. Reinforcement was located $3/8$ in. above the bottom of the panel, to provide minimum recommended cover and to obtain more efficient use of the reinforcement. Reinforcement on the original test panels was located at mid-depth, or 0.675 in. from the bottom of the panel.

The three wire sizes selected for the test were No. 14 wire mesh, 1 by 1 in. spacings, No. 10 wire mesh, 6 by 6 in. spacings, and No. 6 wire mesh, 6 by 6 in. spacings. Table XV gives the dimensions of the

wire used and the number of wires needed to give an almost uniform value of A_s , or area of steel. Additional wires were wired in place to the cross wires to give the spacings listed in Table XV. Cross wires were removed from the No. 10 and No. 6 wires added but a short section, approximately 1/2 inch long, was left to improve bond. The number of wires needed for the No. 14 wire reinforcement was double that provided by the mesh spacing so two layers were wired together to give the required amount of wire. Increasing the width of the panels to nine inches provided sufficient space for the above wires and for an edge spacing of one half inch minimum clearance. The casting bed and reinforcement for validation tests is shown in Figure 25.

TABLE XV
PHYSICAL PROPERTIES OF WIRE FOR VALIDATION TESTS

Wire Size Gage	Diameter in.	A_s /Wire in. ²	No. of Wires 9 in. panel	Spacing in.	Total A_s in. ²
14	0.082	0.00527	17	0.5	0.0896
10	0.139	0.01515	6	1.5	0.0909
6	0.197	0.0309	3	3.0	0.0927

The three wire sizes above provide almost the same total area of wire, the area of the No. 6 wire being 1.5% higher, for each of the nine in. wide panels. The depth of the panels was controlled by using 1½ by 1½ in. steel angles for the side forms for the panels. The No. 14 wire was donated by Sheffield Steel Division, Armco Corporation. The other wire mesh was obtained locally and was of American manufacture. All wire was cleaned and brushed to remove any scale or rust prior to in-

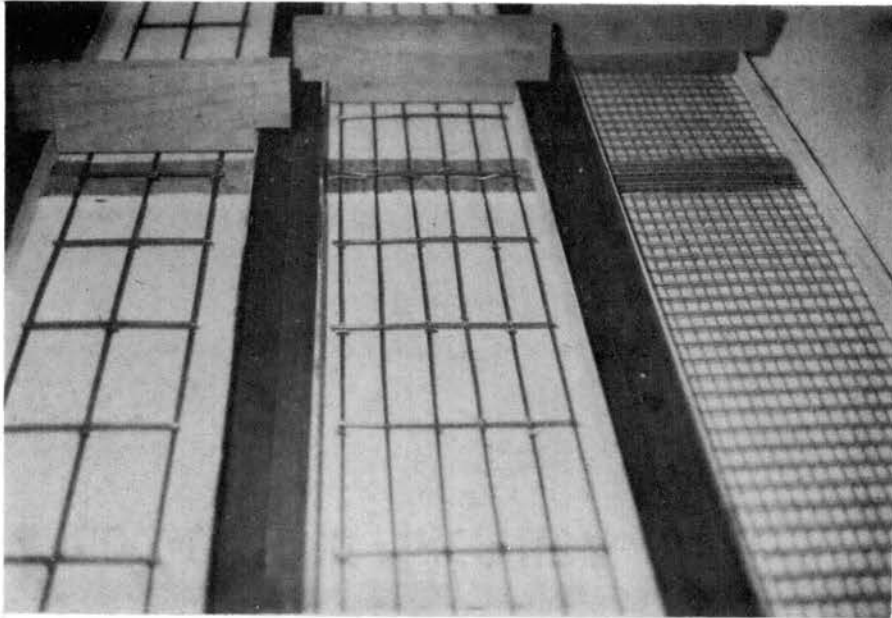


Figure 25. Casting Bed and Reinforcement Used for Validation Tests, Strike Boards in Background. Wire sizes, left to right, No. 6, No. 10 and No. 14.

stalling it in the forms. All wire was tested to determine yield point and minimum strength. A stress-strain diagram for the wire used is shown in Figure 26.

Comparative values for the dimensionless terms, S/d_s , D/d_s and p , plus the wire surface area per unit length of panel are listed Table XVI. The advantage of smaller wire in providing additional surface area for a given value of A_s is obvious. The p terms were included for comparison only since this test was a test of spacing effects only, D and p being constants.

TABLE XVI

WIRE SURFACE AREA AND DIMENSIONLESS TERMS FOR VALIDATION TEST

Wire Size Gage	Surface Area, Wire in. ² /in. panel	S/d_s	D/d_s	p per cent
14	4.375	6.25	18.75	0.895
10	2.623	11.10	11.10	0.910
6	1.855	15.62	7.80	0.929

The six panels tested were cast in the Agricultural Engineering Laboratories and given the identical curing treatment as the panels in the original test. They were removed from the curing bath at 28 days, air dried on open metal racks, and measured for accuracy of dimension. Bending tests of the panels were conducted on the 29th and 30th day after removal from the curing bath.

The panels were loaded in the same manner and data recording followed the same procedure as the original tests. Results of this test are shown in Figure 27. The stress-strain relationship for the concrete

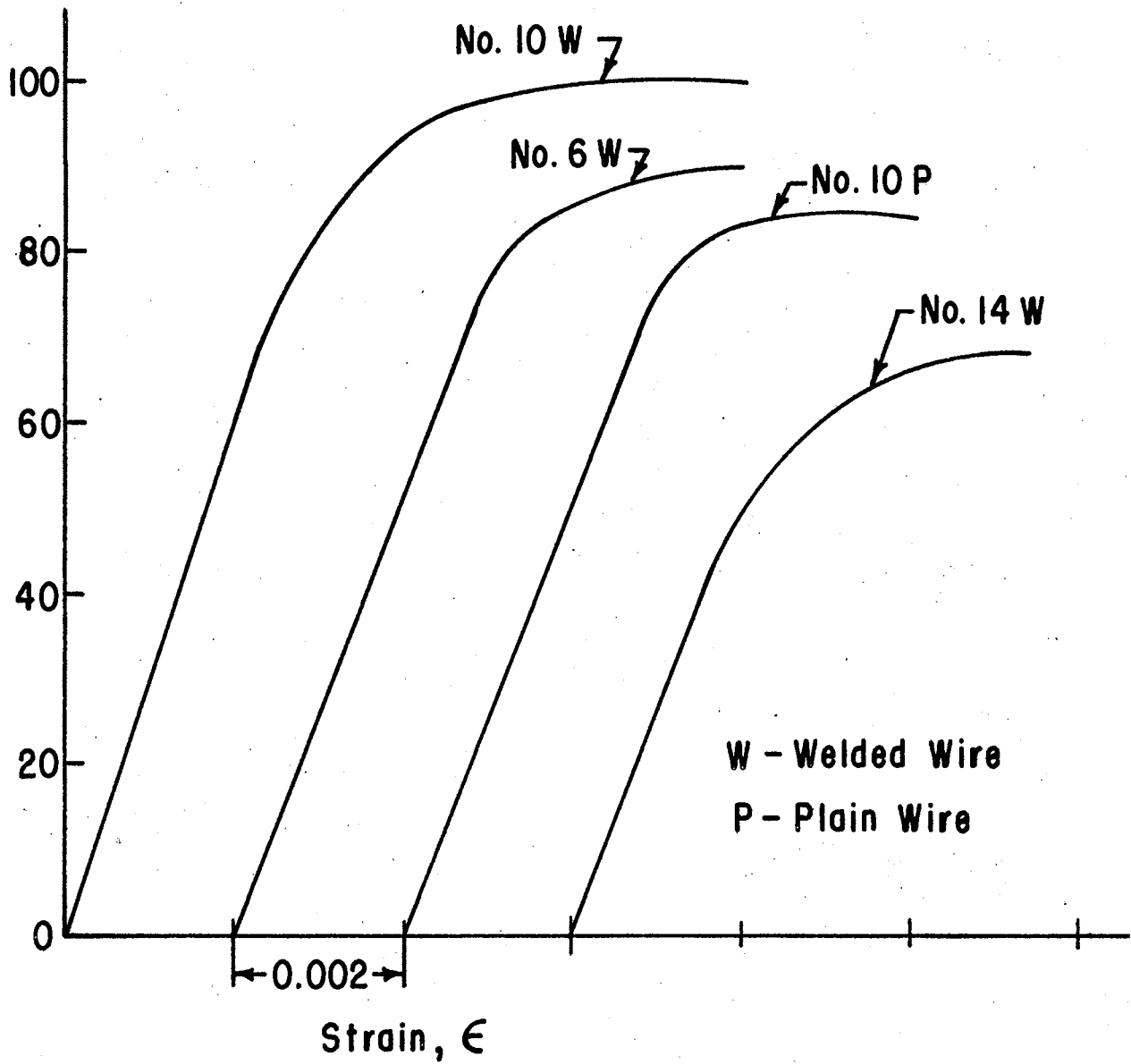


Figure 26. Stress-Strain Plot, Wire for Validation Tests

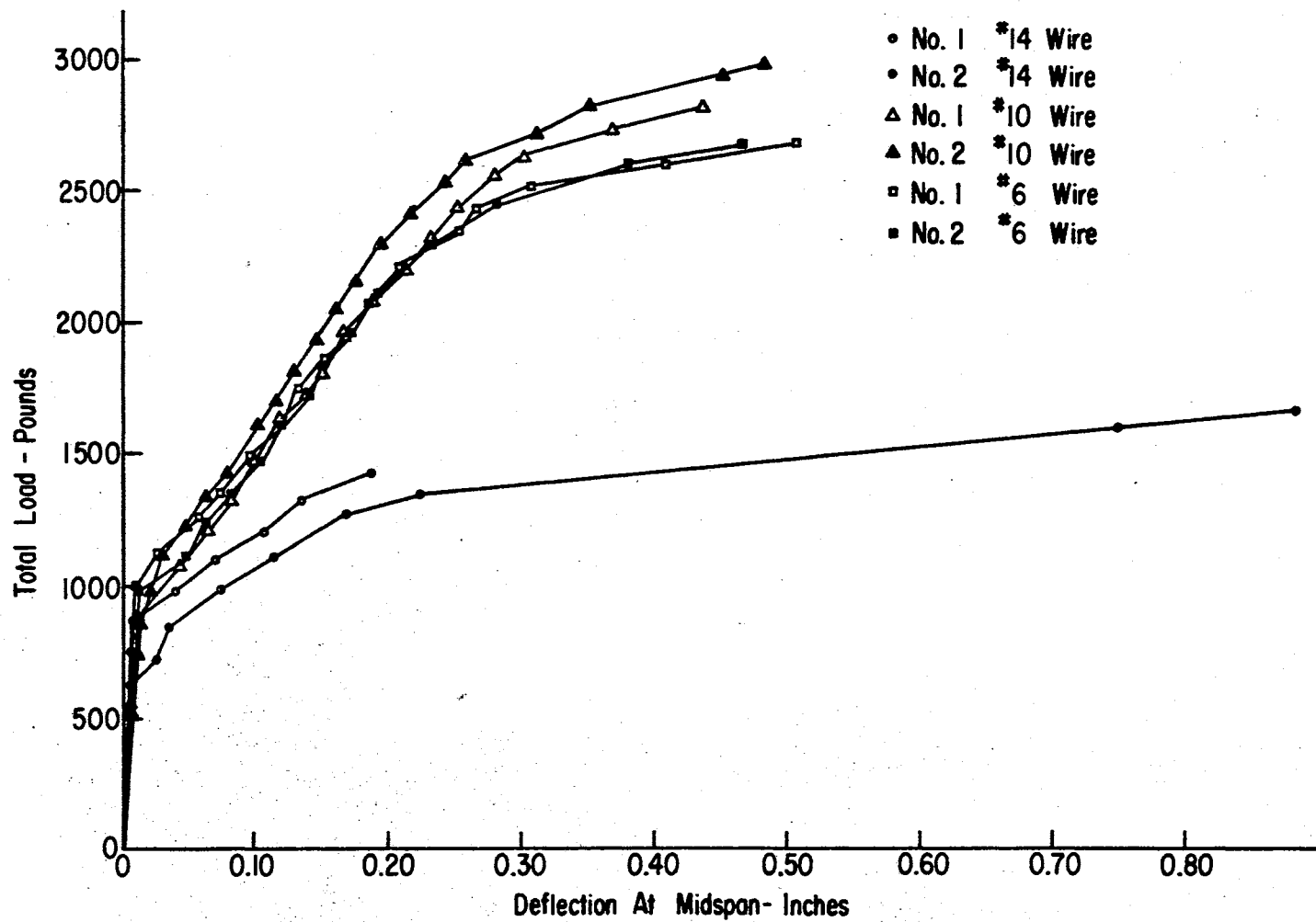


Figure 27. Plot of Validation Test Data

test cylinders for the validation tests is shown in Figure 28. Since only panels with No. 6 and No. 10 wire performed well and only two data points would be available for plotting deflection or ultimate moment equations obtained by regression analysis, no analysis was made.

The panels with 14 gage wire reinforcement failed at much lower loads than the other two sets of panels. Panel 14-1 failed after excessive deflection, primarily due to voids at the crosswires and poor bond, as shown in Figure 29. The close spacing of the cross wires had interfered with the placement of the aggregate and a poor bond was obtained at crosswires. Panel 14-2 failed due to stratification of the concrete in placing and finishing, resulting in a large section spalling off at the compressive surface of the concrete. This failure is shown in Figure 30. Stratification was due to overworking the concrete in an attempt to work all aggregate down through the small mesh of the No. 14 wire. Ultimate loads are given in Table XI.

TABLE XVII

ULTIMATE LOADS FOR VALIDATION TESTS

Panel No.	S/d_s	P_c , Pounds	P_u , Pounds	% Design Load
14-1	6.25	1616	1635	101.2
14-2	6.25	1616	1435	88.7
10-1	11.10	2140	2820	131.5
10-2	11.10	2140	2970	138.5
6-1	15.62	2040	2680	131.3
6-2	15.62	2040	2680	131.3

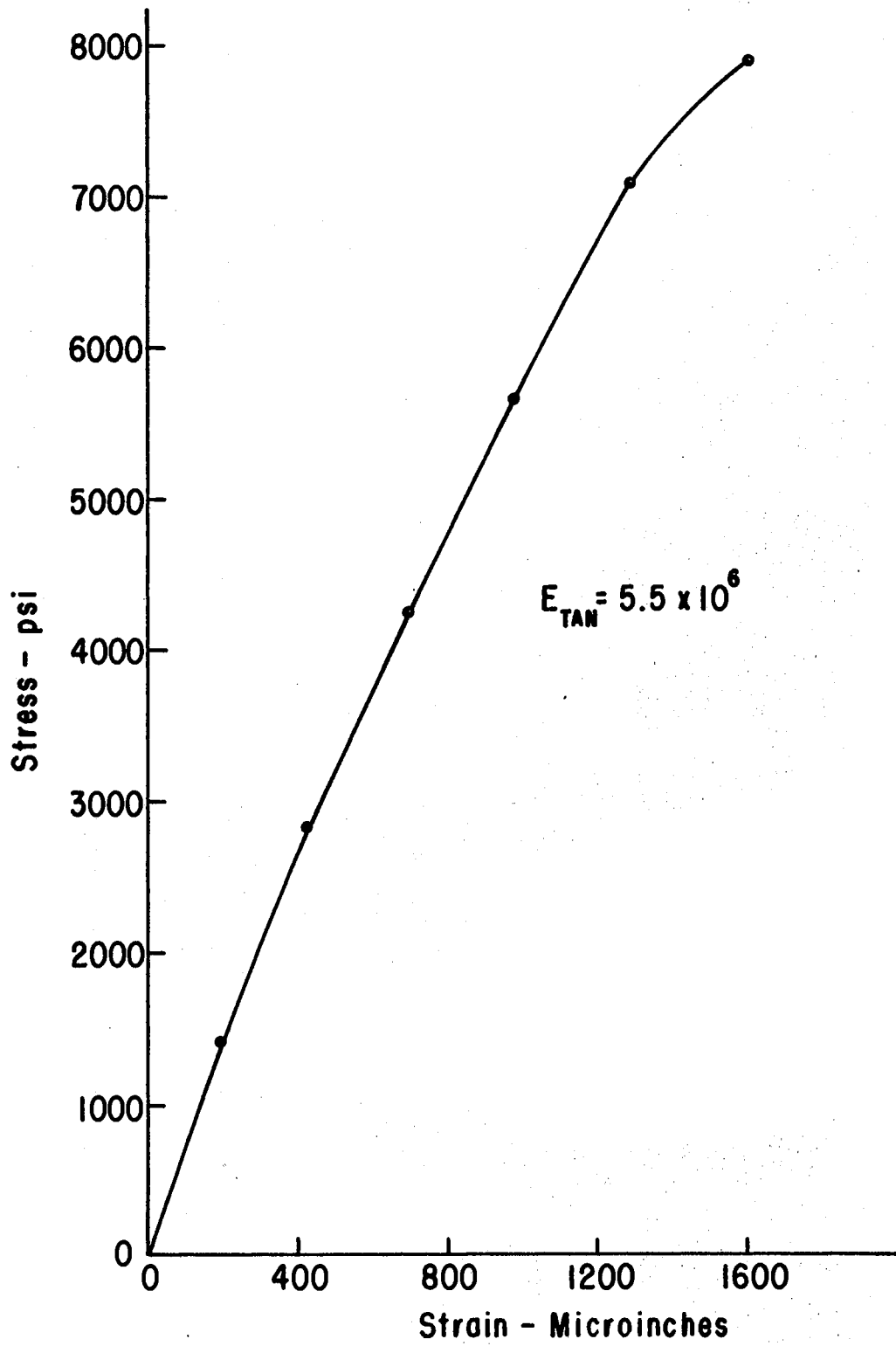


Figure 28. Stress-Strain Plot of Validation Test Cylinder

The above ultimate loads and the graphic presentation of deflection versus load in Figure 27 shows that the panels with No. 10 wire reinforcement were both stronger and stiffer than the panels reinforced with No. 6 wire. Both sets of panels deflected at approximately the same rate, although panel 10-2 deflected less at all loads. When 85 per cent of the ultimate load had been attained, approximately the yield point of the No. 6 wire, deflection increased at a more rapid rate for the panels with the No. 6 wire reinforcement as compared to deflection for those reinforced with No. 10 wire. The reason for this added stiffness and ultimate strength is shown in Figure 26, the No. 10 wire having a yield point of 90,000 psi and an ultimate strength of over 100,000 psi, compared to 80,000 psi yield point and 90,000 psi ultimate strength for the No. 6 wire. As shown in Table XVII, both the panels reinforced with No. 6 wire and panel 10-1 failed at 31% over ultimate design load. Panel 10-2 failed at a slightly higher ultimate load.

Initial cracking for panels with No. 6 and No. 10 wire occurred at loads of approximately 1100 lb. and at strains in the compressive surface of the panel of 250 microinches. Strain increases per unit load was equal in panels 10-1, 6-1 and 6-2 up to yield point for the reinforcement. Strain increased at a slightly lower rate for panel 10-2, which was the stiffest of the four panels. Cracking for all panels occurred at practically the same loads, all panels having a total of four cracks develop by the time the load had increased to 1700 lb. The two panels with No. 14 wire cracked at loads of 723 lb. for panel 14-1 and at 985 lb. for panel 14-2, respectively. Both developed extensive cracking prior to failure, Figures 31 and 32.

The panels reinforced with No. 14 wire were observed to crack at



Figure 29. Failure Section of Panel 14-1, Showing Void Along Crosswire at Failure.

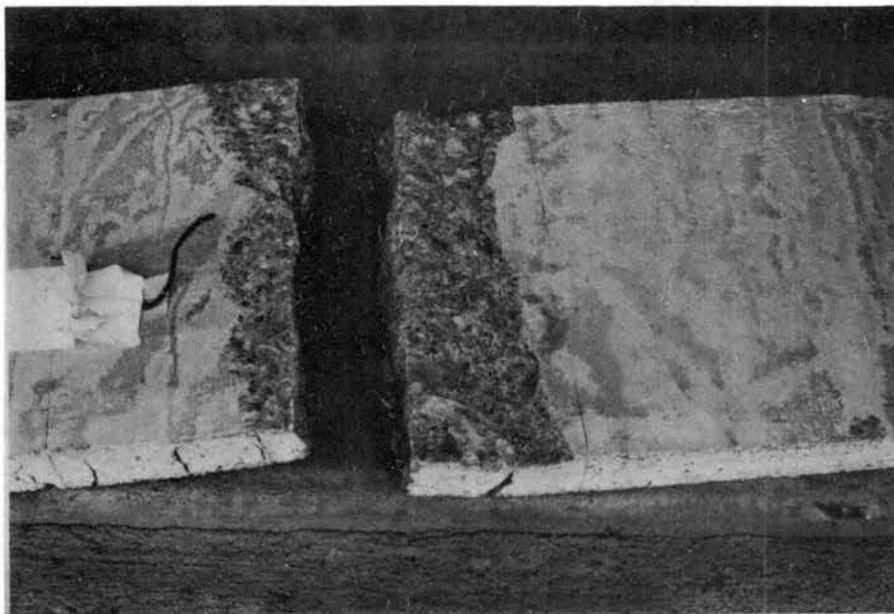


Figure 30. Failure Due to Spalling, or Stratification at Compressive Surface of Panel 14-2.

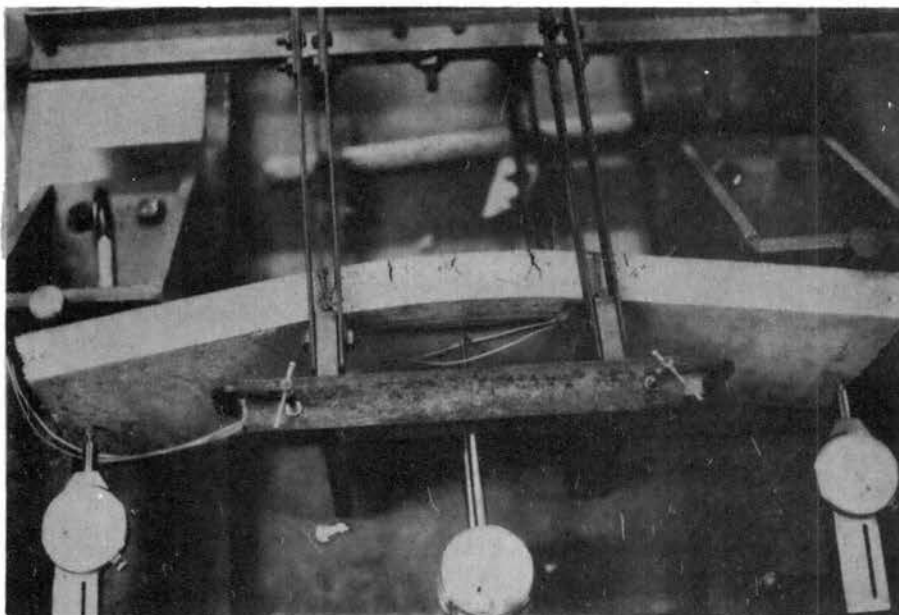


Figure 31. Top View of Panel 14-1 Prior to Failure Showing Cracking and Location of Micro-meter Dial to Measure Deflection.

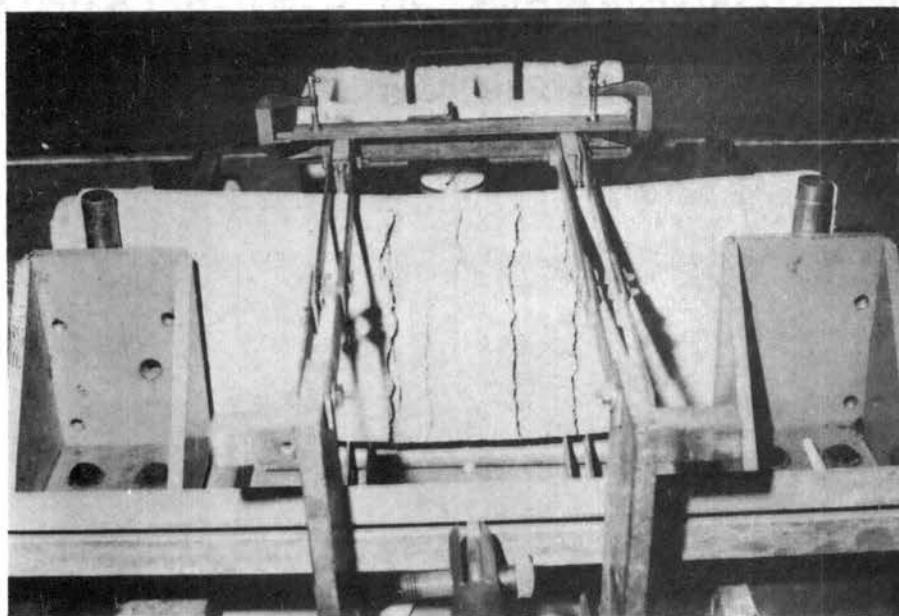


Figure 32. Front View of Panel 14-1 Prior to Failure Showing Crack Development and Crack Spacing.

crosswire locations. Minimum crack spacings were one inch for these panels. This is shown in Figure 33, showing panel 14-1 with three cracks with one in. spacings. Panel 14-2 had five cracks spaced at one inch. All other cracks occurred at cross wire locations. One panel each of the No. 10 wire reinforced panels and the No. 6 wire reinforced panels also failed at, or adjacent to, a cross wire location, as seen in Figure 34. Cracks were also noted at the other cross wire locations in both panels. Both panels reinforced with No. 10 wire and those reinforced with No. 6 wire developed a total of six cracks with an average spacing of two inches.

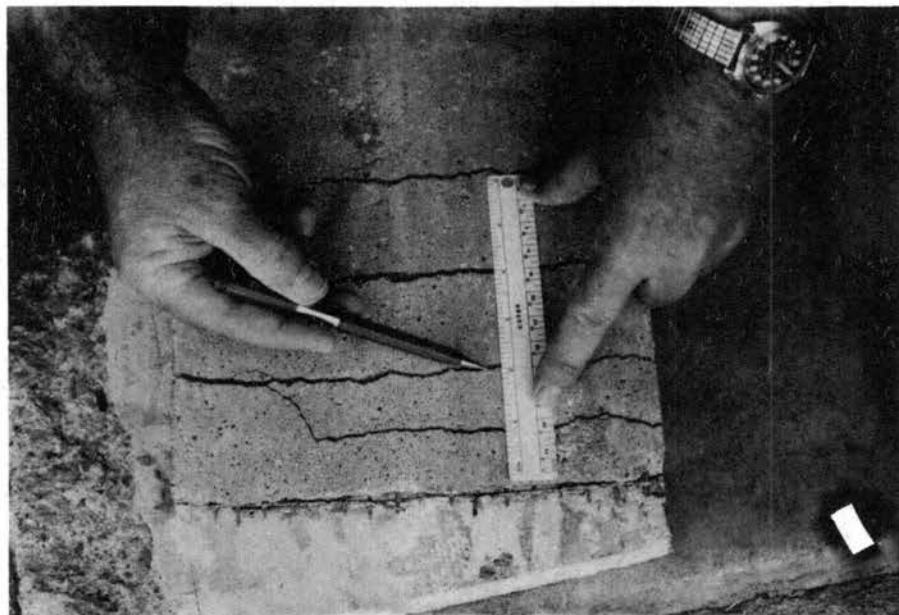


Figure 33. Panel 14-1 Showing Crack Spacing at Cross-wire Locations, With One Inch Crosswire Spacings.

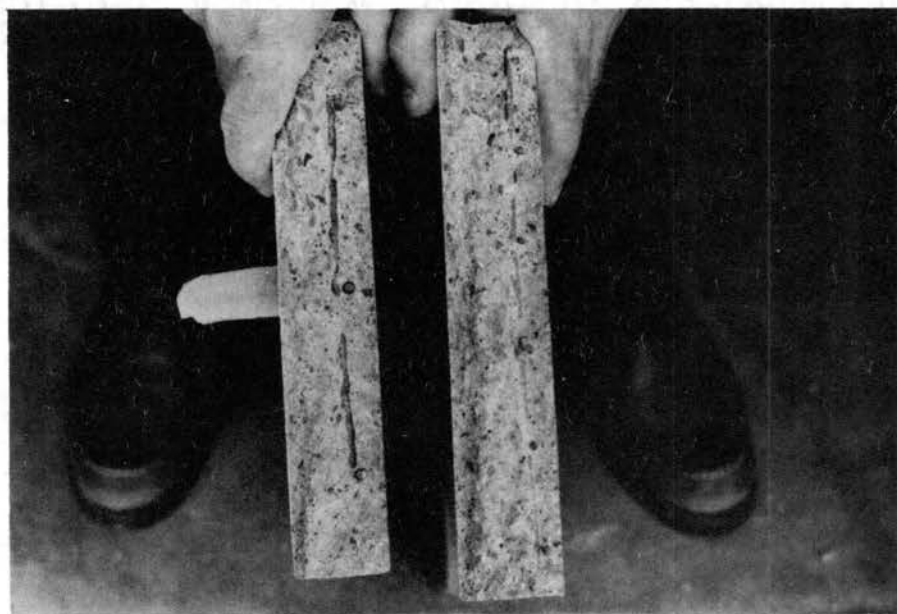


Figure 34. Failure of Panels With Number 6 and 10 Wires With Failure at Crosswires. Failure was outside weld, as shown in the picture.

CHAPTER XII

SUMMARY AND CONCLUSIONS

The primary objective of this study was to determine if proximity effects of reinforcement, or reinforcement spacing, would have a significant effect on the load-deflection performance of uncracked and cracked concrete panels and upon the ultimate load carrying capacity of reinforced concrete panels. Two groups of panels were tested to determine proximity effects by the use of similitude and statistical analysis. One group tested was of constant depth, D , with five reinforcement spacings. The second group had a constant reinforcement spacing, S , and five depths of panel. All panels were of the same width. The length of the panel was proportional to the depth so the group with five depths also had five lengths of panels. Three replications of each depth or spacing of reinforcement treatment were tested, or a total of twenty seven panels.

An experimental design based on the theory of similitude was developed to determine if reinforcement spacing would have a significant effect on load-deflection rate, strain at the compressive surface, and ultimate moment for reinforced concrete panels loaded at the third points. Loads at this location caused uniform moments with zero shear, resulting in a uniform area to measure strain, for the center third of the span. All tests were single cycle monotonic destruction tests of the reinforced concrete panels.

Prediction Equation, Uncracked Panels

The prediction equation developed for determining deflection at the center of the span of an uncracked, reinforced concrete panel was:

$$\Delta/L = 0.00000998 + 0.0129 (PL^2/EI) + 0.00000156 (S/d_s) + 0.0000013 (D/d_s)$$

Prediction Equation, Cracked Panels

The prediction equation developed for determining deflection at the center of the span for a cracked, reinforced concrete panel was:

$$\begin{aligned} \Delta/\Delta_c = & 8.698 - 0.7389 (S/d_s) + 0.02934 (S/d_s)^2 - 0.2975 (D/d_s) \\ & + 0.009945 (D/d_s)^2 - 0.9515 (p) + 0.05094 (p)^2 \end{aligned}$$

Prediction Equation, Ultimate Strength

The prediction developed for determining the ultimate strength and ultimate load of reinforced, concrete panels with closely spaced reinforcement was:

$$P_u/P_c = 0.6697 + 0.005711 (S/d_s) + 0.09955 (D/d_s) - 0.003584 (D/d_s)^2$$

The first prediction equation, $\Delta/L = f[(S/d_s), (D/d_s), (PL^2/EI)]$ shows that the deflection for a specific span is proportional to the load for a given value of L^2/EI , or an uncracked panel of reinforced concrete demonstrates a linear stress-strain-deflection relationship. The effects of spacing and depth of section for constant values of PL^2/EI are not significant at the 0.95 confidence level and proximity effects and, within the limits of this study, will not be a factor in the stiffness of uncracked panels.

The second prediction equation, $\Delta/\Delta_c = f[(S/d_s), (D/d_s)]$, indicates spacing and depth effects on observed versus computed deflection. Since reinforced concrete panels are not a homogeneous material but a composite of concrete and steel, and since deflection at the center of the panels was a function of the extent of cracking and crack location, computed deflections were based on observed cracks and their locations.

Statistical analysis of the Beta terms listed show that none of the parameters tested had a significant effect on panel performance, tested at the 0.95 confidence level. Therefore, proximity effects of reinforcement did not have a significant effect, 0.95 confidence level, on deflection performance of panels tested at stresses less than the yield stress of the reinforcement and the concrete, within the limits of this study.

The third prediction equation, $P_u/P_c = f[(S/d_s), (D/d_s)]$, showed that the recommended ultimate moment and ultimate load was conservative for all panels tested with the exception of the panels with an actual depth of 0.70 in. Spacing effect, as noted in the prediction equation and as shown on the data plot in Figure 24, had no significant effect, 0.95 confidence level, on increased ultimate strength of thin, reinforced concrete panels. Similar results were obtained when the data for depth effect was tested. Therefore, neither spacing effects nor depth effects were significant on ultimate strength of panels in the range tested.

Results of the validation test substantiated the findings of the tests conducted for spacing effects using a single size wire. No difference in ultimate strength was noted for panels with No. 6 wire reinforcement and No. 10 wire reinforcement when the modulus of elasticity

and ultimate strength of the two wire sizes were noted. Panels fabricated with No. 14 wire failed at much lower loads and had excessive deflection prior to failure due to voids and the low yield point of the wire. All panels tested in this series had approximately the same amount of reinforcement.

Increased deflection, or an increased rate of deflection, was noted for the No. 6 wire reinforced panels as compared to the No. 10 wire reinforced panels after 80 per cent of the ultimate load had been reached, or approximately yield point for the No. 6 wire reinforcement. The value of improved stiffness at this point, approximately double design loads, is questionable.

The panels reinforced with No. 14 wire failed primarily because of voids in the concrete, caused by the close spacing of the cross wires, and low yield point of the wire.

Suggestions for Further Study

1. Spacing effects should be investigated at initial cracking to determine if any real advantage is possible with the use of smaller, more closely spaced wire. Such a test would necessitate a continuous monitoring of both deflection and load, or a more sophisticated instrumentation than was available for these tests.

2. Wire sizes smaller than No. 10 are available primarily in galvanized wire. The galvanized wire may have some distinct advantages in farm structures where animal wastes, high humidity and caustic chemicals are commonly encountered. The performance of galvanized wire and cold drawn wire reinforcement should be compared as reinforcement for thin concrete sections to determine the suitability of galvanized wire

for reinforcement with initial cracking and ultimate strength being two test parameters.

A SELECTED BIBLIOGRAPHY

- (1) ACI Committee 324, "Proposed ACI Standards, Minimum Requirements for Thin-Section Precast Concrete Construction", Journal of the ACI, Proceedings, Vol. 59, No. 6, June, 1962, p. 745-753.
- (2) Batson, G. B., "Mechanics of Crack Arrest in Concrete with Closely Spaced Wire Reinforcement, Ph. D. thesis, Carnegie Institute of Technology, January, 1962.
- (3) Billig, Kurt, Structural Concrete, London, MacMillian & Co., Ltd., 1960.
- (4) Billig, Kurt, "CRBI Shell House", Indian Concrete Journal (Bombay), Vol. 28, No. 6, June, 1954, pp. 201-211.
- (5) Cassie, W. Fisher, "Lambot's Boats", Concrete, Vol. 1, No. 11, Nov. 1968, pp. 380-381.
- (6) Ferguson, Phil M. & J. Neils Thompson, "Development Length of High Strength Reinforcing Bars in Bond", Journal of the ACI, Proceedings, Vol. 59, No. 7, July, 1962, pp. 887-922.
- (7) Fukuda, R., "Experimental Studies on Bond Strength Between Cement Paste and Aggregates", Japan Congress on Materials Research, Proceedings, 1967, pp. 147-152.
- (8) Haynes, B. C. and J. W. Simons, "Surface Bonding and Waterproofing Cement Coating for Concrete Block Walls", Georgia Agricultural Experiment Station Research Report No. 30, June 1968.
- (9) Hurd, M. K., "Ferro-Cement Boats", Journal of the ACI, Proceedings, Vol. 66, March, 1969, pp. 202-204.
- (10) Kaplan, M. F., "Strains and Stresses of Concrete at Initiation of Cracking and Near Failure", Journal of the ACI, Proceedings, Vol. 60, No. 7, July, 1963, pp. 853-877.
- (11) Kriz, Ladislav B., "Ultimate Strength Criteria of Reinforced Concrete", ASCE Transactions, Part 1, Vol. 126, 1961, pp. 439-453.
- (12) Little, Wm. A. and Mario Paparoni, "Size Effects in Small-Scale Models of Reinforced Concrete Beams", Journal of the ACI, Proceedings, Vol. 63, Nov. 1966, pp. 1191-1201.

- (13) Lloyd, John P., Hassen M. Rejali, and Clyde E. Kesler, "Crack Control in One-Way Slabs Reinforced With Deformed Welded Fabric", Journal of the ACI, Proceedings, Vol. 66, May, 1969, pp. 366-375.
- (14) Mathey, Robert G. and David Watstein, "Investigation of Bond in Beams and Pullout Specimens With High Strength Deformed Bars", Journal of the ACI, Vol. 32, No. 9, March, 1961, pp. 1071-1090.
- (15) Mensch, Robert, "Theoretical and Experimental Investigation of Concrete Shell Arches for Utility Buildings", M.S. thesis, Oklahoma State University, May, 1962.
- (16) Murphy, Glen, Similitude in Engineering, The Ronald Press Company, New York, 1950.
- (17) Nervi, P. L., Structures, tr. S and M Salvadori, F. W. Dodge, New York, N. Y., 1956.
- (18) Perry, Ervis S. and J. Neils Thompson, "Bond Stress Distribution on Reinforcing Steel in Beams and Pullout Specimens", Journal of the ACI, Proceedings, Vol. 63, Aug. 1966, pp. 865-875.
- (19) Romaldi, James P. and Gordon B. Batson, "Behavior of Reinforced Concrete Beams With Closely Spaced Reinforcement", Journal of the ACI, Proceedings, Vol. 60, No. 6, June, 1963, pp. 775-789.
- (20) Romaldi, James P. and James A. Mandel, "Tensile Strength of Concrete Affected by Uniformly Distributed and Closely Spaced Short Lengths of Wire Reinforcement", Journal of the ACI, Proceedings, Vol. 61, No. 6, June, 1964, pp. 657-670.
- (21) Skoglund, Victor J., Similitude, International Textbook Company, Scranton, Pa., 1967.
- (22) Watstein, David, "Distribution of Bond Stress in Concrete Pull-Out Specimens", Journal of the ACI, Vol. 18, No. 9, May, 1947, pp. 1041-1052.
- (23) Westergaard, H. M., "Stress at a Crack, Size of Crack, and the Bending of Reinforced Concrete", Journal of the ACI, Proceedings, Vol. 30, Nov., Dec., 1933, pp. 93-102.
- (24) Whitney, C. S., "Ultimate Design of Reinforced Concrete", Modern Development in Reinforced Concrete (R/C) No. 11, Portland Cement Assoc., Chicago, 1944.
- (25) "Concrete Reinforced With Glass", Civil Engineering and Public Works Review (London), Vol. 52, No. 615, Sept. 1957, p. 996.

- (26) "Fibrous Reinforcement for Concrete", Chemicals in Building Bulletin CB 68/106, Shell Chemicals, U. K. Ltd.

A P P E N D I C E S

APPENDIX A

PRELIMINARY INVESTIGATIONS

Bond Test

A preliminary test was conducted to determine the minimum bond length required to develop the yield strength of the reinforcing wire. This test consisted of loading three types of wire anchorages in three lengths of test blocks of concrete to determine if pull-out or slip would occur, what bond strength would develop prior to slip and failure, and if failure would be in bond or if the wire would yield. Although pull-out tests are not a true measure of bond as would occur in a reinforced beam, it is a common test to obtain bond characteristics of various types and surface finishes of steel reinforcement.

One factor considered in the experiment was the minimum length of panels to be tested, twelve in., and whether adequate bond stress could be developed in the five in. distance between the load application point and the end of the panel to prevent pull-out of the reinforcement. The second item to be investigated was the comparative bond strength of straight wire and woven or welded wire, and if failure in welded wire specimens would occur at the point of weld in a bond specimen.

A third anchorage was also included, hooked wires to prevent pull-out failures. Therefore, this experiment included three types of wire anchorage, three lengths of bond specimens, and four replications of each, or a total of 36 test specimens.

Wire anchorages tested were:

- 1) Plain wire, ends projecting from the specimen.
- 2) Plain wire, ends hooked and embedded in the concrete.
- 3) Welded wire, one cross wire embedded in the concrete.

Lengths of embedment were:

- 1) 3 inch, minimum length of embedment.
- 2) 4 inch, median length of embedment.
- 3) 5 inch, maximum length of embedment and maximum length of embedment for bond in minimum length test panel.

Casting Procedures

The wire bond test specimens were cast as single wires in the center of a 3 in. by 3 5/8 in. concrete block with depths equal to embedment lengths. Holes were drilled in the bottom of the forms prior to casting the specimens to allow the straight wire and the welded wire to project from the concrete so slippage could be measured and noted at the free, or unloaded end. The concrete mix used was same as used in all tests. The concrete was hand placed and rodded in the forms and the forms were vibrated during the placement of the concrete.

Curing

The specimens were cured for a period of 2 days after placing by covering the forms with wet burlap and keeping them saturated during this time. The specimens were then removed from the forms and cured in water for a period of 26 days, or a total curing time of 28 days. Temperatures were maintained at about 70° during this curing time. After 28 days curing, the pull-out specimens were removed from the water and

placed in a dry location until tested. Tests were conducted 30 days after removal from the curing bath.

Testing Procedures

Pull-out tests were conducted on a universal testing machine. To prevent a conical failure of the concrete at the top of the specimen, around the upper portion of the wire, a bearing plate with a 3/16 in. hole was fabricated to fit the compression head opening of the universal testing machine. The wire was inserted through the hole in the bearing plate and clamped in the upper head of the machine for pull-out tests. The bearing plate and test apparatus are shown in Figure 35.

The tests were conducted using a testing machine load rate of 0.06 in. per minute and end slip of the wire was noted by the dropping of the weigh beam of the machine and visual observation of marks made on the wire projecting from the free end of the concrete bond specimen. The marks were scratches one eighth in. apart on the projecting wire. Tests were continued until failure of the wire occurred or until a total slip of 1/2 in. was noted.

Test results are shown in Table XVIII. All straight wire specimens with one exception, a 5 in. specimen, failed in bond. A second 5 in. specimen slipped once but final failure was a wire failure. The three in. specimens slipped twice during the test prior to final slip failure. All carried higher ultimate bond stress than would be expected from first slip failures. All wires carried stresses in excess of the yield point of the wire prior to ultimate bond failure. All 3 in. embedment specimens with hooked wires and welded wires failed due to wire failures. Therefore, the 4 and 5 in. bond lengths specimens with hooked and welded

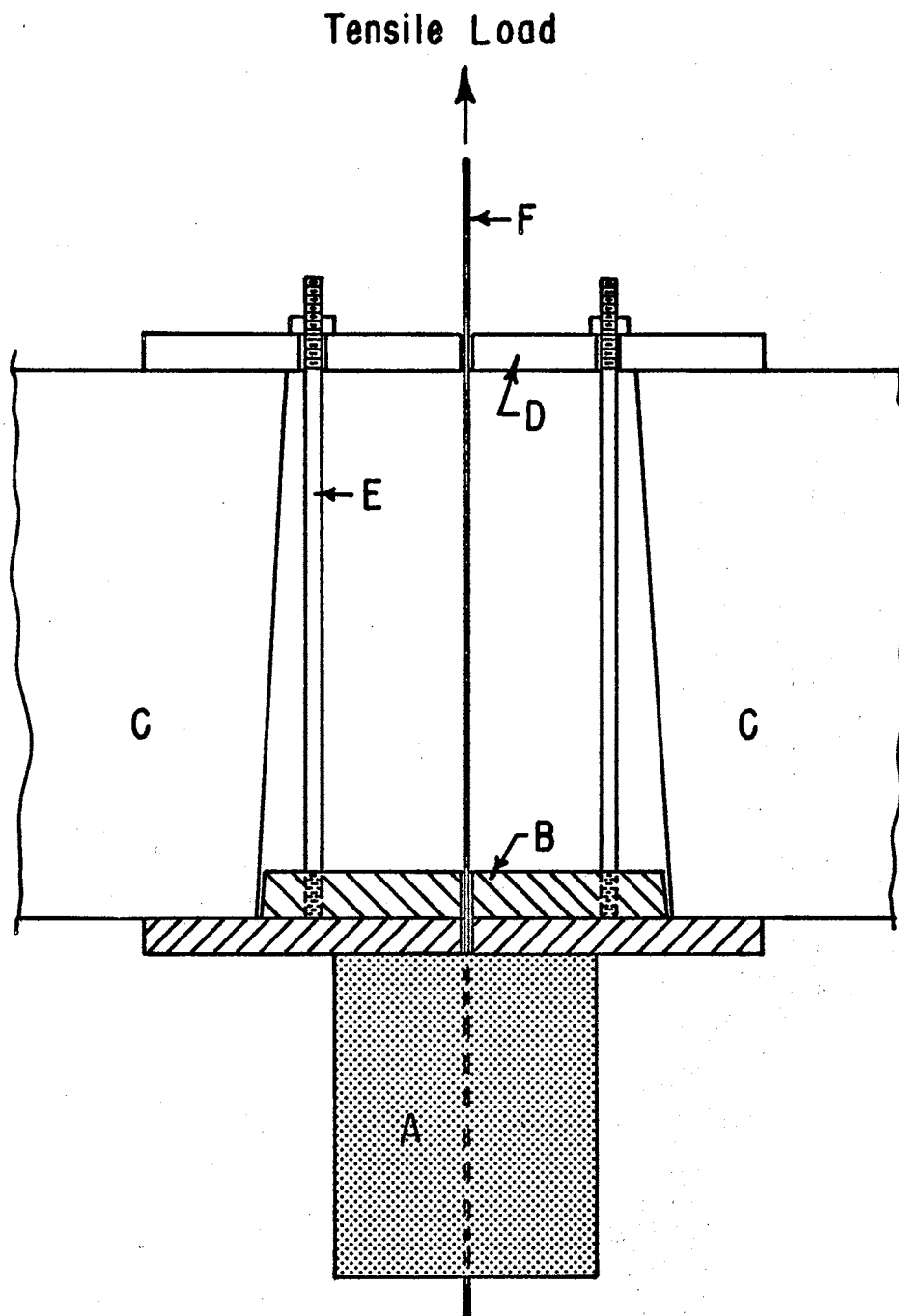


Figure 35. Pull-Out Test Bracket

TABLE XVIII
BOND TEST RESULTS

Specimen Type	First Slip		Second Slip		Ultimate Failure		
	Load lb.	Bond psi	Load lb.	Bond psi	Load lb.	Bond psi	
3" Straight wire	#1	800	630	1000	785	1170	920
	#2	800	630	980	770	1120	880
	#3	720	566			1120	880
	#4	1035	815			1035	815
4" Straight wire	#1	1030	608			1150	680
	#2	1085	640			1300	766*
	#3	1030	608			1250	738
	#4	Wire broken prior to test, no test.					
5" Straight wire	#1	1000	471			1220	580*
	#2	930	438			1120	528
	#3					1275	602*
	#4	1130	533			1180	556
3" Hooked wire	#1					1265*	
	#2					1185*	
	#3					1195*	
	#4					1210*	
3" Welded wire	#1					1270*	
	#2					1135*	
	#3					1260*	
	#4					1070*	

Asterisk (*) denotes wire broke in test.



Figure 36. Pull-Out Test Specimen, 5 Inch Embedment,
Showing Wire Failure.

wires were not tested.

Discussion of Pull-Out Tests

Slip failures in bond pull-out tests were noted by Mathey⁽¹⁴⁾ and Watstein⁽²²⁾ in testing standard reinforcing bars. With 3/4 in. bars, Watstein noted first slip at 225 and 215 psi respectively for eight in. and twelve in. embedment. Mathey and Watstein defined a free end slip of 0.002 in. as critical bond stress, or a loaded end slip of 0.01 in., whichever occurred first. Since slips in these (OSU Agr. Engr.) pull-out tests were noted visually, or by a drop in the weigh beam of the test machine, "first slips" noted would be in excess of the above.

Ferguson and Thompson⁽⁶⁾ found the development lengths of bars for bond stress to increase with decreased steel stress and decrease with increased f'_c , or ultimate strength of concrete. The smallest bar tested was a #3 bar with 1 1/2 in. cover. In 3,000 psi concrete, it developed over 80 kips per square in. in a 7.5 in. (20 d) development length.

The ultimate strength of the concrete for the pull-out specimens tested was obtained by capping the 5 in. pull-out blocks after bond tests were completed, then loading them in a standard compression test. Ultimate loads were reduced 20 per cent for shape factor, as recommended by Billig⁽³⁾. The specimens tested averaged 5193 psi, with 5,040 psi minimum and 5,390 psi maximum.

Based on the above findings, and the relationship of bond stress and the yield strength of the wire, it was assumed that the five in. embedment length would provide sufficient bond to prevent pull-out. Minimum strength of 5,000 psi would be required for the concrete.

Test for E_c for Two Sides of Thin Plates

Mench⁽¹⁵⁾, in his study of small test arches, found a marked difference in the modulus of elasticity, E_c , for concrete on the form side and the outer surface of small arches. The concrete was applied pneumatically and troweled smooth after all arches had been cast. The delay in curing, to allow the surface to be troweled smooth, may have caused the apparent difference. To avoid errors due to variance in EI of the concrete, the stiffness factor, due to variations in E_c , an experiment was conducted to determine if the modulus of elasticity would vary for the two sides of concrete panels cast in the proposed method. If a difference were noted, it would restrict the test procedures and make computations of the stiffness factor, and the computed performance of the panels, more difficult to determine.

Twelve panels were cast to determine finishing effects on the stiffness and strength of panels, and effects of E_c , in bending. Six of the panels cast were duplicates of the proposed "standard" panel, six No. 10 wires in a 1.35 in. deep by 8.1 in. wide by 24 in. long panel. Six more panels, with the same dimensions but with no reinforcement, were also cast. Concrete used was the same mix proposed for the test panels. The panels were cast in plastic lined wood forms, the concrete vibrated and rodded into place, and finished with a steel trowel. The panels were cured in the forms using wet burlap sacking and a plastic cover for 4 days prior to removal. They were then moist cured for the remainder of the 28 days.

The depth of each panel was measured to determine the actual thickness of the center third section. This would be the region of uniform

maximum stress when loaded. The panels were then divided into two groups, each group containing three reinforced panels and three non-reinforced panels. Two batches of concrete had been used to cast the panels so a selection was made to include at least one panel from each mix in the reinforced and unreinforced panels of each group of six. Strain gages were then installed on the form side of one group of six panels and on the troweled side of the other group of panels. The purpose of the strain gages was to measure compressive strain of the panels under bending stress. Strain measurements were not made on the tensile side of the panels.

The panels were loaded at third points with increment loads of approximately 100 lb. Load measurements were made with a load cell in the load linkage. After each load increment was applied, measurements of load, strain and deflection at the centerline of each panel were read and recorded. No effort was made to maintain a specific load rate. All panels were loaded to failure.

Results of the tests of the 12 panels are shown in Table XIX. Unreinforced panels failed when compressive strain exceeded 250 microinches per in., with one exception that failed at 242 microinches per in. strain. Of the six reinforced panels tested, strain gage bonding failures occurred in three panels. Strain recorded for the three panels with operative strain gages showed initiation of cracking at approximately 250 microinches per in. strain on the compression face of the panel.

Slight variations in deflection are shown for the six unreinforced panels tested. This is primarily due to slight variations in the panel thicknesses. Thicknesses of panels, deflection at 400 lb. load, and

TABLE XIX
 PHYSICAL PROPERTIES OF TWELVE PANELS FOR
 PRELIMINARY TESTS FOR E_c FOR CONCRETE

Panel Number	Wires No.	Depth in.	E, psi 10^{-6}	Deflection in. at 400 lb.	Ult. load lb.	Side loaded*
1	0	1.424	4.24	0.0129	636	F
2	0	1.394	3.86	0.0131	595	F
3	0	1.425	4.24	0.0114	699	F
4	0	1.413	3.86	0.0127	601	T
5	0	1.392	4.24	0.0126	580	T
6	0	1.408	3.86	0.0120	619	T
7	6	1.393	4.24	0.0139	848	T
8	6	1.373	4.24	0.0147	867	T
9	6	1.433	3.86	0.0130	981	F
10	6	1.384	3.86	0.0134	1,267	F
11	6	1.424	4.24	0.0116	859	F
12	6	1.445	3.86	0.0133	1,161	T

* F signifies form side loaded in compression, T for troweled side loaded in compression.

ultimate loads for each panel are shown in Table VI. Similar variations were also noted for the reinforced panels. Two panels, Nos. 10 and 12, failed at 1,267 and 1,161 lb. load respectively, compared to 848 to 981 lb. ultimate load for the other four reinforced panels.

A statistical analysis was conducted to determine if form effects were present. The panels were tested for variance in deflection at the 400 lb. load for all panels and at ultimate load for the two groups of panels, nonreinforced and reinforced. Differences in deflection between the reinforced panels tested with the form side in compression and the reinforced panels tested with the finished, or troweled, side in compression were found to be not significant at the 0.95 confidence level. Similar results were obtained with the analysis of ultimate load data. Based on the above results, it was assumed that no significant difference existed in E_c between the form side and the finished side of concrete panels cast when treated and cured as proposed for this experiment.

APPENDIX B

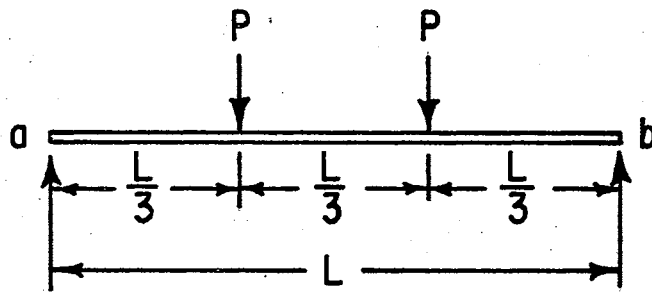
CONJUGATE BEAM THEORY

The conjugate beam method, or elastic weights, was selected for use in this study because it was convenient for determination of deflection of simple beams with large variations in EI, as would occur in cracked sections of thin, concrete beams. This method of deflection determination of beams is closely related to the moment area method and is an analogue application in beam mechanics.

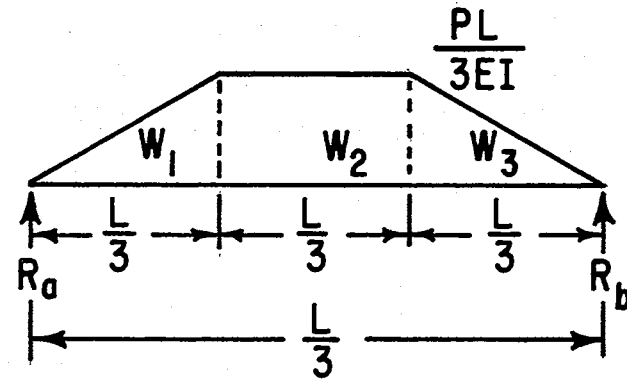
One objectives of this study was to determine the relationship between deflection and spacing of reinforcement for simple, reinforced concrete beams in flexure. If a proximity effect exists, a theoretical equation could be developed to predict increased stiffness as a function of reinforcement spacing. A single, representative deflection, the deflection at the center of the span, was selected to determine relative stiffness of reinforced panels for specific loads.

A real beam, loaded at the third points, and the conjugate beam for computing deflection, are shown in Figure 37. The M/EI diagram from the real beam is shown loaded on the side of the conjugate beam corresponding to the compression side of the real beam. Their relationships are:

1. The span of the conjugate beam is equal to the span of the real beam.
2. The load of the conjugate beam is the M/EI diagram of the real beam.



Real beam, load, P , at third points.
Length = L .



Conjugate beam, Length = L , loaded
with loads W_1 , W_2 and W_3 .

Figure 37. Real Beam and Conjugate Beam

3. The shear at any section of the conjugate beam is equal to the slope of the corresponding section of the real beam.
4. The moment at any section of the conjugate beam is equal to the deflection at the corresponding section of the real beam.

Deflection at the center of the span for a simple beam loaded at the third points can be computed for a beam with a constant section and modulus of elasticity, EI , by taking moments of the M/EI diagram about the center of the beam. The change in slope, θ , from the support to the center of the span, or the slope of the real beam at the support, will be equal to the area of the M/EI diagram for one half the conjugate beam, or the shear of the conjugate beam at the support.

If we assume the load on the conjugate beam is equal to the area of the M/EI diagram for a beam loaded with load P at the third points, we can then describe the load as;

$$W_1 = W_3 = \frac{1}{2} \times \frac{PL}{3EI} \times \frac{L}{3} = \frac{PL^2}{18EI}$$

$$W_2 = \frac{PL}{3EI} \times \frac{L}{3} = \frac{PL^2}{9EI}$$

Therefore, the reactions, R , at each end of the conjugate beam will be equal to:

$$R_L = R_R = W_1 + \frac{W_2}{2}$$

$$= \frac{PL^2}{18EI} + \frac{PL^2}{9EI} \times \frac{1}{2} = \frac{PL^2}{9EI}$$

and the slope at R_L in the real beam equals the shear in the conjugate beam, or;

$$\theta = \frac{PL^2}{9EI} \quad (3)$$

The deflection at the center line of the real beam can be computed by

taking the moment of the conjugate beam at the center line, or;

$$M = \left(\frac{-PL^2}{18EI} \times \frac{5L}{18} \right) + \left(\frac{PL^2}{9EI} \times \frac{L}{2} \right) - \left(\frac{PL^2}{18} \times \frac{L}{12} \right) = \frac{23PL^2}{648EI}$$

Therefore, if the moment of the conjugate beam at the center line equals the deflection of the real beam at the center line,

$$\Delta_c = \frac{23PL^2}{648EI} \quad (4)$$

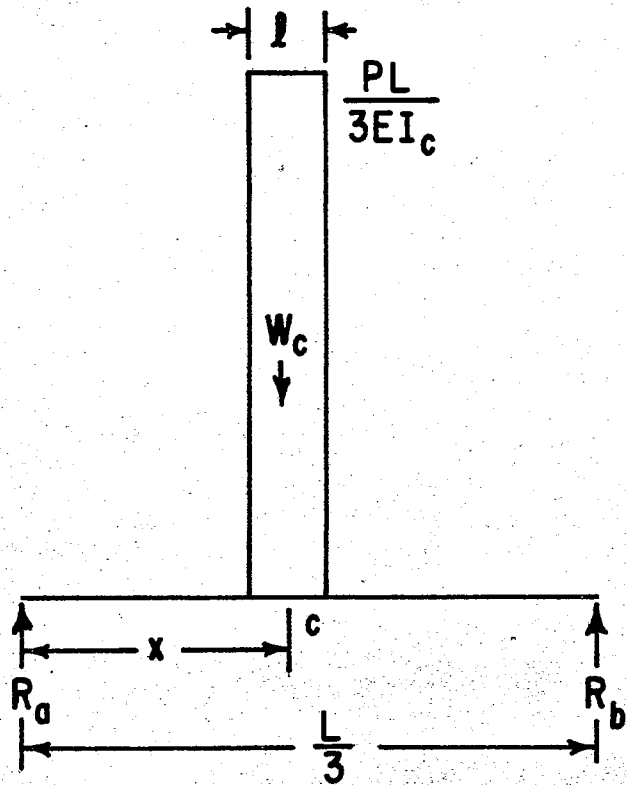
The above equation, Equation 4, will be applicable for determining deflections at midspan for uncracked sections of reinforced concrete beams only. Once cracking occurs, the EI value in the vicinity of the crack will change due to the neutral axis moving up and a reduced moment of inertia at the crack, and a new conjugate load will be applied to the conjugate beam. This will be applied to the conjugate beam for a distance equal to the length tensile stress loss in the concrete on either side of the crack. In thin concrete sections, the magnitude of change of the conjugate load may be quite large due to the greatly reduced moment of inertia of the cracked section.

The load on the conjugate beam due to cracking of the real beam, W_c , is shown in Figure 38. Total load on the conjugate beam will be the initial load, the original M/EI diagram, plus the additional load due to cracking in excess of the original magnitude of M/EI. If the length of tensile stress loss in the concrete is l , the additional conjugate load due to cracking will be;

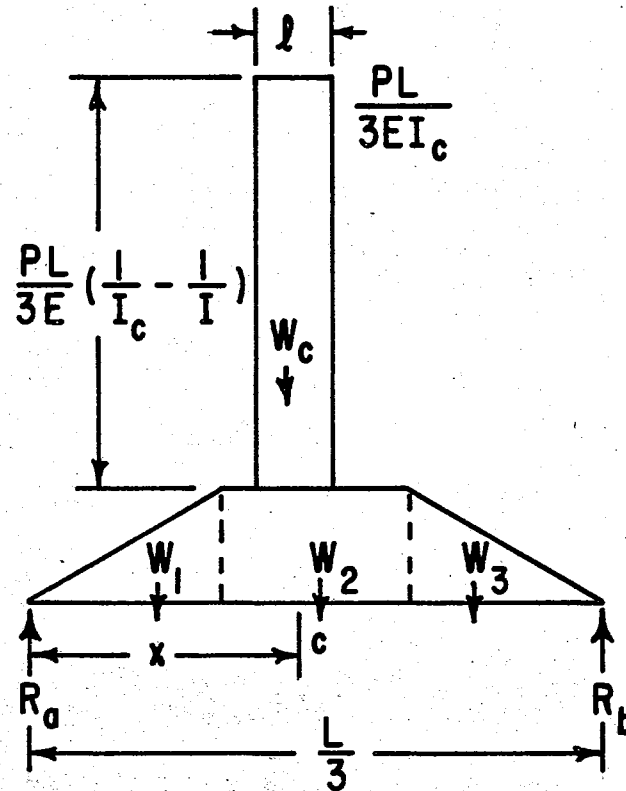
$$W_c = l \left(\frac{PL}{3EI_c} - \frac{PL}{3EI} \right) = \frac{PLl}{3E} \left(\frac{1}{I_c} - \frac{1}{I} \right) \quad (5)$$

where

W_c = additional conjugate load due to crack.



Conjugate beam for load due to crack at c , x distance from R_a . $l =$ length of bond failure.^a



Conjugate beam for loaded, cracked real beam, crack at c .

Figure 38. Cracked Conjugate Beam

l = length of tensile stress loss in the concrete.

I_c = moment of inertia at cracked section.

Deflection of the real beam at any location due to cracking will be equal to the moment of the conjugate beam at that point due to the conjugate load due to cracking, or W_c . Since this study was primarily interested in deflection at the center of the span, deflection at the center of the span can be computed by taking moments of the conjugate beam at that point.

Moments at the center of the conjugate beam can be computed by taking a free body of one-half of the conjugate beam and applying the basic laws of statics.

$$\text{Sum } V = 0$$

$$\text{Sum } H = 0$$

$$\text{Sum } M = 0$$

The total load on the cracked beam will be the conjugate load for the uncracked beam plus the conjugate load due to cracking, or $W_1 + W_2 + W_3 + W_c$.

The reaction at the support, R_a , for the conjugate load due to cracking, can be computed by taking the moments, due to W_c , about the point b, where $M_b = 0$. Therefore;

$$\text{Sum } M_b = 0$$

$$M_b = R_a \times L - W_c (L - x)$$

where

x = distance from R_a to the crack

or,

$$R_a = W_c \left(\frac{L-x}{L} \right)$$

Substituting;

$$R_a = \frac{PL\ell}{3E} \left(\frac{1}{I_c} - \frac{1}{I} \right) \left(\frac{L-x}{L} \right) \quad (6)$$

Moments at the center of the span due to load W_c can now be computed using the above value for R_a , or;

$$\begin{aligned} M_{c1} &= R_a \left(\frac{L}{2} \right) - W_c \left(\frac{L}{2} - x \right) \\ &= \frac{PL\ell}{3E} \left(\frac{1}{2} \right) \left(\frac{L-x}{L} \right) \left(\frac{1}{I_c} - \frac{1}{I} \right) - \frac{PL\ell}{3E} \left(\frac{L}{2} - x \right) \left(\frac{1}{I_c} - \frac{1}{I} \right) \\ &= \frac{PL\ell}{3E} \left(\frac{1}{I_c} - \frac{1}{I} \right) \left[\left(\frac{L-x}{2} \right) - \left(\frac{L-2x}{2} \right) \right] \\ &= \frac{PL\ell}{3E} \left(\frac{x}{2} \right) \left(\frac{1}{I_c} - \frac{1}{I} \right) \end{aligned}$$

Therefore, if the deflection of the real beam is equal to the moment of the conjugate beam, the deflection due to cracking only will be;

$$\Delta_{cc} = \frac{PL\ell}{3E} \left(\frac{x}{2} \right) \left(\frac{1}{I_c} - \frac{1}{I} \right) \quad (7)$$

Total deflection of the real beam at midspan will now be equal to the sum of the moments of the uncracked conjugate beam plus the moment of the cracked conjugate beam due to W_c , or:

$$\begin{aligned} \Delta_c &= \Delta + \Delta_{cc} \\ &= \frac{23PL^3}{648EI} + \frac{PL\ell}{3E} \left(\frac{x}{2} \right) \left(\frac{1}{I_c} - \frac{1}{I} \right) \quad (8) \end{aligned}$$

Where two or more cracks occur in the center third of the real beam, deflection due to these additional cracks can be computed using the same

procedure. In each case, x will be the distance measured from the nearest end of the real beam to the crack. The total x , or the sum of the x 's, can then be substituted in the above equation since the deflection at the center will be dependent upon the distance from the center of the span to the cracks, irrespective of which side of the center line the cracks occur, or;

$$\Delta_c = \frac{23PL^3}{648EI} + \frac{PL\ell}{3E} \left(\frac{1}{I_c} - \frac{1}{I} \right) \left(\frac{x_1 + \dots + x_n}{2} \right) \quad (9)$$

Total load on the real beam was measured and used for computations in the analysis of the experiments. Therefore, the applied load at the third points was one-half the total load, or $P/2$. Substituting for the P value in the above equation, computed deflections were:

$$\Delta = \frac{23PL^3}{1296EI} \quad (10)$$

for the uncracked beam, and

$$\Delta_c = \frac{23PL^3}{1296EI} + \frac{PL\ell}{6E} \left(\frac{1}{I_c} - \frac{1}{I} \right) \left(\frac{\sum x}{2} \right) \quad (12)$$

for the cracked beam.

The above assumption is based on a rectangular shape of the M/EI diagram for the cracked section of length ℓ , or the effective length of tensile stress loss at a crack. The actual shape of the M/EI diagram at a crack would not be a rectangular shape but, since we can assume any shape for the elastic weight effective at the centroid, or at the crack, the rectangular shape is the most convenient for computation.

The length of tensile stress loss at a crack was determined experimentally for this analysis. The testing method used to obtain an effective length, ℓ , of three in. for No. 10 wire stresses at 55,000 to

70,000 psi is explained in Chapter IV, Theoretical Analysis, on page 28.

The values of the moment of inertia, I , for cracked and uncracked sections of thin, reinforced concrete panels varied greatly, as previously stated. Illustrated are two reinforced panels, 1.35 in. thick with six No. 10 wires at the center of the panel. See Figure 39 and Figure 40. Since the reinforcement is located at the center of the panel, it will contribute little to the panel prior to cracking and can be ignored. It could also be ignored in a thin section of uncracked concrete if it were not located at the center of the panel but were moved down to 0.35 inches from the bottom, providing one inch of concrete above the reinforcement. If it were moved, the center of gravity, or the neutral axis of the panel, would only move down 0.015 in. and the increase in the value of moment of inertia would be negligible.

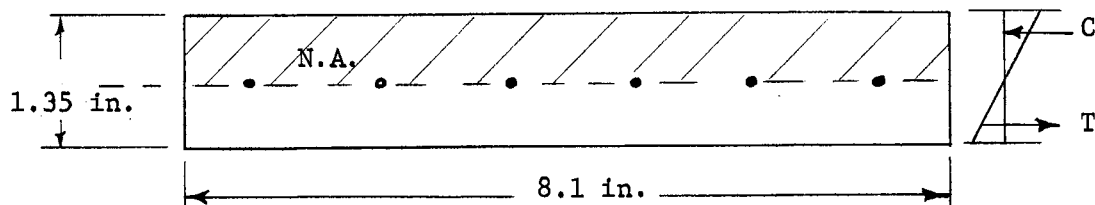


Figure 39. Cross Section for Computing Moment of Inertia of an Uncracked Panel

The moment of inertia for the above section would be computed for a solid, rectangular panel,

$$I = 1/12 bd^3 = 1.66 \text{ in.}^4$$

All concrete above the neutral axis is considered in compression and all concrete below the neutral axis is assumed to be tension. The wire, located at or near the neutral axis, allowing slight displacement during placing and tamping of the concrete, would contribute little or nothing.

Once the panel has cracked, all concrete below the neutral axis is assumed cracked and will contribute nothing to the moment of inertia. The moment of inertia for the cracked panel can now be computed using the transformed section, assuming both the concrete and the reinforcement are stressed in the linear range and stresses have not exceeded yield point. The effective depth of the section is now $D/2$, with the reinforcement carrying all tensile stresses and the concrete carrying all compressive stresses. Moment of inertia for the cracked section, using the transformed section method, will be;

$$I_c = I_o + Ah^2 = 1/12 Bx^3 + Bx(x/2)^2 + nA_s(D/2(-x))^2$$

where:

x = computed distance from compressive surface to neutral axis using transformed section analysis.

n = $E_s/E_c = 6$ for wire reinforcement, $f'_c = 6,000$ psi.

I_c = moment of inertia of cracked section.

Therefore, $I_c = 0.1327 \text{ in.}^4$

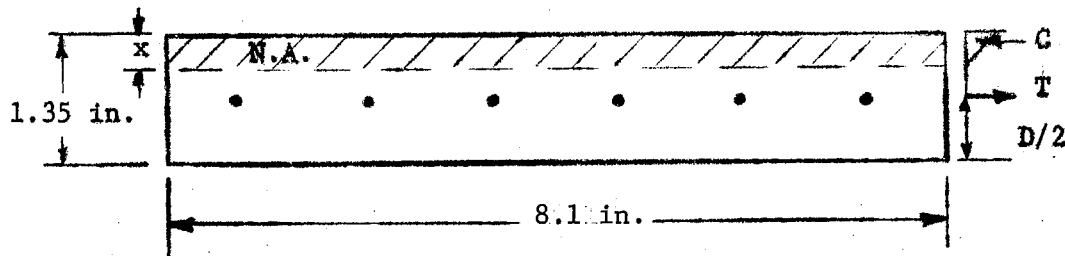


Figure 40. Cross Section for Computing Moment of Inertia of a Cracked Panel

The value for the moment of inertia, I_u , for the uncracked section will be approximately 12.5 times as large as the moment of inertia for the cracked section I_c . Since the stiffness of the concrete panels will be inversely proportional to I , the cracked panel will be 12.5 times more flexible over approximately the length equal to the tensile stress loss in the concrete on either side of the crack.

The above value for I_c is valid only for concrete in the linear range of the stress-strain relationship. Therefore, a concrete mix with a linear stress-strain ratio would be needed for the above value to be valid over much of the test range.

An example of crack effect in deflection is given in the example problem below. Assume a 1.35 in. thick concrete panel, 8.1 in. wide and 24 in. long. The panel is reinforced with six (6) number 10 wire located at the center of the panel. See Figure 8. The moment of inertia I_u of the uncracked section is 1.66 in.^4 . The moment of inertia at a crack, I_c , is 0.1327 in.^4 . Modulus of elasticity of the concrete $5 \times 10^6 \text{ psi}$. Modulus of elasticity of the steel is $30 \times 10^6 \text{ psi}$.

Example:

Compute deflection at the center of the span for a 730 pound total load, = 3 inches;

- a) No cracks.
 b) Crack at midspan, $x = 12$ inches.

$$a) = \frac{23PL^3}{1296EI} = \frac{23 \times 730 \text{ lb.} \times 24 \times 24 \times 24 \text{ in.}^3}{1296 \times 5 \times 10^6 \text{ psi} \times 1.66 \text{ in.}^4}$$

$$\Delta = 0.0269 \text{ in.}$$

$$b) c = \frac{23PL^3}{1296EI} + \frac{PL}{6E} \left(\frac{1}{I_c} - \frac{1}{I} \right) \left(\frac{\Sigma x}{2} \right)$$

$$= \Delta + \frac{730 \text{ lb.} \times 24 \text{ in.} \times 3 \text{ in.}}{6 \times 4 \times 10^6 \text{ psi}} \left(\frac{1}{0.1327 \text{ in.}^4} - \frac{1}{1.66 \text{ in.}^4} \right)$$

$$\left(\frac{12 \text{ in.}}{2} \right)$$

$$= 0.0269 \text{ in.} + 0.0912 \text{ in.}$$

$$c = 0.1181 \text{ inches.}$$

The above example shows that the midspan deflection due to a crack at midspan increases total deflection 340 per cent over an uncracked section. The above computed deflections compare with actual deflections of 0.0228 in. and 0.1229 in. for midspan deflections of Panel 20 for uncracked and cracked conditions and a load of 732 lb. The actual crack in Panel 20 also occurred at midspan.

APPENDIX C

LOAD-DEFLECTION PLOTS, TEST PANELS

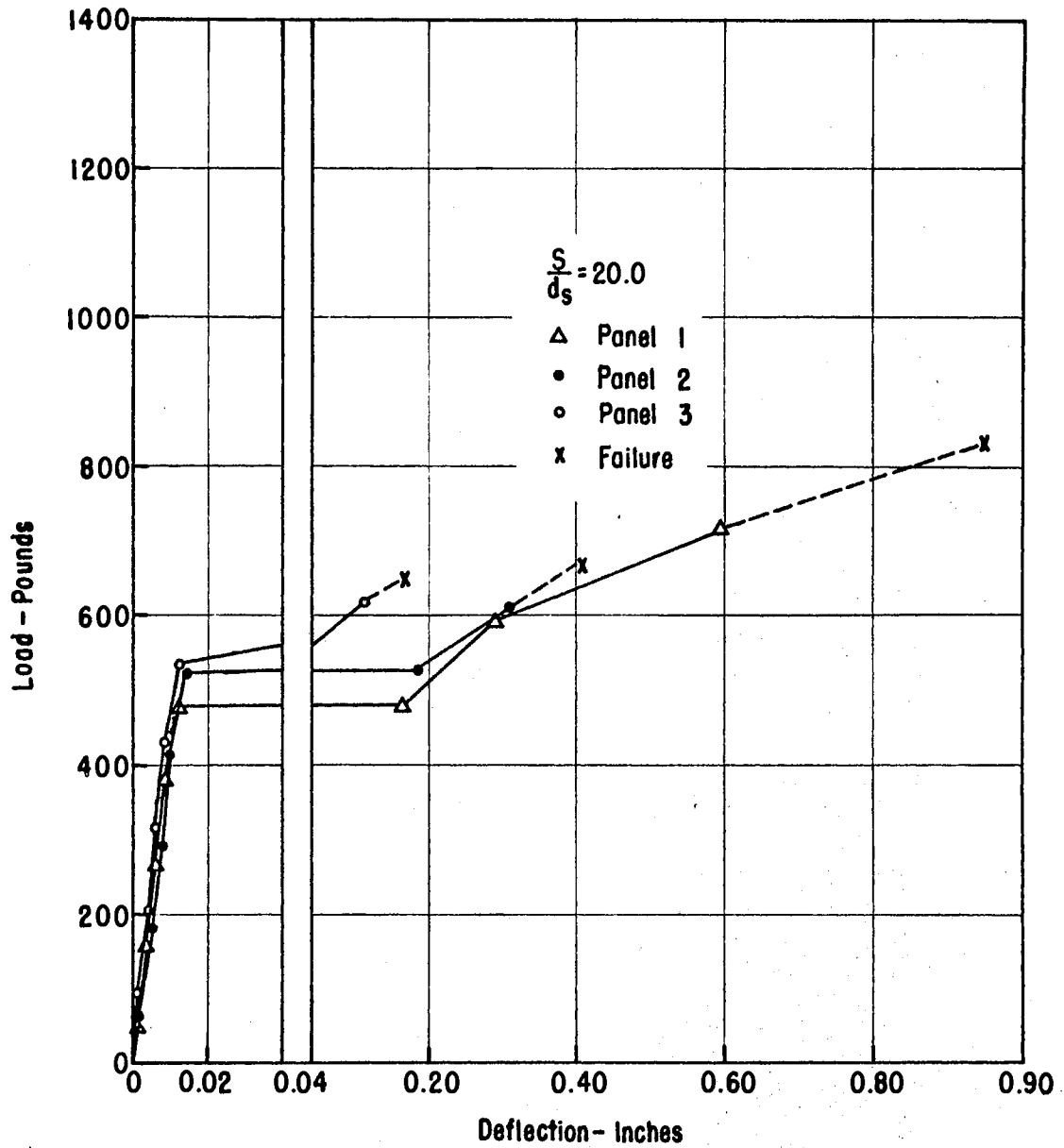


Figure 41. Load-Deflection Plots, Panels 1, 2 and 3

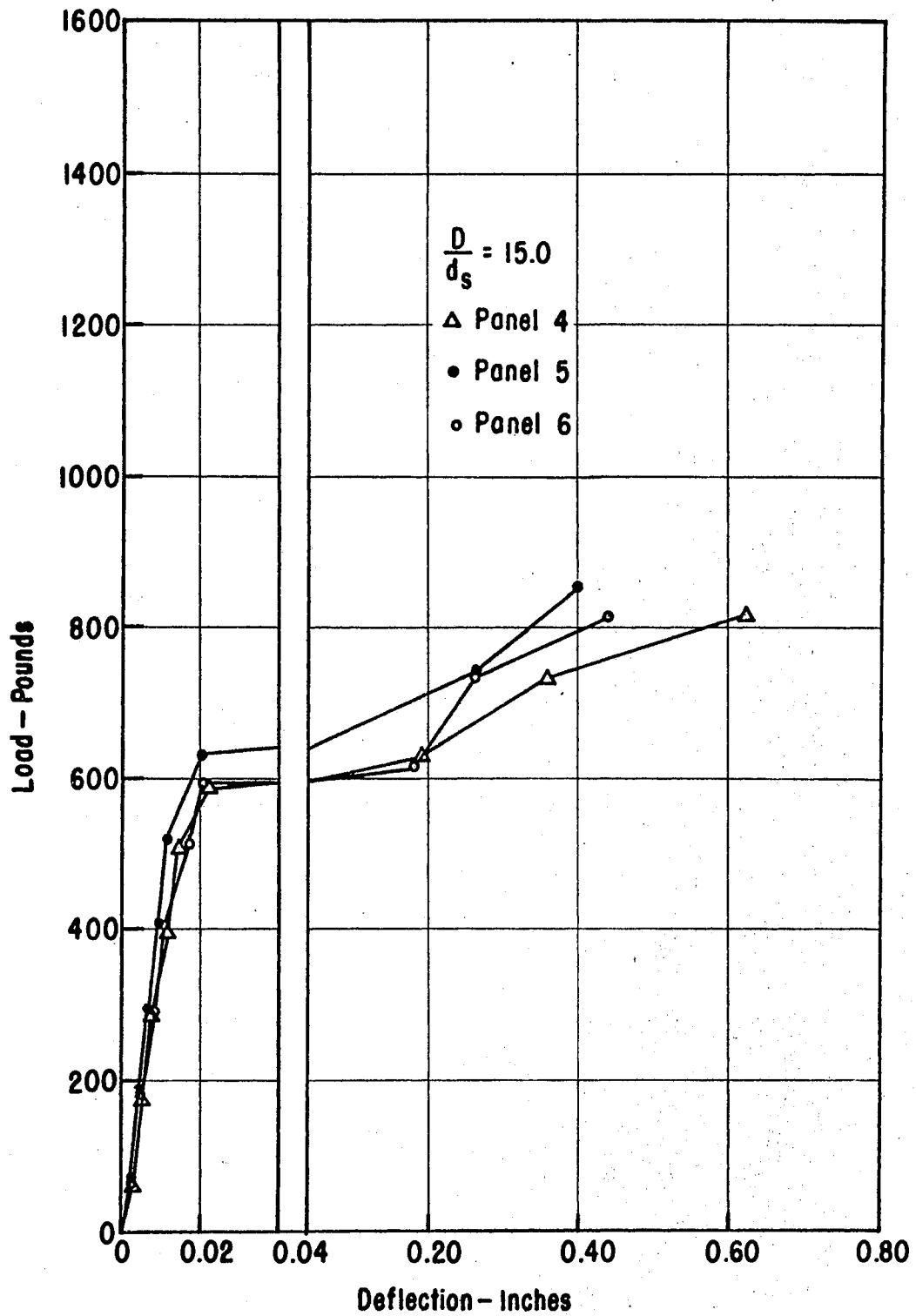


Figure 42. Load-Deflection Plots, Panels 4, 5 and 6

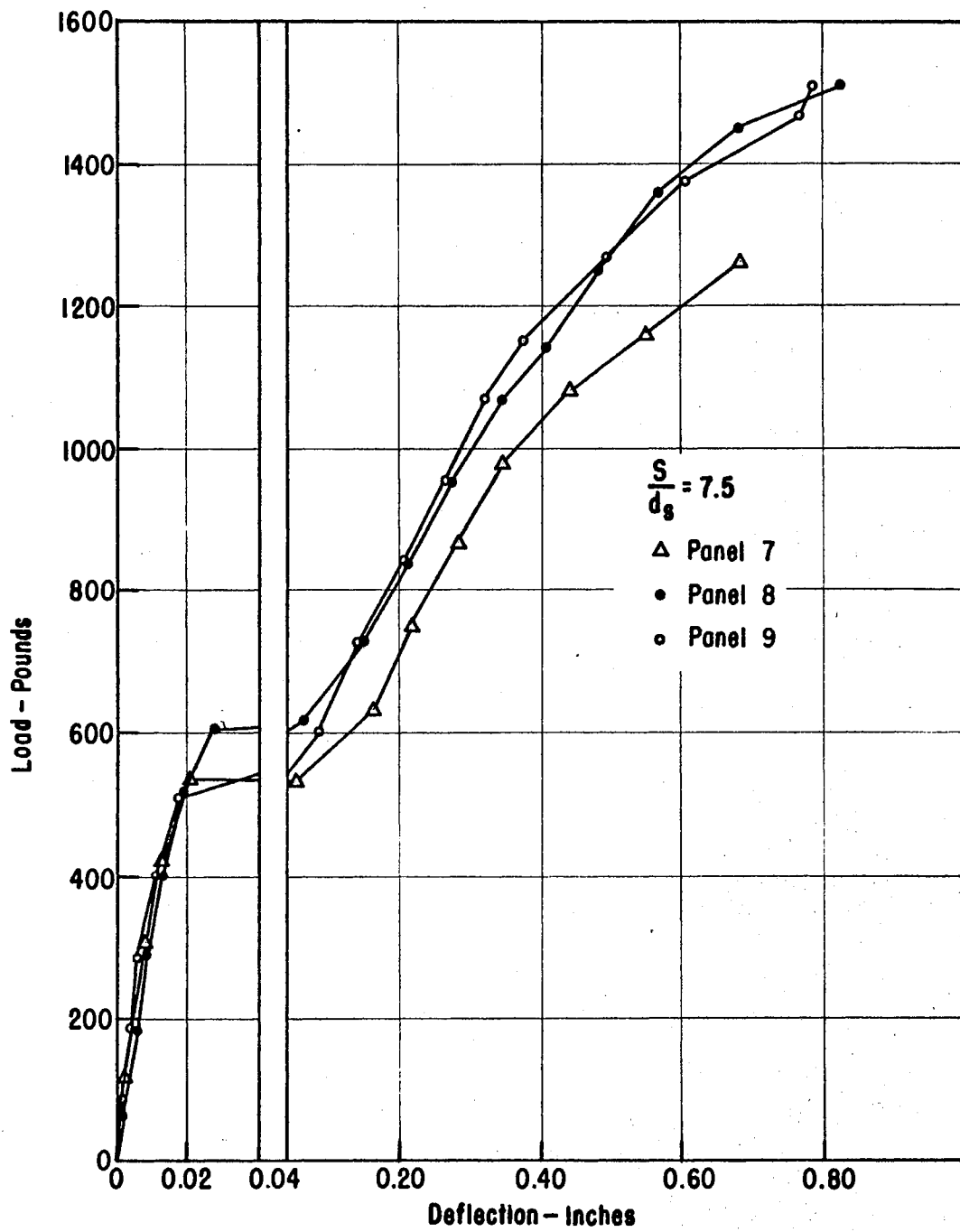


Figure 43. Load-Deflection Plots, Panels 7, 8 and 9

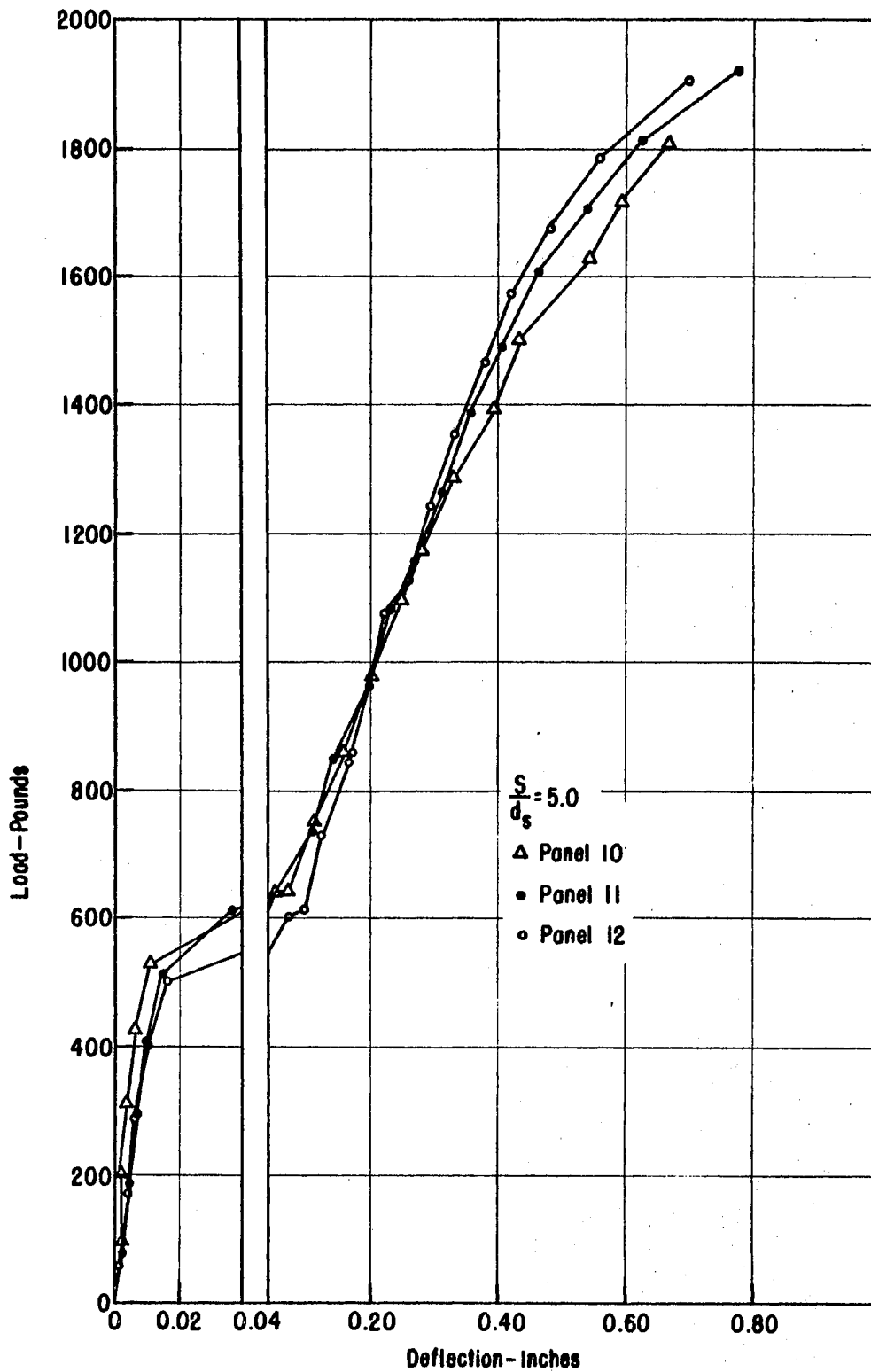


Figure 44. Load-Deflection Plots, Panels 10, 11 and 12

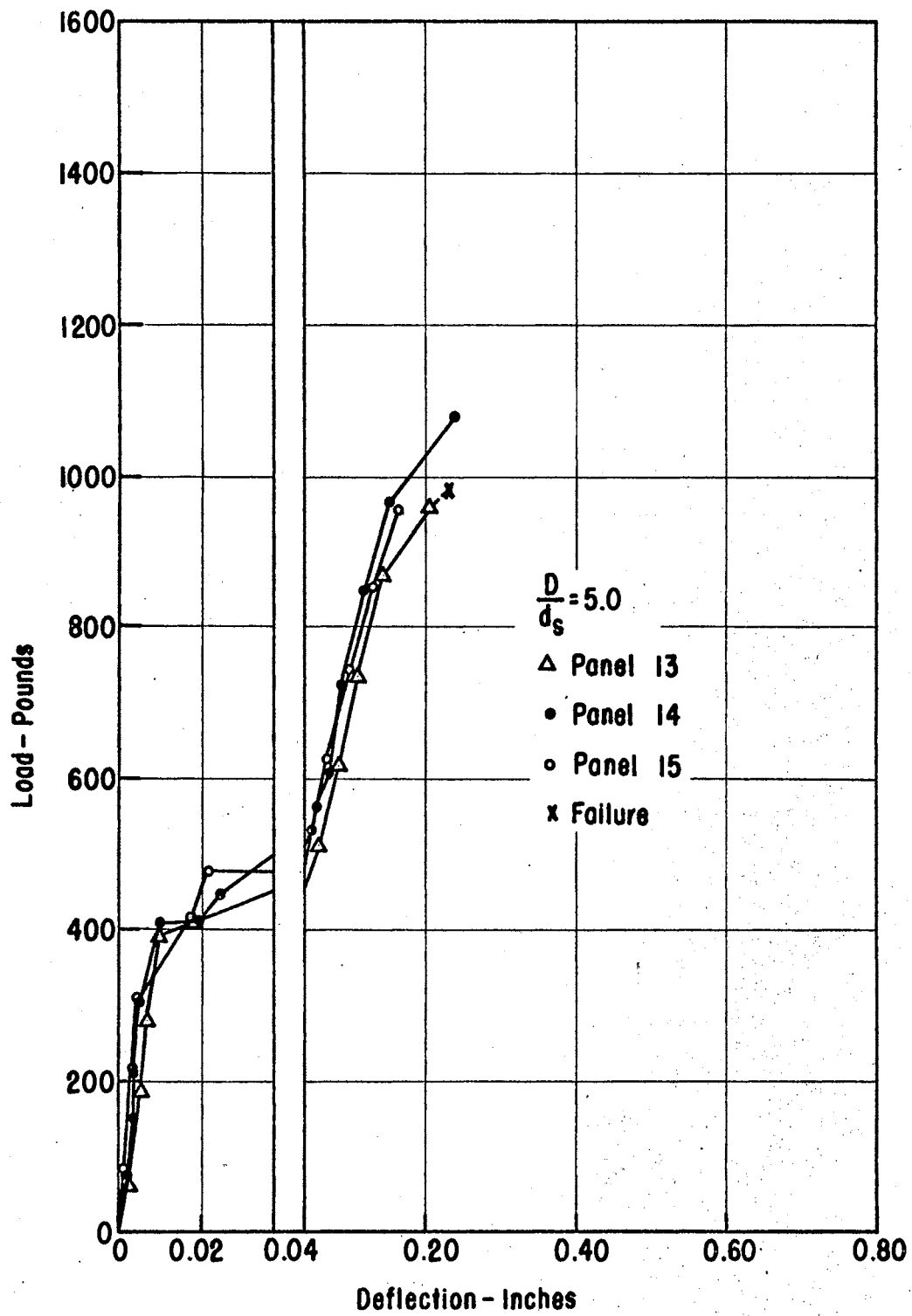


Figure 45. Load-Deflection Plots, Panels 13, 14, and 15

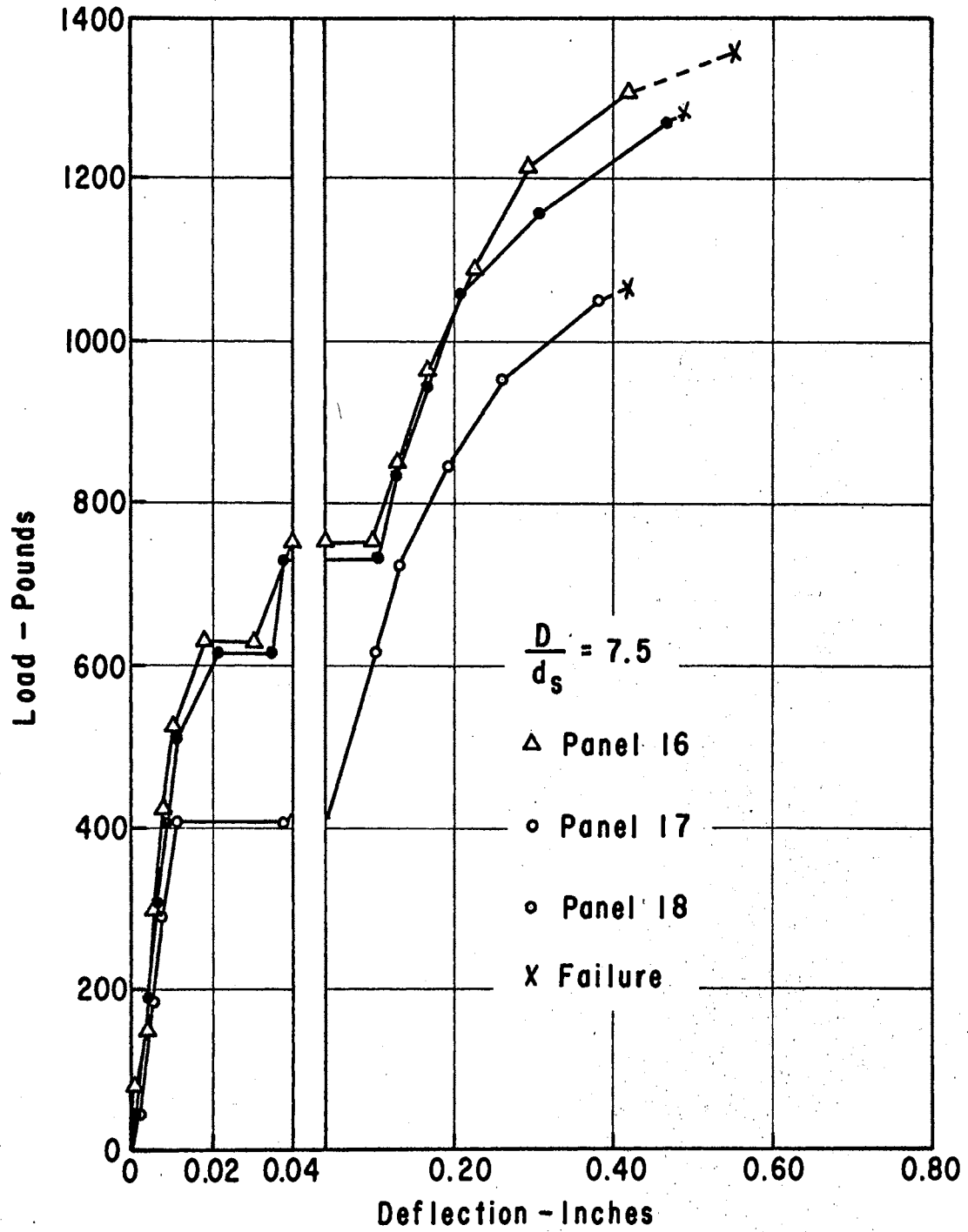


Figure 46. Load-Deflection Plots, Panels 16, 17 and 18

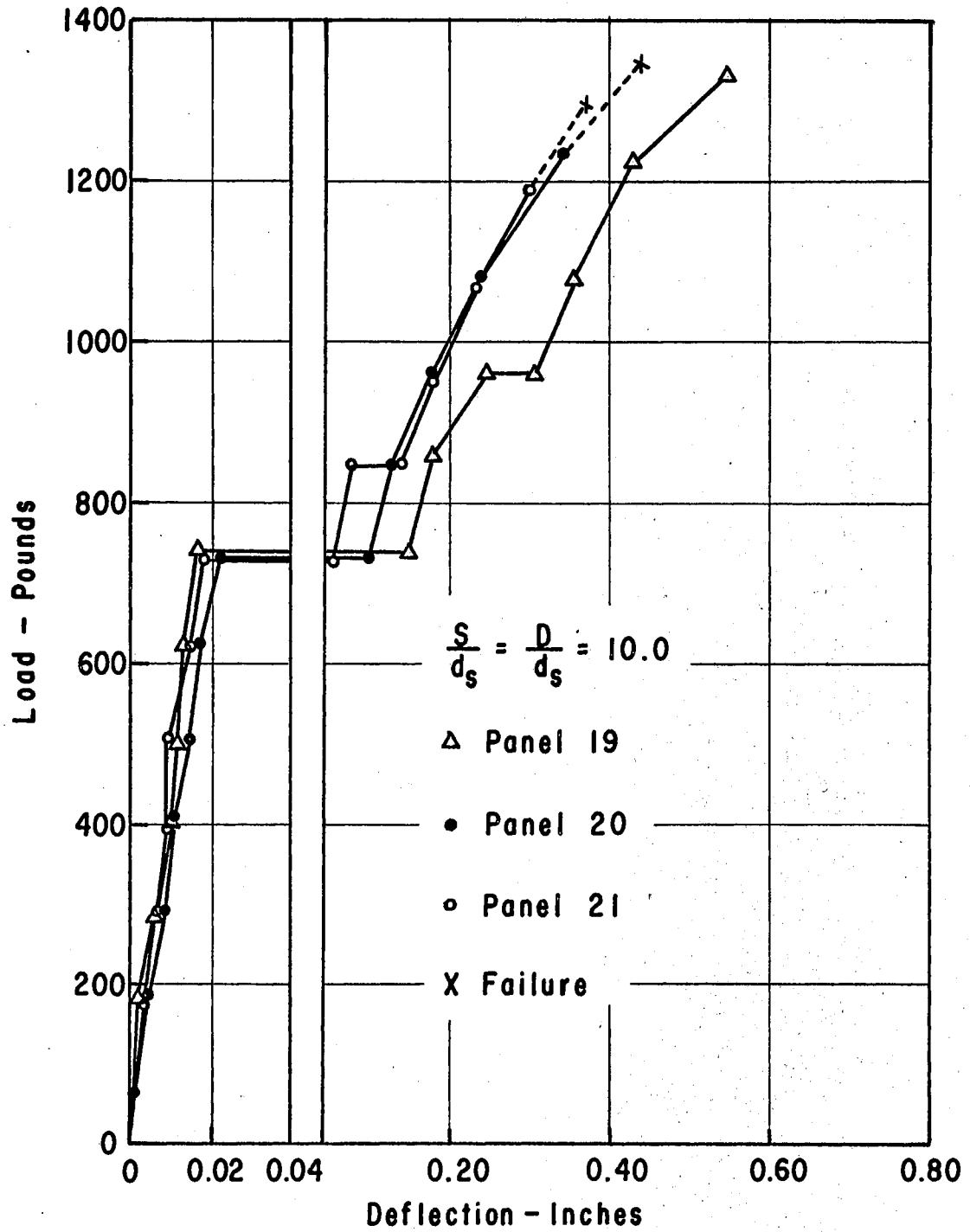


Figure 47. Load-Deflection Plots, Panels 19, 20 and 21

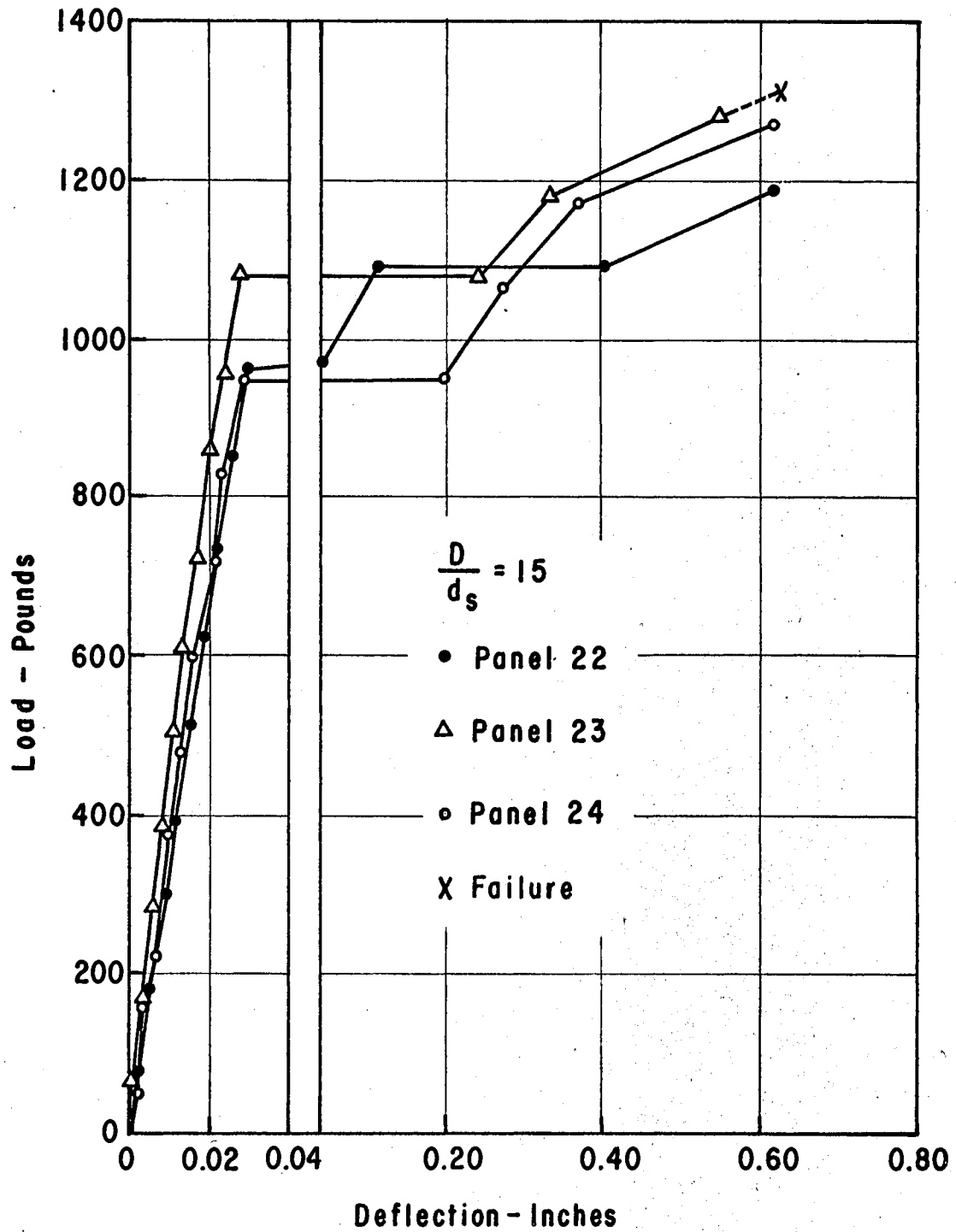


Figure 48. Load-Deflection Plots, Panels 22, 23 and 24

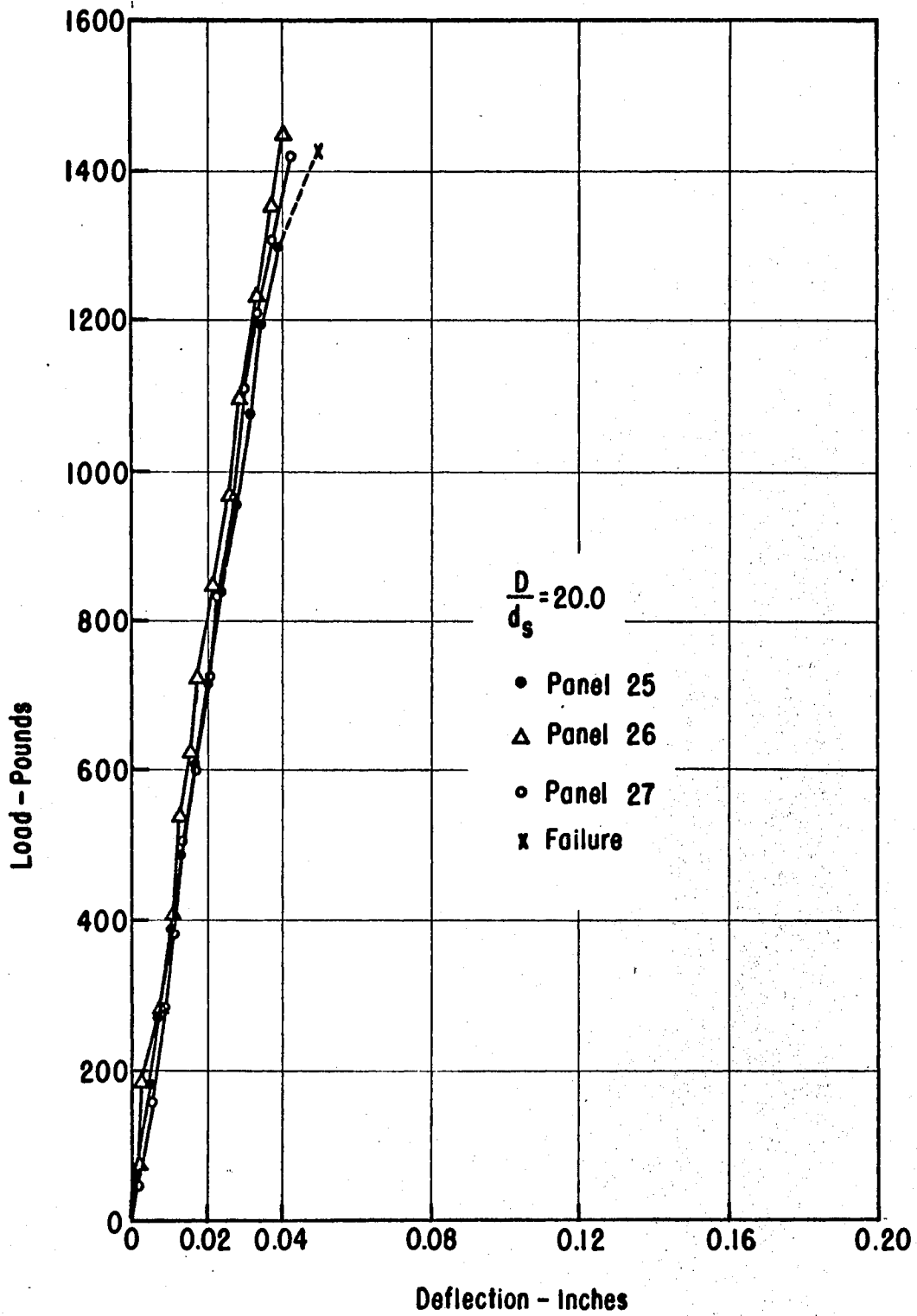


Figure 49. Load-Deflection Plots, Panels 25, 26 and 27

VITA

George William Arthur Mahoney

Candidate for the Degree of

Doctor of Philosophy

Thesis: AN EXPERIMENTAL ANALYSIS OF DEFLECTION AND ULTIMATE MOMENT IN THIN, REINFORCED CONCRETE PANELS AS A FUNCTION OF REINFORCEMENT SPACING

Major Field: Agricultural Engineering

Biographical:

Personal Data: Born in Springfield, Sangamon County, Illinois, January 23, 1925, the son of Edward J. and Mercedes M. Mahoney.

Education: AUS Cadet Training Detachment, University of Florida, 1943; graduated in absentia from Cathedral Boys High School, Springfield, Illinois, in 1945; graduated from Springfield Junior College, Springfield, Illinois, with an Associates Arts Degree in 1947; graduated from the University of Illinois with a Bachelor of Science degree in Agricultural Engineering in 1949; received the Master of Science degree in Agricultural Engineering from Oklahoma State University in 1953; attended Iowa State University the academic year 1964-65 as an NSF Faculty Fellow; completed the requirements for the Doctor of Philosophy degree from Oklahoma State University in May, 1971.

Professional Experience: AUS Air Corps, first lieutenant, 1943-1945; Engineers Aide with the Illinois Highway Department, summer of 1948; Instructor in Agricultural Engineering, Oklahoma State University, 1949-1953; Assistant Professor of Agricultural Engineering, Oklahoma State University, 1953 to 1971.

Professional and Honorary Organizations: Phi Theta Kappa, Member of the American Society of Agricultural Engineers, Member of Sigma Xi, Lieutenant Colonel in the United States Air Force Reserve, Registered Professional Engineer in Oklahoma.